



**HAL**  
open science

# Implementation of Model Predictive Control for Three-Phase Inverter with Output LC Filter Using DSP

Ihab S. Mohamed

► **To cite this version:**

Ihab S. Mohamed. Implementation of Model Predictive Control for Three-Phase Inverter with Output LC Filter Using DSP. Electric power. 2014. hal-02557286

**HAL Id: hal-02557286**

**<https://inria.hal.science/hal-02557286>**

Submitted on 30 Apr 2020

**HAL** is a multi-disciplinary open access archive for the deposit and dissemination of scientific research documents, whether they are published or not. The documents may come from teaching and research institutions in France or abroad, or from public or private research centers.

L'archive ouverte pluridisciplinaire **HAL**, est destinée au dépôt et à la diffusion de documents scientifiques de niveau recherche, publiés ou non, émanant des établissements d'enseignement et de recherche français ou étrangers, des laboratoires publics ou privés.

بِحَمْدِهِ تَعَالَى



**IMPLEMENTATION OF MODEL PREDICTIVE  
CONTROL FOR THREE PHASE INVERTER WITH  
OUTPUT *LC* FILTER USING DSP**

By

Ihab Sami Mohamed Mohamed

A Thesis Submitted to the  
Faculty of Engineering at Cairo University  
in Partial Fulfillment of the  
Requirements for the Degree of  
MASTER OF SCIENCE  
in  
Electronics and Communications

FACULTY OF ENGINEERING , CAIRO UNIVERSITY  
GIZA, EGYPT  
JUNE 2014

# **IMPLEMENTATION OF MODEL PREDICTIVE CONTROL FOR THREE PHASE INVERTER WITH OUTPUT LC FILTER USING DSP**

By

**Ihab Sami Mohamed Mohamed**

A Thesis Submitted to the  
Faculty of Engineering at Cairo University  
in Partial Fulfillment of the  
Requirements for the Degree of  
**MASTER OF SCIENCE**  
in  
Electronics and Communications

Under the Supervision of

**Prof. Dr. Mohamed Fathy Abu-Elyazeed**

Professor

Electronics and Communications Department

Faculty of Engineering , Cairo University

**Dr. Sherif Ahmed Zaid**

Associate Professor

Electrical Power and Machines Department

Faculty of Engineering , Cairo University

**Dr. Hany Mohamed Elsayed**

Assistant Professor

Electronics and Communications Department

Faculty of Engineering , Cairo University

**FACULTY OF ENGINEERING , CAIRO UNIVERSITY**

**GIZA, EGYPT**

**JUNE 2014**

**IMPLEMENTATION OF MODEL PREDICTIVE  
CONTROL FOR THREE PHASE INVERTER WITH  
OUTPUT LC FILTER USING DSP**

By

Ihab Sami Mohamed Mohamed

A Thesis Submitted to the  
Faculty of Engineering at Cairo University  
in Partial Fulfillment of the  
Requirements for the Degree of  
**MASTER OF SCIENCE**  
in  
Electronics and Communications

Approved by the Examining Committee:

---

Prof. Dr. El Sayed Mostafa Saad, External Examiner

---

Prof. Dr. Magdi Fikri Mohamed, Internal Examiner

---

Prof. Dr. Mohamed Fathy Abu-Elyazeed, Thesis Main Advisor

FACULTY OF ENGINEERING , CAIRO UNIVERSITY  
GIZA, EGYPT  
JUNE 2014

**Engineer's Name:** Ihab Sami Mohamed Mohamed  
**Date of Birth:** 22/12/1987  
**Nationality:** Egyptian  
**E-mail:** ihab.s.mohamed@gmail.com  
**Phone:** ....  
**Address:** El-Sheikh Zayed, Giza, Egypt  
**Registration Date:** 1/10/2011  
**Awarding Date:** 24/6/2014  
**Degree:** Master of Science  
**Department:** Electronics and Communications



**Supervisors:**

Prof. Dr. Mohamed Fathy Abu-Elyazeed  
Dr. Sherif Ahmed Zaid  
Dr. Hany Mohamed Elsayed

**Examiners:**

Prof. Dr. El Sayed Mostafa Saad (External examiner)  
Prof. Dr. Magdi Fikri Mohamed (Internal examiner)  
Prof. Dr. Mohamed Fathy Abu-Elyazeed (Thesis main advisor)

**Title of Thesis:**

Implementation of Model Predictive Control for Three Phase Inverter With Output *LC* Filter Using DSP

**Key Words:**

Predictive control; Model Predictive Control; power conversion; uninterruptible power systems; hysteresis control; PWM control; DSP; HIL

**Summary:**

Model predictive control (MPC) is an advanced method of process control that has been enormously used in industry. In recent years, there has been a rapid increase in the use of digital controllers in control systems. Digital controls are used for achieving optimal performance in the form of maximum productivity, maximum profit, minimum cost, or minimum energy use. The control of inverters with output *LC* filter has a special importance in applications where the high quality voltage is needed. Several control schemes have been proposed for the control of three-phase inverter. This thesis presents a new and simple control scheme using predictive control and implementing the proposed MPC on the eZdsp F28335 kit. The controller uses a discrete-time model of the system to predict the behavior of the output voltage for all possible switching states generated by the inverter. Then, a cost function is used as a criterion for selecting the switching state that will be applied during the next sampling interval. There is no need of internal current-control loops and no modulators because the gate-drive signals are generated directly by the controller.

# Table of Contents

<b>List of Tables</b>	<b>iii</b>
<b>List of Figures</b>	<b>iv</b>
<b>List of Symbols and Abbreviations</b>	<b>vii</b>
<b>Acknowledgements</b>	<b>ix</b>
<b>Dedication</b>	<b>x</b>
<b>Abstract</b>	<b>xi</b>
<b>1 Introduction</b>	<b>1</b>
<b>2 DSP for Control Systems</b>	<b>7</b>
2.1 What is Digital Signal Processing? . . . . .	7
2.2 DSPs and Microprocessors . . . . .	7
2.3 Fixed–point vs. Floating–point DSPs . . . . .	8
2.4 Choosing the Processor . . . . .	9
2.5 TMS320 DSP Product Review . . . . .	11
2.5.1 Power Efficiency: TMS320C5000 DSP Platform . . . . .	11
2.5.2 Control Optimized: TMS320C2000 DSP Platform . . . . .	12
2.5.3 Highest Performance: TMS320C6000 DSP platform . . . . .	12
2.6 DSP for Control Systems . . . . .	13
2.6.1 Benefits of DSPs . . . . .	14
2.6.2 Typical DSP Control Applications . . . . .	15
2.7 Overview of the Used eZdsp F28335 Kit . . . . .	16
<b>3 System Model and Predictive Control Strategies</b>	<b>20</b>
3.1 The Proposed System Description . . . . .	20
3.1.1 The Inverter Model . . . . .	20
3.1.2 The Filter Models . . . . .	22
3.1.2.1 The Filter Types . . . . .	22
3.1.2.2 The <i>LC</i> Filter Model . . . . .	23
3.2 Overview of Predictive Control Strategies . . . . .	25
3.2.1 Classification Based on Operational Principle . . . . .	26
3.2.1.1 Hysteresis–Based Predictive Control . . . . .	26
3.2.1.2 Trajectory–Based Predictive Control . . . . .	27
3.2.1.3 Deadbeat–Based Predictive Control . . . . .	29
3.2.1.4 Model Predictive Control . . . . .	29
3.2.2 Classification Based on Prediction Horizon and Control Principle . . . . .	30

<b>4</b>	<b>The Proposed MPC</b>	<b>32</b>
4.1	Model Predictive Control . . . . .	32
4.2	Improved Model Predictive Control . . . . .	37
4.3	The Cost Function . . . . .	41
4.4	Classical Control Methods . . . . .	41
4.4.1	Hysteresis Voltage Control . . . . .	41
4.4.2	Linear Voltage Control with PWM . . . . .	44
<b>5</b>	<b>Results</b>	<b>46</b>
5.1	Simulation Results . . . . .	46
5.1.1	MPC . . . . .	46
5.1.2	MPC and Classical Methods . . . . .	54
5.1.3	Improved MPC . . . . .	60
5.2	Hardware Testing . . . . .	67
5.2.1	System Verification Using Software Simulation . . . . .	67
5.2.2	System Verification Using Hardware Testing . . . . .	67
5.2.3	Hardware-in-the-Loop (HIL) Simulation . . . . .	68
5.2.4	Experimental Results . . . . .	69
<b>6</b>	<b>Conclusions and Future Work</b>	<b>81</b>
	<b>References</b>	<b>83</b>

# List of Tables

1.1	IEEE 519 standards for total harmonic voltage distortion. . . . .	4
3.1	Possible switching states and voltage vectors for a three phase inverter . .	21
5.1	System Parameters . . . . .	46
5.2	The effect of varying the filter capacitance value on the performance of MPC. . . . .	47
5.3	A summary for different values of a resistive load . . . . .	64
5.4	A summary for the nonlinear load with different values of $R$ and $C$ . . . .	66
5.5	System Parameters . . . . .	74
5.6	A comparison between simulation and experimental results for different values of a resistive load . . . . .	77

# List of Figures

1.1	Ideal Sine wave. . . . .	2
1.2	Distorted Waveform. . . . .	2
1.3	Fundamental Frequency (50 Hz) Sine Wave and Harmonics: 2nd Harmonic (100 Hz); 3rd Harmonic (150 Hz); 4th Harmonic (200 Hz). . . . .	3
2.1	Digital signal processing logic. . . . .	7
2.2	Fixed point versus floating point DSP. . . . .	9
2.3	TMS Product Generation. . . . .	13
2.4	The functional block diagram for eZdsp F28335 Kit. . . . .	18
2.5	The platform picture of the eZdsp TMS320F28335 Kit. . . . .	19
3.1	The three phase inverter with output $LC$ filter. . . . .	20
3.2	Possible voltage vectors generated by the inverter. . . . .	21
3.3	The types of filter . . . . .	23
3.4	The $LC$ filter model. . . . .	23
3.5	Classification of predictive control methods used in power electronics. . . . .	25
3.6	Predictive current control, boundary circle, and space vector. . . . .	27
3.7	DSPC: Trajectories in the $e/a$ -state plane. . . . .	28
4.1	The block diagram of MPC with only one prediction step. . . . .	32
4.2	The simulation model of the voltage vector $v_i$ . . . . .	34
4.3	The simulation model of the filter current $i_f$ . . . . .	34
4.4	The simulation model of the output voltage $v_c$ . . . . .	34
4.5	The simulation model of the output current $i_o$ . . . . .	35
4.6	The simulation model of the output voltage reference $v_c^*$ . . . . .	35
4.7	The inverter system simulation model using MPC with one prediction step. . . . .	36
4.8	The flow chart of the proposed predictive control algorithm. . . . .	37
4.9	The block diagram of the Improved MPC with two prediction steps. . . . .	38
4.10	The inverter system simulation model using Improved MPC. . . . .	40
4.11	The block diagram of hysteresis voltage control. . . . .	42
4.12	The simulation model of the transformation $\alpha\beta/abc$ . . . . .	42
4.13	The inverter system simulation model using hysteresis voltage control. . . . .	43
4.14	The block diagram of PWM voltage control. . . . .	44
4.15	The inverter system simulation model using PWM voltage control. . . . .	45
5.1	The simulated three phase output voltages and currents at steady state for a resistive load of 3- $\Omega$ . Voltage THD: 0.71%. . . . .	48
5.2	The simulated three phase output voltages and currents at steady state for a resistive load of 20- $\Omega$ . Voltage THD: 1.71%. . . . .	48
5.3	The effect of varying the inverter output voltage reference value on the THD at different resistive loads. . . . .	49
5.4	The simulated output voltages and currents according to full load step change at $t = 0.05sec$ . . . . .	49
5.5	The inverter nonlinear load. . . . .	50

5.6	The simulated three phase output voltages and currents at steady state for a nonlinear load. Voltage THD: 4.75%. . . . .	50
5.7	The simulated three phase output voltages and currents at steady state for a nonlinear load with a sampling time of $T_s = 10 \mu s$ . Voltage THD: 2.18%. . . . .	51
5.8	The effect of varying the inverter output voltage reference value on the THD at different nonlinear loads. . . . .	51
5.9	The simulated three phase output voltages and currents at steady state for a resistive load of 20- $\Omega$ with the filter capacitance of 20 $\mu F$ (-50%). Voltage THD: 2.60%. . . . .	52
5.10	The simulated three phase output voltages and currents at steady state for a resistive load of 20- $\Omega$ with the filter capacitance of 100 $\mu F$ (+150%). Voltage THD: 1.01%. . . . .	52
5.11	The simulated three phase output voltages and currents at steady state for a nonlinear load with the filter capacitance of 20 $\mu F$ (-50%). Voltage THD: 4.53%. . . . .	53
5.12	The simulated three phase output voltages and currents at steady state for a nonlinear load with the filter capacitance of 100 $\mu F$ (+150%). Voltage THD: 4.66%. . . . .	53
5.13	The simulated three phase output voltages and currents at steady state for a resistive load of 3- $\Omega$ in case of MPC. Voltage THD: 0.71%. . . . .	55
5.14	The simulated three phase output voltages and currents at steady state for a resistive load of 3- $\Omega$ in case of PWM control. Voltage THD: 3.13%. . . . .	55
5.15	The simulated three phase output voltages and currents at steady state for a resistive load of 3- $\Omega$ in case of hysteresis control. Voltage THD: 4.21%. . . . .	56
5.16	The simulated three phase output voltages and currents at steady state for a resistive load of 20- $\Omega$ in case of MPC. Voltage THD: 1.71%. . . . .	56
5.17	The simulated output voltages and currents according to full load step change at $t = 0.05 sec$ for a MPC. . . . .	57
5.18	The simulated output voltages and currents according to full load step change at $t = 0.05 sec$ for a PWM control. . . . .	57
5.19	The simulated output voltages and currents according to full load step change at $t = 0.05 sec$ for a hysteresis control. . . . .	58
5.20	The simulated three phase output voltages and currents at steady state for a nonlinear load for a MPC. Voltage THD: 3.02%. . . . .	58
5.21	The simulated three phase output voltages and currents at steady state for a nonlinear load for a hysteresis control. Voltage THD: 50.66%. . . . .	59
5.22	The simulated three phase output voltages and currents at steady state for a nonlinear load for a PWM control. Voltage THD: 40.75%. . . . .	59
5.23	The simulated three phase output voltages and currents for a MPC with 50- $\Omega$ load. Voltage THD: 2.30%. . . . .	61
5.24	The simulated three phase output voltages and currents for a MPC with 2-k $\Omega$ load. Voltage THD: 3.84%. . . . .	61
5.25	The simulated three phase output voltages and currents for a MPC with 4-M $\Omega$ load. Voltage THD: 6.12%. . . . .	62
5.26	The simulated three phase output voltages and currents for the Improved MPC with 50- $\Omega$ load. Voltage THD: 0.74%. . . . .	62

5.27	The simulated three phase output voltages and currents for the Improved MPC with 2-k $\Omega$ load. Voltage THD: 0.76%. . . . .	63
5.28	The simulated three phase output voltages and currents for the Improved MPC with 4-M $\Omega$ load. Voltage THD: 0.77%. . . . .	63
5.29	The simulated three phase output voltages and currents for a MPC with a nonlinear load of $R = 60\Omega$ and $C = 3000\mu F$ . Voltage THD: 2.34%. . . .	64
5.30	The simulated three phase output voltages and currents for a MPC with a nonlinear load of $R = 1000\Omega$ and $C = 3000\mu F$ . Voltage THD: 3.06%. . .	65
5.31	The simulated three phase output voltages and currents for the Improved MPC with a nonlinear load of $R = 60\Omega$ and $C = 3000\mu F$ . Voltage THD: 1.06%. . . . .	65
5.32	The simulated three phase output voltages and currents for the Improved MPC with a nonlinear load of $R = 1000\Omega$ and $C = 3000\mu F$ . Voltage THD: 0.75%. . . . .	66
5.33	The schematic diagram of the proposed HIL platform. . . . .	69
5.34	The Code Composer Studio (CCS) screen. . . . .	71
5.35	The Host-PC program for a three phase inverter with $LC$ filter using HIL simulation. . . . .	72
5.36	The implementation of the proposed MPC on eZdsp F28335 Kit. . . . .	73
5.37	The simulated three phase output voltages and currents for a MPC with resistive load of 20- $\Omega$ load. Voltage THD: 0.57%. . . . .	75
5.38	The experimental three phase output voltages and currents for a MPC with resistive load of 20- $\Omega$ load. Voltage THD: 0.7%. . . . .	75
5.39	The simulated three phase output voltages and currents for a MPC with resistive load of 100- $\Omega$ load. Voltage THD: 1.44%. . . . .	76
5.40	The experimental three phase output voltages and currents for a MPC with resistive load of 100- $\Omega$ load. Voltage THD: 1.7%. . . . .	76
5.41	The simulated three phase output voltages and currents for a MPC with a nonlinear load. Voltage THD: 1.9 %. . . . .	77
5.42	The experimental three phase output voltages and currents for a MPC with a nonlinear load. Voltage THD: 1.98 %. . . . .	78
5.43	The simulated filter current for a MPC with a nonlinear load. Current THD: 3.07%. . . . .	78
5.44	The experimental filter current for a MPC with a nonlinear load. Current THD: 3.07%. . . . .	79
5.45	The simulated three phase output voltages and currents for a MPC with resistive load of 20- $\Omega$ and according to the previous modifications. Voltage THD: 6%. . . . .	80

# List of Symbols and Abbreviations

MPC	Model Predictive Control
<i>THD</i>	Total Harmonic Distortion
IEEE 519	The IEEE standard for total harmonic voltage distortion
UPS	The Uninterruptible Power Supply system
LRPC	Long-Range Predictive Control
DSPC	Direct Speed Control
GPC	Generalized Predictive Control
S	The switching states of the inverter
$v_i$	The voltage vectors generated by the inverter
$V_{dc}$	The dc-link voltage
$i_f$	The filter current in the vectorial form
$v_c$	The output voltage in the vectorial form
$i_o$	The output current in the vectorial form
$L$	The filter inductance
$C$	The filter capacitance
$f_c$	The filter cut-off frequency
$F(s)$	The Transfer function of the <i>LC</i> filter
$T_s$	The sampling time
$g_N$	The cost function for $N$ step predictions
$g_1$	The cost function for a MPC with one step prediction $N = 1$
$g_2$	The cost function for the Improved MPC with two steps prediction $N = 2$
$v_c^*$	The output voltage reference vector
$v_{c\alpha}$	The real part of the predicted output voltage vector
$v_{c\beta}$	The imaginary part of the predicted output voltage vector
$v_{c\alpha}^*$	The real part of the reference output voltage vector
$v_{c\beta}^*$	The imaginary part of the reference output voltage vector

DSP	Digital Signal Processor
MAC	The multiply and accumulate operation of DSP
MIPS	The millions of instructions per second
HIL	Hardware-In-the-loop testing
CCS	The Code Composer Studio

# Acknowledgements

In the Name of Allah, the Most Merciful, the Most Compassionate all praise be to Allah, the Lord of the worlds; and prayers and peace be upon Mohamed His servant and messenger. First and foremost, I must acknowledge my limitless thanks to Allah, the Ever-Magnificent; the Ever-Thankful, for His help and bless. I am totally sure that this work would have never become truth, without His guidance.

I would like to express my special appreciation and thanks to my supervisors Prof. Dr. Mohamed Fathy Abu-Elyazeed, Dr. Hany Mohamed Elsayed, and Dr. Sherif Ahmed Zaid, whose expertise, understanding, and patience, added considerably to my graduate experience. I appreciate their vast knowledge and skill in many areas. I would like to thank you for encouraging my research and for allowing me to grow as a research scientist. Your advice on both research as well as on my career have been priceless.

I would also like to thank my committee members, Prof. Dr. Magdi F. Mohamed and Prof. Dr. El Sayed Mostafa Saad, for the assistance they provided at all levels of the research project. I also want to thank you for letting my defense be an enjoyable moment, and for your brilliant comments and suggestions, thanks to you.

I would like to appreciate the help offered by the Electronics and Communications department staff, especially Prof. Dr. Mohamed Mostafa, Dr. Hossam A. Fahmy, and Dr. Mohsen Mahroos, and library staff, Faculty of Engineering, Cairo University.

Also, I would like to thank my friends, especially Dr. Mohamed Ibrahim, Dr. Gamal El Ghazaly, Eng. Ramez Mohamed, Eng. Nasr El-khateeb, Eng. Mohamed Sobhy, Eng. Ahmed Samir, Eng. Anas M. Thabet, Eng. Amr Noor Eldeen, Eng. Mohamed Hussein Amin, and Eng. Emad Badr El Deen, for real support during my postgraduate study and thesis works.

A special thanks to my family. Words cannot express how grateful I am to my mother, father, mother-in-law, and father-in-law for all of the sacrifices that you've made on my behalf. Your prayer for me was what sustained me thus far. I would also like to thank all of my friends who supported me in writing, and incited me to strive towards my goal. At the end I would like express appreciation to my beloved wife who spent sleepless nights with me and was always my support in the moments when there was no one to answer my queries.

# Dedication

I dedicate my dissertation work to Allah, the major source of strength and success in my life. This work is dedicated to the sake of Allah, my Creator and my Master.

I dedicate my dissertation work to my family and many friends who have supported me throughout the process. A special feeling of gratitude to my beloved wife who spent sleepless nights with me.

I also dedicate this dissertation to the leader and the President-elect Mohamed Morsy who is a symbol of freedom and national in Egypt and the free world. Finally, I dedicate my dissertation work to all those who sacrificed their lives for this country, especially Eng. Hassan Eid, Mr. Ashraf Abdel Tawab, and Mr. Sherif El Wakeel, as well as for all prisoners, especially Prof. Dr. Essam Hashish, Ahmed Abu El Maati, and Mohamed Hamdy.

# Abstract

Control systems engineering activities focus on the implementation of control systems mainly derived from mathematical modeling of systems. Many control systems are used today in large number of industrial applications. There are a lot of control strategies such as adaptive control, intelligent control, optimal control, robust control, model predictive control (MPC), and stochastic control. Model predictive control (MPC) is an advanced method of process control that has been used in the process industries since the 1980s. In recent years, it has also been used in power system balancing models. The main advantage of MPC is the fact that it allows the current timeslot to be optimized, while keeping future timeslots in account. This is achieved by optimizing a finite time-horizon, but only implementing the current timeslot. In recent years there has been a rapid increase in the use of digital controller in control systems. Digital controllers are used for achieving optimal performance in the form of maximum productivity, maximum profit, minimum cost, or minimum energy use.

The control of inverters with output LC filter has a special importance in applications where a high quality voltage is needed. The objective is implementing MPC of Three-phase inverter using DSP. The total harmonic distortion (THD) plays a major role in determining the quality of the inverter output waveform. The use of an inverter with an output LC filter allows for generation of sinusoidal voltages with low harmonic distortion. Several control schemes have been proposed for the control of three-phase inverter. This work presents a new and simple control scheme using predictive control. The controller uses a discrete-time model of the system to predict the behavior of the output voltage for all possible switching states generated by the inverter. Then, a cost function is used as a criterion for selecting the switching state that will be applied during the next sampling interval. A simple estimation of the load-current can be calculated from filter-current and output voltage. Therefore, there is no need of internal current-control loops and no modulators; the gate-drive signals are generated directly by the controller.

The simulation results under linear and nonlinear loads are presented, using Matlab/Simulink tools, verifying the feasibility and good performance of the proposed control scheme. The effects of changing the values of the system parameters are presented. The performance of the proposed predictive control method is compared with classical control methods. Moreover, this work presents the effect of considering different number of prediction steps in terms of THD and the number of cycles to reach steady state operation. Finally, the implementation of the proposed MPC is carried out on DSP kit using Hardware-In-the-Loop testing (HIL), to verify and observe the performance of the design under real-life conditions. It is observed that, the performance of the proposed MPC is very close to that in the simulation.

# Chapter 1: Introduction

Control systems engineering is the discipline that applies control theory to design systems with desired behaviors. The practice uses sensors to measure the output performance of the device being controlled and those measurements can be used to give feedback to the input actuators that can make corrections toward desired performance. When a device is designed to perform without the need of human inputs for correction it is called automatic control (such as cruise control for regulating a car's speed). Control systems engineering activities focus on implementation of control systems mainly derived by mathematical modeling of systems of a diverse range. Control system engineering is a relatively field of study that gained a significant attention during 20th century with the advancement in technology. It has an essential role in a wide range of control systems, from simple household washing machines to high-performance fighter aircraft. It seeks to understand physical systems, using mathematical modeling, in terms of inputs, outputs and various components with different behaviors; use control systems design tools to develop controllers for those systems; and implement controllers in physical systems employing available technology. A system can be mechanical, electrical, fluid, chemical, and the mathematical modeling, analysis and controller design uses control theory in one or many of the time, frequency and complex-s domains, depending on the nature of the design problem.

Many control systems are used today in a large number of industries consisting of applications from all kinds. The common factor of all control types is to sustain a desired outcome that may change during a process. There are a lot of control strategies such as adaptive control, intelligent control, optimal control, robust control, predictive control, and stochastic control. Model predictive control (MPC) is an advanced method of process control that has been used in the process industries in chemical plants and oil refineries since 1980s. In recent years it has also been used in power system balancing models [1]. MPCs rely on dynamic models of the process, most often linear models obtained by system identification. The main advantage of MPC is the fact that it allows the current timeslot to be optimized, while keeping future timeslots in account. This is achieved by optimizing a finite time-horizon, but only implementing the current timeslot. MPC has the ability to expect future events and can take control actions accordingly. PID and LQR controllers do not have this predictive ability. [2], [3].

In recent years there has been a rapid increase in the use of digital controller in control systems. Digital controls are used for achieving optimal performance - for example, in the form of maximum productivity, maximum profit, minimum cost, or minimum energy use. At the same time, the "digital revolution" or "computer revolution" is providing the means for practical implementation of these new control-system methodologies. Microprocessors, microcontrollers, and digital signal processors have become extremely powerful with minimum cost of implementation. Modern integrated circuit technology has produced the Digital Signal Processor (DSP), which offers substantial computational power at readily affordable prices. These parallel developments offer an unprecedented opportunity for practical implementation of advanced control techniques. As a result, sophisticated control-system applications using DSPs have increased exponentially in recent years. At the same time that advanced control "techniques" are being developed, engineers now have extremely effective design and synthesis techniques for digital control, plus

processors with increasing capabilities. This parallel development of complementary technologies produces an era that is truly exciting; powerful control theories can now be easily implemented into practical working applications [4]. For power systems, there has been a rapid increase in the use of digital controller in control systems.

In an ideal power system, the voltage supplied to customer equipment and the resulting load currents are perfect sine waves. In practice, however, conditions are never ideal, so these waveforms are often quite distorted, as shown in Figure 1.1 and Figure 1.2. This deviation from perfect sinusoids is usually expressed in terms of harmonic distortion of the voltage and current waveforms. Power system harmonic distortion is not a new phenomenon - efforts to limit it to acceptable proportions have been a concern of power engineers from the early days of utility systems. The distortion was typically caused by the magnetic saturation of transformers or by certain industrial loads, such as arc furnaces or arc welders. Moreover, Harmonics are caused by nonlinear loads. A load is said to be nonlinear when the current it draws does not have the same wave form as the supply voltage. The major concerns were the effects of harmonics on synchronous and induction machines, telephone interference, and power capacitor failures.

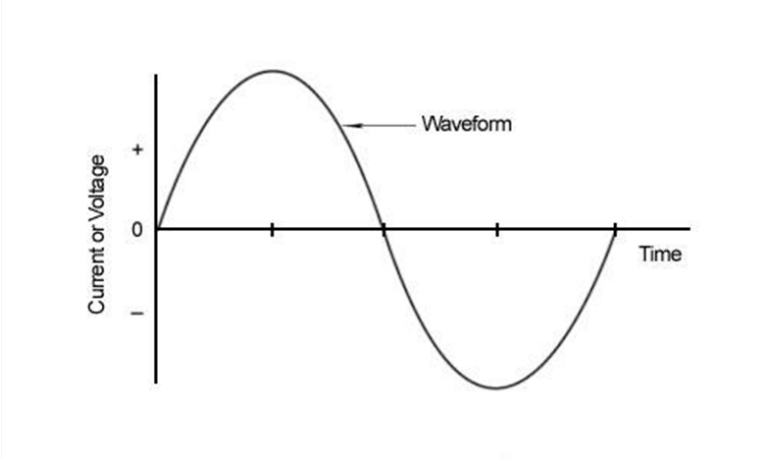


Figure 1.1: Ideal Sine wave.

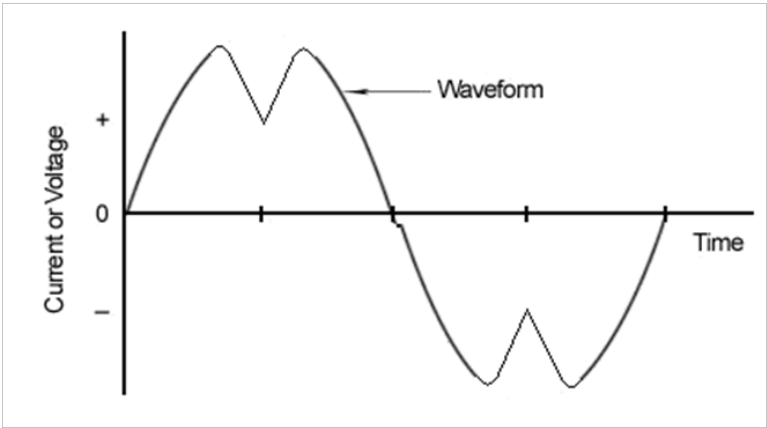


Figure 1.2: Distorted Waveform.

Distortions of the fundamental sinusoid generally occur in multiples of the fundamental frequency. Thus on a 50 Hz power system, a harmonic wave is a sinusoid having a

frequency expressed by the following formula, where  $n$  is an integer:

$$f_{\text{harmonics}} = n * 50 \text{ Hz}$$

For example, given a 50 Hz fundamental waveform, the 2nd, 3rd, 4th and 5th harmonic components will be at 100 Hz, 150 Hz, 200 Hz, and 250 Hz respectively as shown in Figure 1.3. Thus, harmonic distortion is the degree to which a waveform deviates from its pure sinusoidal values as a result of the summation of all these harmonic elements. The ideal sine wave has zero harmonic components. In that case, there is nothing to distort this perfect wave.

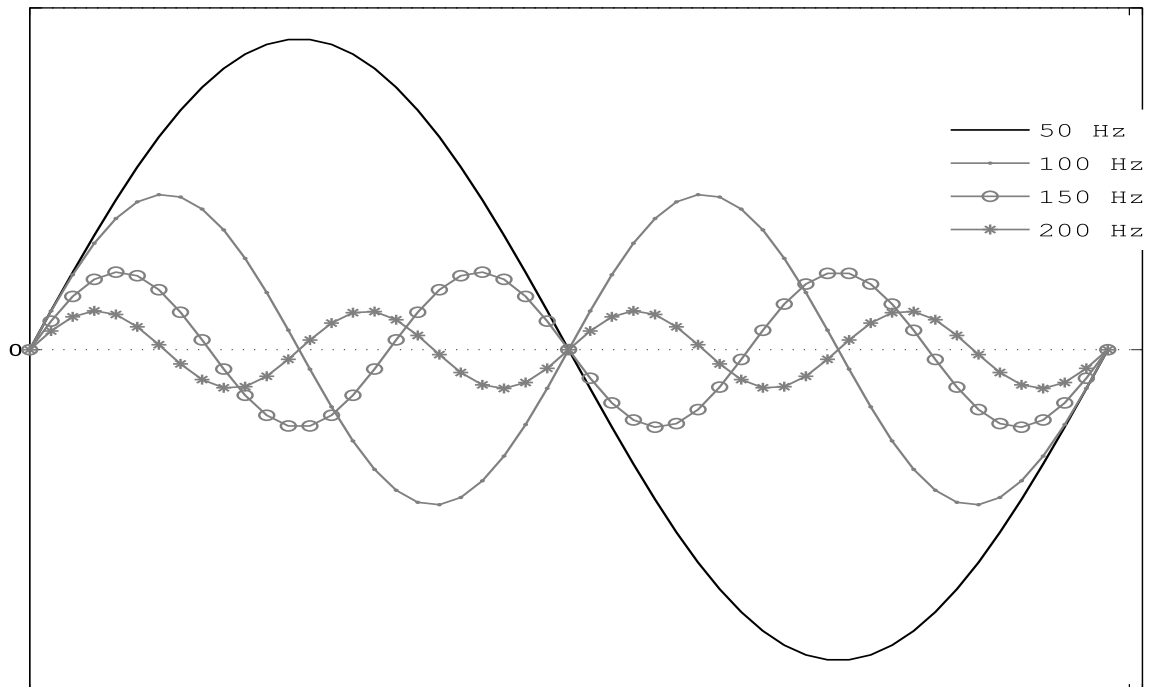


Figure 1.3: Fundamental Frequency (50 Hz) Sine Wave and Harmonics: 2nd Harmonic (100 Hz); 3rd Harmonic (150 Hz); 4th Harmonic (200 Hz).

Total Harmonic Distortion, or THD, is the summation of all harmonic components of the voltage or current waveform compared against the fundamental component of the voltage or current wave:

$$THD = \frac{\sqrt{V_2^2 + V_3^2 + V_4^2 + \dots + V_n^2}}{V_1} * 100\% \quad (1.1)$$

Because harmonic voltage distortions can affect the operation of other devices connected to the same power grid, various standards have been established to judge the severity of harmonic distortion. One of these is IEEE 519 by the American Institute of Electrical and Electronic Engineers. This standard recognizes the sensitivity of electrical equipment in a building as the limiting factor on how much voltage distortion is acceptable. IEEE 519 therefore provides limits for different types of buildings. As can be seen in Table 1.1, the limitation is more stringent in facilities likely to contain sensitive electronic

Table 1.1: IEEE 519 standards for total harmonic voltage distortion.

Application Class	THD (%)
Sensitive Applications <ul style="list-style-type: none"> <li>• Airports/Hospitals</li> <li>• Telecommunication Facilities</li> </ul>	3%
General Applications <ul style="list-style-type: none"> <li>• Office Buildings/Schools</li> </ul>	5%
Dedicated Systems <ul style="list-style-type: none"> <li>• Factories</li> </ul>	10%

equipment. To sum up, THD of voltage is usually less than 5%. Voltage THDs below 5% are widely considered to be acceptable, but values above 10% are definitely unacceptable and will cause problems for sensitive equipment and loads [5].

The use of a three phase inverter has become very popular in the recent decades for a wide range of applications. The control of a three-phase inverter is one of the most important and classical subjects in power electronics and has been extensively studied in the last decades [6]. The control of inverters with output  $LC$  filter has a special importance in applications where a high quality voltage is needed. Such applications include distributed generation, energy-storage systems, stand-alone applications based on renewable energy, and uninterruptible power supplies (UPSs) [7], [8], [9]. UPS systems provide uninterrupted, reliable, and high quality power for vital loads. In fact, they protect sensitive loads against power outages as well as overvoltage and undervoltage conditions. Applications of UPS systems include medical facilities, data storage and computer systems, emergency equipment, telecommunications, industrial processing, and on-line management systems.

In UPS systems, it is desired, to achieve a good sinusoidal output voltage regulation independent of the changes in the input voltage or in the load, linear or non-linear, balanced or unbalanced, high reliability and high efficiency. Therefore, low total harmonic distortion (THD) in the output voltage of UPS inverter under various loads and fast dynamic response are the main requirement for high-performance UPS. The output voltages of the inverter pass through the second order  $LC$  low pass filter to reduce the higher-order harmonic components and produce a nearly sinusoidal output waveform. To reduce the harmonic distortion, the  $LC$  filter is connected at the point of common coupling to the distribution system. In the other hand, the inclusion of a  $LC$  filter at the output of the inverter makes more difficult the controller design and controller parameters' adjustment [10].

Several control schemes have been proposed for this converter, including nonlinear methods (like hysteresis control), linear methods (like proportional-integral controllers using pulse-width modulation (PWM)) [6], [11], [12], deadbeat control [13], [14], [15], multiloop feedback control [16], [17], [18], adaptive control based on bank resonant filters [19], [20], and repetitive-based controllers [21]. Some tuning strategies have been presented including H-infinity control design [22]. In most of these schemes the output

voltage and one of two currents are used by a cascaded control considering outer and inner control loops, with linear or nonlinear controllers and a modulator is needed to generate the drive signals for the inverter switches [10].

Predictive control is a very wide class of controllers that have found application in the control of power converters due to its fast dynamic response [23]. It can be applied to a variety of systems, constraints and nonlinearities can be easily included, multivariable case can be considered, and the resulting controller is easy to implement. It requires a high amount of calculations, compared to a classic control scheme; however, the fast microprocessors available today make possible the implementation of predictive control. The main characteristic of predictive control is the use of the model of the system for the prediction of the future behavior of the controlled variables. This information is used by the controller in order to obtain the optimal actuation, according to a predefined optimization criterion. Several control algorithms have been presented under the name of predictive control like hysteresis-based predictive control, trajectory-based predictive control, deadbeat control, model predictive control (MPC) and MPC with finite control set, as presented in [10], [23]. The difference between these algorithms of controllers is that deadbeat control and MPC with continuous control set need a modulator, in order to generate the required voltage. This will result in having a fixed switching frequency. The other controllers directly generate the switching signals for the converter, do not need a modulator, and present a variable switching frequency.

A well-known type of predictive controller is the deadbeat controller. It has been applied for current control in three phase inverters [24], [25], active filters [26], [27], power factor preregulators [28], uninterruptible power supplies [15], [29], and dc-dc converters [30]. One of disadvantage of these deadbeat control schemes is that non-linearities and constraints of the system variables are difficult to incorporate. Another approach is the model predictive control (MPC), also known as receding-horizon control; it uses a model of the system to predict the behavior of the variables until a certain horizon of time, and a cost function is used as criterion to select the optimal future actions [23], [31], [32], [33]. MPC is a very flexible control scheme that allows the easy inclusion of system constraints and nonlinearities in the controller design stage [9]. In MPC, different formulations of the cost function are possible, considering different norms and including several variables and weighting factors [23]. It is also possible to consider different prediction horizons for improving the behavior of the system, but increasing the complexity of the system and the computational cost, as shown in [34]. In order to simplify the implementation of MPC, the converter can be modeled as a system with a finite number of switching states, and only one time step horizon can be considered for the optimization. This way, all possible switching states can be evaluated online; then, the one that minimizes the cost function is selected during the next instant.

This work mainly focused on MPC scheme for a three phase inverter with output *LC* filter and implementing the controller on eZdsp F28335 Kit. The controller uses a model of the system to predict, on each sampling interval, the behavior of the output voltage for each possible switching state. Then, a cost function is used as a criterion for selecting the switching state that will be applied during the next sampling interval. A simple estimation of the load-current can be calculated from filter-current and output voltage. Therefore, there is no need of internal current-control loops and no modulators; the gate-drive signals are generated directly by the controller.

System development testing is mainly done using two approaches. First, the performance of the system is observed and tuned using software simulation tools. Second, the design is deployed on a target platform to verify the functionality and measure the performance under more realistic conditions. This approach is also known as hardware testing. Hardware-in-the-loop (HIL) testing is a technique that is used in the development and test of complex process systems.

The simulation results under linear and nonlinear loads are presented, using Matlab/Simulink tools, verifying the feasibility and good performance of the proposed control scheme. The effect of error in system parameters values are presented. The performance of the proposed predictive control method is compared with hysteresis and pulsewidth modulation control under linear and nonlinear loads. The results show that the predictive method controls very effectively the output voltage and performs very well compared with the classical solutions. Moreover, this work presents the effect of considering different number of prediction steps in terms of THD and the number of cycles or the settling time to reach steady state operation. The simulation results for MPC with only one prediction step and the Improved MPC with two prediction steps are presented and compared. The experimental results, using HIL testing, are carried out for linear and nonlinear loads, to verify the proposed MPC using eZdsp F28335 Kit. It is observed that, the performance of the proposed MPC is very close to that in the simulation.

This thesis is organized as follows. Chapter 2 presents an overview for DSPs types, TMS320 DSP Product, digital control, benefits of DSPs for control, its typical applications, and the features of the used eZdsp F28335. Chapter 3 describes the proposed three phase inverter model, the types of filters for inverters, the benefit of  $LC$  filter in the system, and continuous and discrete-time model of the  $LC$  filter. Also, it presents a survey of the most important types of predictive control applied in power electronics and drives. Chapter 4 introduces the proposed Model Predictive Control (MPC) method, considering different prediction steps  $N$ , and two of classical control methods. Chapter 5 then combines the simulation results for linear and non-linear loads, to verify the proposed Model Predictive Control (MPC), considering one and two prediction steps, and compare its performance with classical control methods. Moreover, it presents the experimental results, using HIL testing, to verify the proposed MPC using eZdsp F28335 Kit. Finally, chapter 6 presents conclusions and future work.

# Chapter 2: DSP for Control Systems

Signal processing and control are closely related. In fact, many controllers can be viewed as a special kind of signal processor that converts an input signal and a feedback signal into a control signal. This chapter presents an overview for DSPs types, DSP families which are used in this thesis, benefits of DSPs for control, and its typical applications. Finally, the features of the used eZdsp F28335 are presented.

## 2.1 What is Digital Signal Processing?

Digital signal processing or digital signal processor (DSP) is a method of processing real world signals (represented by a sequence of numbers) using mathematical techniques to perform transformations or extract information. A digital signal is a language of 1s and 0s that can be processed by mathematics. Analog signals are real world signals that we experience everyday - sound, light, temperature, pressure, and so on. A digital signal is a numerical representation of the analog signal. It may be easier and more cost effective to process these signals in the digital world. In the real world, we can convert these signals into digital signals through our analog-to-digital conversion process, process the signals, and if needed, bring the signals back out to the analog world through the digital-to-analog converter as shown in Figure 2.1.

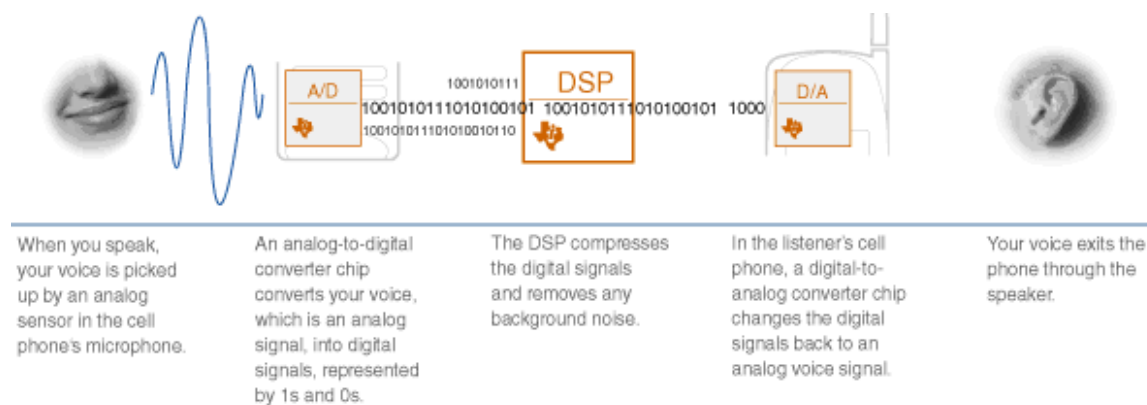


Figure 2.1: Digital signal processing logic.

The result is crystal clear sound, with no annoying echoes. That's a basic explanation of what a DSP does. It takes a digital signal and processes it to improve the signal. The improvement may be clearer sound, sharper images, or faster data [35].

## 2.2 DSPs and Microprocessors

If a universal microprocessor solution existed with which every design could be realized, the electronics industry wouldn't be a very competitive place. However, typically in most electronic designs, more than one processor technology can be used to implement the required functions. The trick is, of course, to choose the one that best delivers the

performance, size, power consumption, features, software and tools to get the job done fast - without breaking the budget. After almost two decades of development, digital signal processors continue to take the place of competitive processors. Digital signal processors are, after all, at the center of signal processing [36].

DSPs differ from microprocessors in a number of ways. A DSP is a type of microprocessor - one that is incredibly fast and powerful. The real-time capability makes a DSP perfect for applications that cannot tolerate any delays. Real-time DSP applications limited to cases where the required sampling rate is sufficiently lower than the processors instruction rate or the DSP can perform and complete its operations between two samples. Microprocessors are typically built for a range of general purpose functions, and normally run large blocks of software, such as operating systems like Windows or UNIX [37]. Although today's microprocessors, including the popular and well-known Pentium family, are extremely fast-as fast or faster than some DSPs-they are still not often called upon to perform real-time computation or signal processing. Usually, their bulk processing power is directed more at handling many tasks at once, and controlling huge amounts of memory and data, and controlling a wide variety of computer peripherals (disk drive, modem, video display, etc). However, microprocessors, such as Pentiums and Dual Core, are notorious for their size, cost, and power consumption to achieve their muscular performance, whereas DSPs are more dedicated, racing through a smaller range of functions at lightning speed, yet less costly and requiring much less space (size) and power consumption to achieve their purpose.

To sum up, some of the advantages of designing with DSPs over other microprocessors are flexibility, reliability, increased system performance, reduced system cost, and real-time performance, simulation, and emulation [4], [37].

## **2.3 Fixed–point vs. Floating–point DSPs**

The application determines the type of DSP used in order to achieve optimum performance at a low cost. Most DSPs use fixed point arithmetic, while other processors using floating-point arithmetic. Floating-point arithmetic is a more flexible and general mechanism than fixed-point. With floating-point, system designers have access to wider dynamic range (the ratio between the largest and smallest numbers that can be represented). As a result, floating-point DSP processors are generally easier to program than their fixed point, but usually are also more expensive and have higher power consumption. The increased cost and power consumption result from the more complex circuitry required within the floating-point processor, which implies a larger silicon die. The ease-of-use advantage of floating-point processors is due to the fact that in many cases the programmer doesn't have to be concerned about dynamic range and precision.

In contrast, on a fixed-point processor, programmers often must carefully scale signals at various stages of their programs to ensure adequate numeric precision with the limited dynamic range of the fixed-point processor. Most high-volume, embedded applications use fixed point processors because the priority is on low cost and, often, low power. Programmers and algorithm designers determine the dynamic range and precision needs of their application, either analytically or through simulation, and then add scaling operations into the code if necessary [35]. Figure 2.3 illustrates the primary trade-offs between fixed and floating point DSPs.

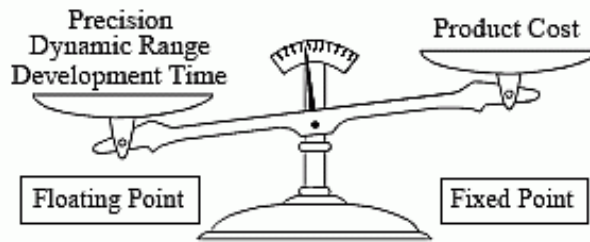


Figure 2.2: Fixed point versus floating point DSP.

For applications that have extremely demanding dynamic range and precision requirements, or where ease of development is more important than unit cost, floating-point processors have the advantage. It's possible to perform general-purpose floating point arithmetic on a fixed-point processor by using software routines that emulate the behavior of a floating point device. However, such software routines are usually very expensive in terms of processor cycles. Consequently, general-purpose floating-point emulation is seldom used. A more efficient technique to boost the numeric range of fixed-point processors is block floating point, wherein a group of numbers with different mantissas but a single, common exponent is processed as a block of data. Block floating-point is usually handled in software, although some processors have hardware features to assist in its implementation [38], [35].

## 2.4 Choosing the Processor

The right DSP processor for a job depends heavily on the application. One processor may perform well for some applications, but be a poor choice for others. With this in mind, one can consider a number of features that vary from one DSP to another in selecting a processor. These features are discussed below.

- **Arithmetic Format**- One of the most fundamental characteristics of a programmable digital signal processor is the type of native arithmetic used in the processor. Most DSPs use fixed point arithmetic, while other processors using floating-point arithmetic.
- **Data Width**- All common floating-point DSPs use a 32-bit data word. For fixed-point DSPs, the most common data word size is 16 bits.
- **Speed**- There are a number of ways to measure a processor's speed. Perhaps the most fundamental is the processor's instruction cycle time: the amount of time required to execute the fastest instruction on the processor. The reciprocal of the instruction cycle time divided by one million and multiplied by the number of instructions executed per cycle is the processor's peak instruction execution rate in millions of instructions per second, or MIPS.

Some newer DSPs allow two MACs to be specified in a single instruction, which makes MIPS-based comparisons even more misleading. One solution to these

problems is to decide on a basic operation (instead of an instruction) and use it as a yardstick when comparing processors. A common operation is the MAC operation. Unfortunately, MAC execution times provide little information to differentiate between processors: on many DSPs a MAC operation executes in a single instruction cycle, and on these DSPs the MAC time is equal to the processor's instruction cycle time.

- **Memory Organization-** The organization of a processor's memory subsystem can have a large impact on its performance. As mentioned earlier, the MAC and other DSP operations are fundamental to many signal processing algorithms. Fast MAC execution requires fetching an instruction word and two data words from memory at an effective rate of once every instruction cycle. There are a variety of ways to achieve this, including multiported memories (to permit multiple memory accesses per instruction cycle), separate instruction and data memories (the "Harvard" architecture and its derivatives), and instruction caches (to allow instructions to be fetched from cache instead of from memory, thus freeing a memory access to be used to fetch data).
- **Multiprocessor Support-** Certain computationally intensive applications with high data rates (e.g., radar and sonar) often demand multiple DSP processors. In such cases, ease of processor interconnection (in terms of time to design interprocessor communications circuitry and the cost of linking processors) and interconnection performance (in terms of communications throughput, overhead, and latency) may be important factors. Some DSP families-notably the Analog Devices ADSP-2106x-provide special-purpose hardware to ease multiprocessor system design. ADSP-2106x processors feature bidirectional data and address buses coupled with six bidirectional bus request lines. These allow up to six processors to be connected together via a common external bus with elegant bus arbitration. Moreover, a unique feature of the ADSP-2106x processor connected in this way is that each processor can access the internal memory of any other ADSP-2106x on the shared bus. Six four-bit parallel communication ports round out the ADSP-2106x's parallel processing features.
- **Power Consumption and Management-**DSPs are increasingly being used in portable applications (such as cellular phones and portable audio players) where power consumption is a major concern. As a result, many processor vendors are reducing processor supply voltages and adding power management features to give programmers greater influence over processor power consumption. Power management features available on some DSPs include:
  - **Reduced voltage operation:** Many vendors offer low-voltage (3.3-, 2.5-, or 1.8-volt) versions of their DSP processors. These processors consume far less power than five-volt equivalents at the same clock rate.
  - **Sleep or idle modes:** Most DSPs feature modes that turn off the processor's clock to all but certain sections of the processor, reducing power consumption. In some cases, any unmasked interrupt will bring the processor back from sleep mode, while in other cases, only a few designated external interrupt lines

will wake the processor. Some processors provide multiple sleep modes with different power savings and wakeup latencies.

- **Programmable clock dividers:** Some DSPs allow the processor's clock frequency to be varied under software control to use the minimum clock speed required for a particular task.
- **Peripheral control:** Some DSPs allow the programmer to disable peripherals that are not in use. Regardless of power management features, it is often difficult for design engineers to obtain meaningful power consumption figures for DSPs. This is because a DSP's power consumption may vary by as much as a factor of three depending on the instructions it executes.
- **Cost-** Obviously, processor cost is a major concern for products that are to be produced in volume. For such applications, designers try to use the lowest cost DSP that meets the requirements of the application, even though such devices may be considerably less flexible and more difficult to program than costlier processors. Among processor families, the least expensive family members tend to have significantly fewer features, less on-chip memory, and lower performance than the more expensive members [39], [40], [36], [41].

## 2.5 TMS320 DSP Product Review

Since the launch of Texas Instruments' first single-chip Digital Signal Processor (DSP) in 1982, it has provided designers an accelerated next-generation, breakthrough systems as well as complementary technology and support. DSPs are one of the most microprocessors types that are programmable and operate in real-time much faster than general-purpose microprocessors. The ability to crunch vast quantities of numbers is the value digital signal processors bring to the electronics science [42].

The TMS320 DSP family offers more extensive selection than other families, with a balance of general-purpose and application-specific processors to suit application needs. There are three distinct Instruction Set Architectures that are completely code-compatible within platforms:

### 2.5.1 Power Efficiency: TMS320C5000 DSP Platform

TMS320C5000 DSP Platform is optimized for the consumer digital market - the heart of the mobile Internet. With a roadmap to power consumption as low as 0.33mA/MHz, the TMS320C55x and TMS320C54x DSPs are optimized for personal and portable products like digital music players, GPS receivers, portable medical equipment, 3G cell phones, and digital cameras as well as MIPS-intensive voice and data applications and extremely cost effective single and multi-channel applications.

Based on the C55x DSP core, the OMAP5910 processor integrates a C55x DSP core with a ARM925 on a single chip for the optimal combination of high performance with low power consumption. This unique architecture offers a solution to both DSP and ARM developers, providing the low power real-time signal processing capabilities of a DSP coupled with the command and control functionality of an ARM. Sampling today,

the OMAP5910 is optimal for designers working with devices that require embedded applications processing in a connected environment [41].

### **2.5.2 Control Optimized: TMS320C2000 DSP Platform**

TMS320C2000 DSP Platform provides on-chip integration and computational abilities that produce unparalleled improvements in energy efficiency. For example, the TMS320C28x DSP generation is the highest-performance solution for digital control. The C28x core is a high performance control optimized controller and offers up to 150 MIPS of computational bandwidth to handle numerous sophisticated control algorithms in real-time, such as sensorless speed control, PWM, and power factor correction. It provides hardware and software tools for control applications such as Fuzzy Logic, PID controller, PWM, Clarke transformation, and other optimized blocks for control. The TMS320C24x DSP generation is the foundation for this diverse platform. This generation delivers power and control advantages that allow designers to implement advanced, cost-efficient control systems. The TMS320C2000 Platforms target industrial control such as automation and drives, optical networking, and automotive control applications [41].

### **2.5.3 Highest Performance: TMS320C6000 DSP platform**

The C6000 DSP platform optimized for highest performance and ease-of-use in high-level language programming with three device generations. It offers fastest running at clock speeds up to 1 GHz. The platform consists of the TMS320C64x and TMS320C62x fixed-point generations as well as the TMS320C67x floating-point generation. Optimal for broadband infrastructure, performance audio and imaging applications, the C6000 DSP platform's performance ranges from 1200 to 8000 MIPS for fixed-point and 600 to 1350 MFLOPS for floating point. For example, for designers of high-precision applications, C67x floating-point DSPs offer the speed, precision, power savings and dynamic range to meet a wide variety of design needs. These dynamic DSPs are the ideal solution for demanding applications like audio, medical imaging, instrumentation and automotive. The TMS Product Generations shown in Figure 2.3 [35], [41].

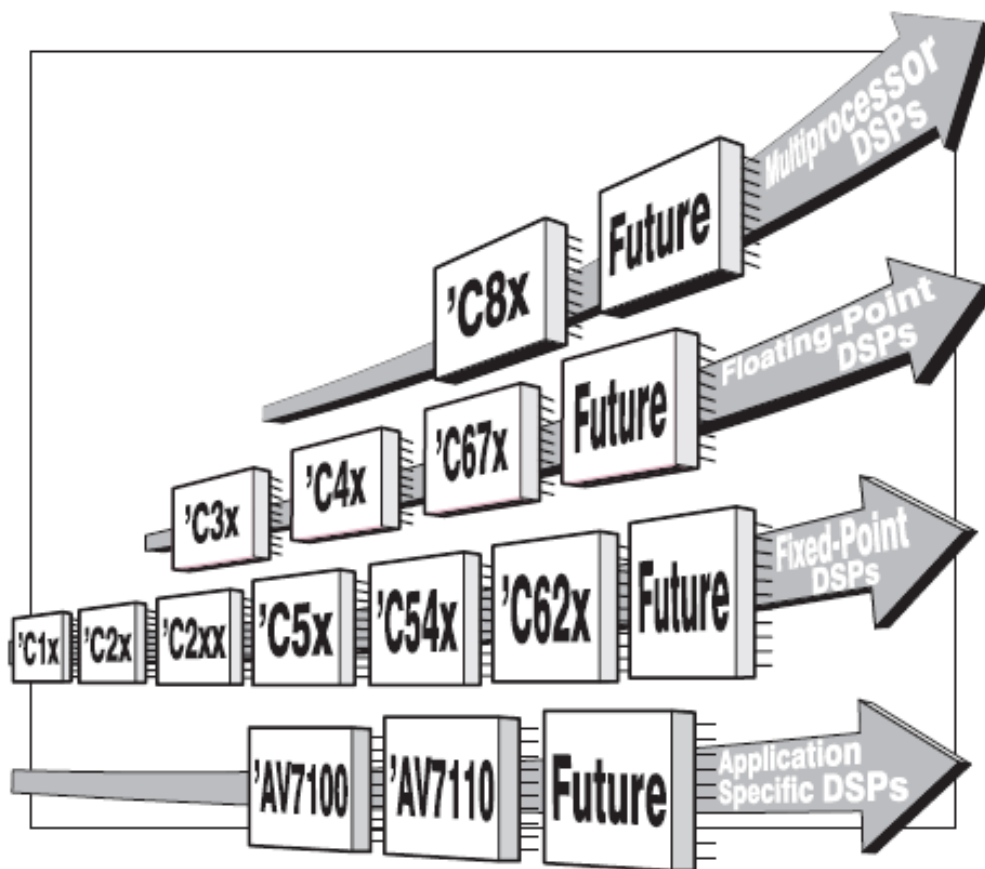


Figure 2.3: TMS Product Generation.

## 2.6 DSP for Control Systems

Control system engineers eagerly welcomed development of the digital computer. [43] Even in its early configurations, the computer was viewed as a tool that would improve system performance by overcoming the familiar limitations of analog designs: periodic adjustments to maintain performance when components change with age and/or temperature, frequent repairs (or preventative maintenance) due to reliability problems, and difficult design modifications of inflexible “hard-wired” analog implementations. In addition, analog designs are generally limited to fairly simple control techniques, since each function requires additional hardware components. On the other hand, digital computers offered great promise for control–system designers:

- Easier control of complex, multivariable, linear or nonlinear systems with feedback from many sensors.
- Easier adjustment and modification of control compensation algorithms (software changes rather than hardware modifications).
- Easier incorporation of advanced methods such as adaptation, estimation, optimization, and on-line identification.

- Improved analysis of system models/simulations and easier debugging of candidate designs.
- Shorter and more cost-effective development, design, and product manufacturing.
- Improved operational monitoring and easier maintenance.

Although digital implementations did not have the legacy of analog systems, and even though they were somewhat more difficult to analyze (in early applications), control engineers eagerly faced this challenge and developed very effective analysis and synthesis techniques. As computers became more prevalent, the promises of digital control were indeed realized in practical systems. However, the majority of these early digital applications were confined to large complex systems (chemical/petroleum processing, space flight), or to specialized applications (computer controlled machines, robots) [4].

The DSP's architecture and instruction set are optimized specifically for signal-processing-type algorithms which contain repetitive multiplications and additions or accumulations. [42] These operations dominate algorithms used in both signal processing and modem control systems, so the DSP is therefore well suited for digital control. In any event, multiplication and addition still remain as the basic operations. State variable controllers, Kalman filters, and least-square estimation are common examples of vector/matrix equations using these operations. The above mathematical examples point out the basic importance of the multiplication and addition operations in almost all digital signal processing algorithms. These same operations are likewise fundamental to control algorithms for digital filtering, convolution, prediction and estimation, auto- and cross-correlation operations that are used in different forms and shapes in linear, nonlinear, random and stochastic filtering, identification, adaptive and optimal control methods, as well as intelligent control techniques such as fuzzy logic, neural networks, and genetic algorithms that have been applied to control-system designs [36], [41], [4].

### 2.6.1 Benefits of DSPs

Although early control-system applications only used DSPs to implement digital “controller” algorithms, they are capable of much more. During the last decade as demands for increased reliability, improved efficiency, better accuracy, compactness, lower cost, and higher performance have increased, a dramatic increase in utilization of the DSPs capabilities has taken place [41], [4]. Today's DSPs have on-chip features and peripherals that are particularly useful for control systems: A/Ds, large memory blocks, 16-bit and 32-bit timers, compare modules, capture modules, PWM waveform generation, fast interrupt handling capabilities, and high-speed serial and I/O ports. As a result, control-system designers can now incorporate any/all of the control functions into a DSP solution.

- **Pulse width modulation (PWM):** Control systems, especially those using electric motors frequently control switching power converters by PWM techniques. PWM generations, and electronic commutation of DC motors, are often carried out by DSP devices. PWM eliminates D/A converters, thus reducing component counts and decreasing power dissipation and drive system size (compared to current-driven, bipolar transistor power converters). Advanced PWM methods, such as the Space Vector PWM, that require intensive calculation within a few microseconds, can

also be part of the DSP's tasks. These new methods improve the efficiency and utilization of the supply voltage and, at the same time, reduce undesired harmonics of the motor currents [4].

- **Control Laws:** DSPs allow effective real-time implementation of advanced algorithms that result in improved system control. Single- and/or multiple-axis control systems can be realized by a single DSP. Adaptive and optimal multivariable control methods, dual control, learning, neural networks, genetic algorithms, and fuzzy logic, as well as other control methodologies, are among those using the DSP's speed and performance. [44], [45], [41].
- **System identification:** In many control systems, it is necessary to estimate some system parameters and/or the system model before or during normal operation. DSP performance offers enough spare processing power that an identification process or parameter estimation may be included along with other DSP tasks [44], [45], [46].
- **Power conditioning/power supply control:** In many digital motor control systems, power supply signal conditioning and power factor correction are required. This task commonly uses PWM techniques which may be incorporated into the DSP function. PWM methods are also used for soft-switching of the power transistors/switches in order to reduce power dissipation during transient states [46], [41], [4].
- **Diagnostics and protection:** Often, a major part of the processor task in a practical control system is diagnostics and safety supervision of system operation. DSPs can also handle these responsibilities.
- **Noise control:** Control and reduction of the noise level in a control system have become more important to system designers, manufacturers, and end-users. Attenuation of acoustic noise, mechanical vibrations, signal harmonic noise, and measurement noise by active methods using advanced algorithms requires additional computational power that can be met by today's DSPs at practically no cost penalty [47], [4].
- **Other DSP tasks:** In many control systems, the DSP has been used to handle other non-control system tasks in addition to its role as the digital controller. Communication with the host computer, data filtering, and data bus control protocol (such as SCSI) are among demonstrated DSP tasks.

## 2.6.2 Typical DSP Control Applications

DSP-based control systems are already used in a broad range of applications and products from simple or low-end products to complex, high-performance or high-end products. Some of the current and possible applications include the following:

1. **Automotive** - Many control systems in automotive applications require DSPs to implement sophisticated control tasks. Electric motors and electronic controllers are replacing many hydraulic mechanisms used in automotive control, such as power steering and anti-lock brakes. Electric motor control leaves more engine horsepower for other tasks, and also provides enhanced system performance over hydraulic and mechanical control for better handling and smoother operation [41].

2. **Industrial applications** - Inexpensive and reliable AC motors such as AC-induction, brushless DC, and switched reluctance have become quite popular in motor and motion control applications that span both industrial and consumer products. Quiet and smooth operation of such nonlinear electric machines at variable speeds and high efficiency can now be achieved with low cost DSPs and power electronics for even low-end products. Examples include HVAC (heating, ventilation, and air conditioning), fans, heatpumps, compressors, motors and generators, and appliances. High-performance switching power supplies, uninterruptable power supplies (UPS), industrial drives, and power converters also benefit from DSPs. More complex systems such as manufacturing processes, industrial robots, and precision tooling machines use single and multiple fixed- and floating-point DSPs for both high-accuracy servo systems and intensive image processing [41].
3. **Office equipment** - Control of several independent Position and speed control systems today use reliable, low-cost AC motors in printers and copiers. Full automation of these products, at improved speeds, require high-performance Compact DSPs. Tape drives from low- to high-end products are another application area where multi-axis, multivariable control design is used, and reduction of sensors and mechanical/moving parts is desired [4].
4. **Active noise and active vibration control systems** - Industrial, medical, consumer, and automotive systems (such as cabin quieter, active exhaust systems, and motor vibration suppression controls), MIR systems, hearing devices, manufacturing, and construction machines are good candidates for application of active noise and vibration control. Such systems are inherently adaptive, and require real-time implementation of complex algorithms. The capability of DSPs to realize such applications has been used for these practical applications [48].
5. **Robotics** - Multiple-axis, multivariable linear and nonlinear controllers for industrial, medical, military, and space applications are candidates for DSPs. Visual and other high-performance sensors can quickly add large amounts of signal processing to an application; these may be in addition to complex control algorithms already underway. DSPs have been used as the main computational engines in a variety of robotic applications, from servo motor control to image signal processors [4], [41].
6. **Other applications** include camcorders, radar and missile control, aircraft and jet engine control, CNC and tooling machines, and seismic and geophysical instrument control.

## 2.7 Overview of the Used eZdsp F28335 Kit

The TMS320C2000 family of digital signal controllers with its performance and peripheral integration offers flash memory, ultra-fast A/D converters, and robust CAN modules and ease of use. The high-precision control DSPs are TMS320C28x and The TMS320C24x generations. They target industrial control, optical networking, and automotive control applications. The used DSP is the F28335 DSP due to the following features.

The computing unit of the F28335 DSP consists of a 32-bit CPU and a single-precision 32-bit floating-point unit(FPU), which enables the floating-point computation to be performed in hardware. Besides, the CPU of the F28335 has a 8-stage pipeline structure, which makes the CPU be able to execute eight instructions simultaneously in one system clock period. The 150MHz system clock is provided by an on-chip oscillator and a phase-locked loop(PLL) circuit. The oscillator generates a 50MHz clock signal, which is tripled to 150MHz by the PLL circuit. The F28335 applies the Harvard Bus Architecture, which means that there are independent logical memory spaces and separated memory buses for the program and the data.

The memory bus contains a program read bus, a data read bus and a data write bus. The physical memory of the F28335 comprises of a 34Kx16 single-access random-access memory(SARAM), a 256Kx16 Flash, a 8Kx16 read-only memory(ROM), a 1Kx16 one-time programmable memory(OTP) and the registers. SARAM, OTP and Flash memories are assigned and used according to the practical demands. The ROM has been pre-programmed by the DSP manufacturer. The program existing in the ROM provides a standard procedure for DSP booting as well as some optimized codes for mathematical functions. The registers control the behavior of the DSP and each peripheral module.

For the F28335, reading from or writing to registers applies the bit-field address structure. F28335 also has the feature of directmemory access(DMA). With the DMA bus, the data can be passed from one part of the DSP to the other part without the interaction of the CPU [49], which increases the data transmission speed. As it is designed mainly for industrial applications, the F28335 has plenty of peripheral circuits. For example, the 16-channel, 12-bit ADC module, the PWM module and the encoder module could be used for motor control purposes. Five kinds of communications could be achieved with by the controller area network(CAN) module, the serial communication interface(SCI) module, the serial peripheral interface(SPI), the multichannel buffered serial port(McBSP) module and the inter-integrated circuit(I2C) module. 96 interrupts are supported by F28335. These interrupts are governed by the peripheral interrupt expansion(PIE) block, which could enable or disable some interrupts, decide the interrupts' priorities and inform the CPU of the occurrence of a new interrupt. The joint test action group(JTAG) interface, which supports the real-time debugging. With the help of the JTAG, the user can watch and modify the contents of the memory and the registers without stopping the processor [35], [40], [50]. The functional block diagram for eZdsp F28335 Kit, which presents the previously mentioned features, and the board of the eZdsp TMS320F28335 Kit are shown in Figure 2.4 and Figure 2.5 [50].

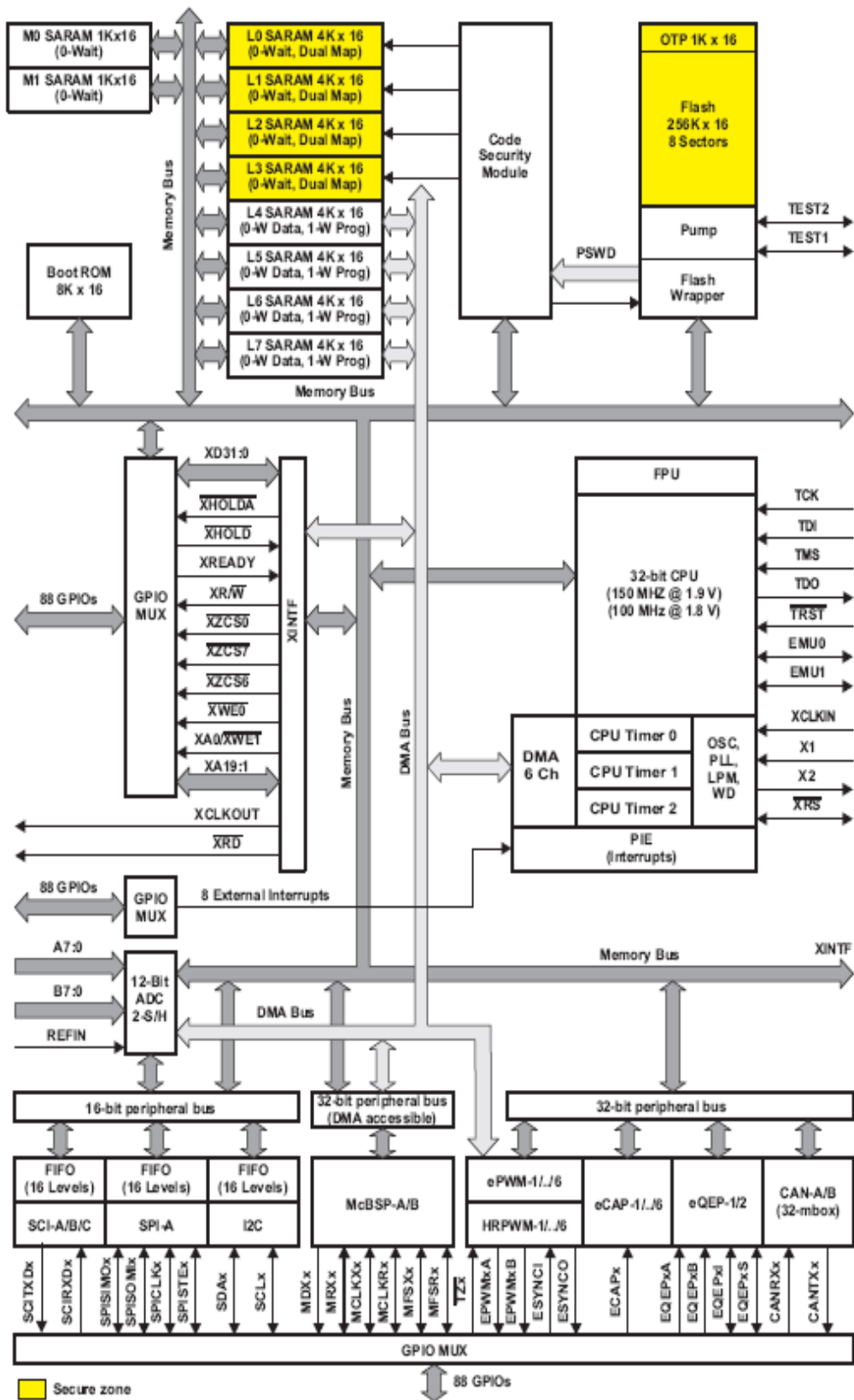


Figure 2.4: The functional block diagram for eZdsp F28335 Kit.

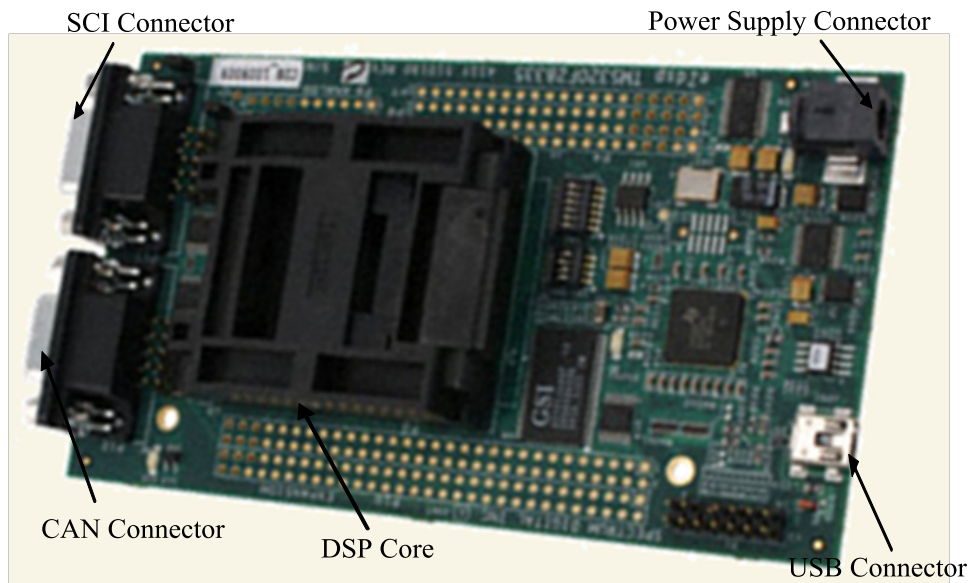


Figure 2.5: The platform picture of the eZdsp TMS320F28335 Kit.

In this work, the ezdsp F28335 Kit is used due to the following:

- One of the highest-performance solution for digital control and offers up to 150 MIPS.
- It provides hardware and software tools for control applications such as Fuzzy Logic, PID controller, PWM, Clarke transformation, and other optimized blocks for control.
- On-chip, there are 16-channel, 12-bit ADC module, PWM module, and encoder module. So, it is therefore well suited for control purposes.
- For HIL testing, it is easy to interface with Matlab/Simulink tools without using other devices for connection. The data are directly transmitted and received through serial port (SCI module).

DSP and control engineering are closely related. This chapter focused on DSPs types, TMS320 DSP Product, the relation between signal processing and control engineering, the typical control applications, and the features of the used ezdsp F28335 Kit. The next chapter will present the proposed three phase inverter with output *LC* filter and an overview of the most important types of predictive control applied in power electronics and drives.

# Chapter 3: System Model and Predictive Control Strategies

This chapter presents the three phase inverter with output  $LC$  filter, its possible switching states and corresponding voltage vectors, and the types of filters for inverters. Moreover, it presents the continuous–time model and discrete–time model of the  $LC$  filter. Finally, this chapter presents a survey of the most important types of predictive control applied in power electronics and drives.

## 3.1 The Proposed System Description

The proposed system is a three phase inverter with output  $LC$  filter which is used to convert DC to AC. This system consists of a converter, the  $LC$  filter, and the load.

### 3.1.1 The Inverter Model

The three phase inverter with output  $LC$  filter considered in this work is shown in Figure 3.1. The converter and filter models are presented here, and the load is assumed unknown.

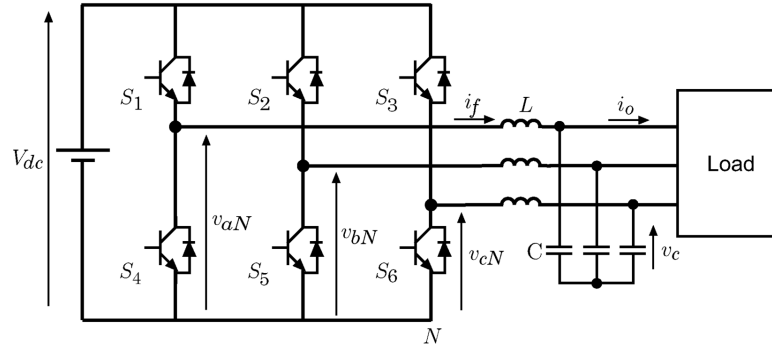


Figure 3.1: The three phase inverter with output  $LC$  filter.

The switching states of the converter are determined by the gating signals  $S_a$ ,  $S_b$ , and  $S_c$  as follows:

$$S_a = \begin{cases} 1, & \text{if } S_1 \text{ on and } S_4 \text{ off} \\ 0, & \text{if } S_1 \text{ off and } S_4 \text{ on} \end{cases} \quad (3.1)$$

$$S_b = \begin{cases} 1, & \text{if } S_2 \text{ on and } S_5 \text{ off} \\ 0, & \text{if } S_2 \text{ off and } S_5 \text{ on} \end{cases} \quad (3.2)$$

$$S_c = \begin{cases} 1, & \text{if } S_3 \text{ on and } S_6 \text{ off} \\ 0, & \text{if } S_3 \text{ off and } S_6 \text{ on} \end{cases} \quad (3.3)$$

It can be expressed in vectorial form by

$$\mathbf{S} = \frac{2}{3}(S_a + aS_b + a^2S_c) \quad (3.4)$$

where  $a = e^{j(2\pi/3)}$ .

In this work, it is assumed that the switching devices are ideal switches so the process of switching on and switching off is not taken into consideration.

The output–voltage space vectors generated by the inverter are defined by

$$v_i = \frac{2}{3}(v_{aN} + av_{bN} + a^2v_{cN}) \quad (3.5)$$

where  $v_{aN}$ ,  $v_{bN}$ , and  $v_{cN}$  are the phase voltages of the inverter, with respect to the negative terminal of the dc–link N. Then, the load voltage vector  $v_i$  can be related to the switching state vector  $S$  by

$$v_i = V_{dc}S \quad (3.6)$$

where  $V_{dc}$  is the dc–link voltage.

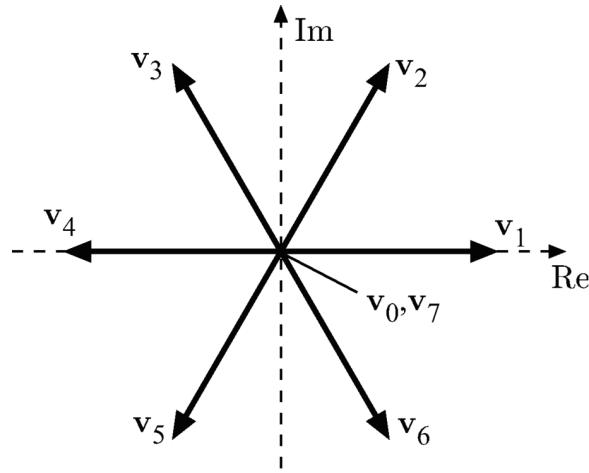


Figure 3.2: Possible voltage vectors generated by the inverter.

Considering all the possible combinations of the gating signals  $S_a$ ,  $S_b$ , and  $S_c$ , eight switching states and consequently eight voltage vectors are obtained, as shown in Table 3.1, using (3.6). Here, variables  $S_a$ ,  $S_b$ , and  $S_c$  represent the switching states of the a, b, and c legs of the inverter. Note that  $v_0 = v_7$ , resulting in only seven different voltage vectors, as shown in Figure 3.2.

Table 3.1: Possible switching states and voltage vectors for a three phase inverter

$S_a$	$S_b$	$S_c$	$v_i$
0	0	0	$v_0 = 0$
1	0	0	$v_1 = \frac{2}{3}V_{dc}$
1	1	0	$v_2 = \frac{V_{dc}}{3} + j\frac{\sqrt{3}}{3}V_{dc}$
0	1	0	$v_3 = -\frac{V_{dc}}{3} + j\frac{\sqrt{3}}{3}V_{dc}$
0	1	1	$v_4 = -\frac{2}{3}V_{dc}$
0	0	1	$v_5 = -\frac{V_{dc}}{3} - j\frac{\sqrt{3}}{3}V_{dc}$
1	0	1	$v_6 = \frac{V_{dc}}{3} - j\frac{\sqrt{3}}{3}V_{dc}$
1	1	1	$v_7 = 0$

In this work, the inverter is considered as a nonlinear discrete system with only seven different voltage vectors as possible outputs. Nevertheless, using modulation techniques like PWM, the inverter can be modeled as a continuous system.

Using vectorial notation, the filter current  $i_f$ , the output voltage  $v_c$ , and the output current  $i_o$  can be expressed as space vectors and defined as

$$i_f = \frac{2}{3}(i_{fa} + ai_{fb} + a^2i_{fc}) \quad (3.7)$$

$$v_c = \frac{2}{3}(v_{ca} + av_{cb} + a^2v_{cc}) \quad (3.8)$$

$$i_o = \frac{2}{3}(i_{oa} + ai_{ob} + a^2i_{oc}) \quad (3.9)$$

### 3.1.2 The Filter Models

This section presents an overview of the most important types of filters and the modeling of *LC* filter in continuous and discrete time domain.

#### 3.1.2.1 The Filter Types

The output filter reduces the harmonics in generated current caused by semiconductor switching. There are several types of filters. The simplest variant is filter inductor connected to the inverter's output. But also combinations with capacitors like *LC* or *LCL* can be used.

The first type is the *L* filter, as shown in Figure 3.3(a). It is the first order filter with attenuation 20 dB/decade over the whole frequency range. This filter type is suitable for converters with high switching frequency. The second type is the *LC* filter, as shown in Figure 3.3(b). It is second order filter and it has better damping behavior than *L* filter. This simple configuration is easy to design and it works mostly without problems. The second order filter provides 12 dB/octave of attenuation after the cut-off frequency [51]. Transfer function of the *LC* filter is

$$F(s) = \frac{1}{1 + s^2LC} \quad (3.10)$$

The cut-off frequency  $f_c$  of the *LC* filter can be calculated as

$$f_c = \frac{1}{2\pi\sqrt{LC}} \quad (3.11)$$

The own design of the *LC* filter is a compromise between the value of the capacity and inductance. The high capacity has positive effects on the voltage quality. On the other hand, higher inductance value is required to achieve demanded cut-off frequency of the filter therefore this filter is suitable for the proposed system. The third type is the *LCL* filter, as shown in Figure 3.3(c). The attenuation of the *LCL* filter is 60 dB/decade for frequencies above resonant frequency, therefore lower switching frequency for the converter can be used. The *LCL* filter has good current ripple attenuation even with small inductance values. However it can bring also resonances and unstable states into the system. Therefore, the filter must be designed precisely according to the parameters of the specific converter [51].

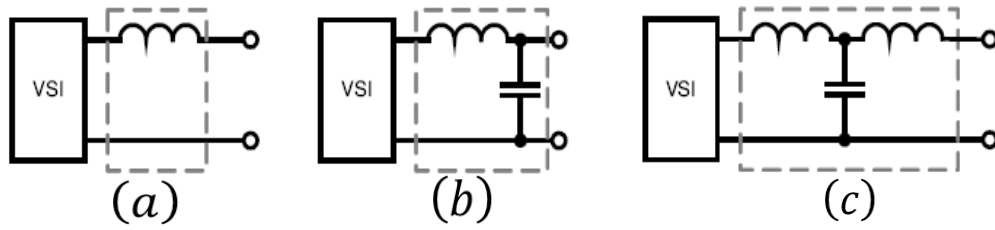


Figure 3.3: The types of filter

### 3.1.2.2 The LC Filter Model

The output voltage waveform of the inverter is generally non-sinusoidal and contains undesirable harmonics especially with non-linear loads. The use of an inverter with an output LC filter allows for generation of output sinusoidal voltages with low harmonic distortion. The LC filter in this system acts as a low pass filtering circuit which inductors block high-frequency signals and conduct low-frequency signals, while capacitors do the reverse. A filter in which the signal passes through an inductor, or in which a capacitor provides a path to ground, presents less attenuation to low-frequency signals than high-frequency signals and is therefore a low-pass filter and thereby minimizes harmonics of the output voltage. The cut-off frequency of the output LC filter of inverters limits the control bandwidth of the converter system while it attenuates voltage ripples that are caused by inverter switching activities. For a selected cut-off frequency of an output LC filter, an infinite number of L-C combinations is possible [51], [9], [52].

#### 1. Continuous-Time Model of the LC Filter

The LC filter is modeled as shown in the block diagram in Figure 3.4. This model can be described by two equations, one that describes the inductance dynamics and the other describing the capacitor dynamics.

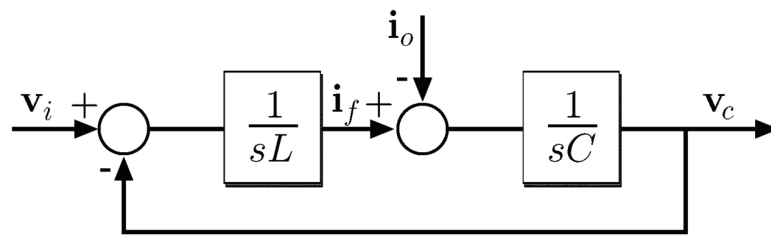


Figure 3.4: The LC filter model.

The equation of the filter inductance expressed in vectorial form is:

$$L \frac{di_f}{dt} = v_i - v_c \quad (3.12)$$

where  $L$  is the filter inductance.

The dynamic behavior of the output voltage can be expressed by the following:

$$C \frac{dv_c}{dt} = i_f - i_o \quad (3.13)$$

where  $C$  is the filter capacitance.

These equations can be rewritten as a state–space system as

$$\frac{dx}{dt} = Ax + Bv_i + B_d i_o \quad (3.14)$$

where

$$x = \begin{bmatrix} i_f \\ v_c \end{bmatrix} \quad (3.15)$$

$$A = \begin{bmatrix} 0 & -1/L \\ 1/C & 0 \end{bmatrix} \quad (3.16)$$

$$B = \begin{bmatrix} 1/L \\ 0 \end{bmatrix} \quad (3.17)$$

$$B_d = \begin{bmatrix} 0 \\ -1/C \end{bmatrix}. \quad (3.18)$$

Variables  $i_f$  and  $v_c$  are measured, while  $v_i$  can be calculated using (3.6), and  $i_o$  is considered as an unknown disturbance. In this work, the value of  $V_{dc}$  is assumed fixed and known.

The output of the system is the output voltage  $v_c$  and written as a state equation

$$v_c = [0 \quad 1] x \quad (3.19)$$

## 2. Discrete–Time Model of the LC Filter

A discrete–time model of the filter is obtained from (3.14) for a sampling time  $T_s$ , and is expressed as:

$$x(k+1) = A_q x(k) + B_q v_i(k) + B_{dq} i_o(k) \quad (3.20)$$

where

$$A_q = e^{AT_s} \quad (3.21)$$

$$B_q = \int_0^{T_s} e^{A\tau} B d\tau \quad (3.22)$$

$$B_{dq} = \int_0^{T_s} e^{A\tau} B_d d\tau \quad (3.23)$$

This model is used to calculate predictions of the output voltage  $v_c$  for a given input voltage vector  $v_i$ , and the selection of the optimal voltage vector is made using the predictive control scheme. In order to predict the output voltage  $v_c$  using (3.20), the output current  $i_o$  is needed. So it can be estimated using the following equation, obtained from (3.13):

$$i_o(k-1) = i_f(k-1) - \frac{C}{T_s} (v_c(k) - v_c(k-1)) \quad (3.24)$$

For sufficiently small sampling times  $T_s$ , it can be supposed that the output load does not change considerably in one sampling interval and, in that case, assume  $i_o(k-1) = i_o(k)$  [9], [52].

## 3.2 Overview of Predictive Control Strategies

This section presents a survey of the most important types of predictive control applied in power electronics and drives. Finally, the classification and each type of predictive control are explained.

Predictive control is a very wide class of controllers that have found rather recent application in power converters. The first ideas for predictive control methods have been published in the 1960s by Emeljanov [53]. After a rather quiet period in the next decade many predictive control algorithms, which are fundamental for drive technology, like Direct Torque Control (DTC) [54], [55] or Predictive Current Control [56] were developed in the 1980s. Further publications concerned the control of armature current of DC drives with the help of line-commutated converters [57]; however, this field of research has lost more and more of its significance. After 1990 further publications about predictive drive control appeared; some of them, like [58], show extensions and improvements of known control methods, while other authors, e.g. [59], published completely new control strategies. But at the end, in most cases, these methods turned out to be only further enhancements or combinations of already published fundamental predictive control strategies. Hence, it makes sense to point out the basic functional and fundamental principles of predictive control strategies first.

The classification for different predictive control methods is shown in Figure 3.5. The difference between these groups of controllers is that deadbeat control and MPC with continuous control set need a modulator, in order to generate the required voltage. This will result in having a fixed switching frequency. The other controllers directly generate the switching signals for the converter, do not need a modulator, and present a variable switching frequency.

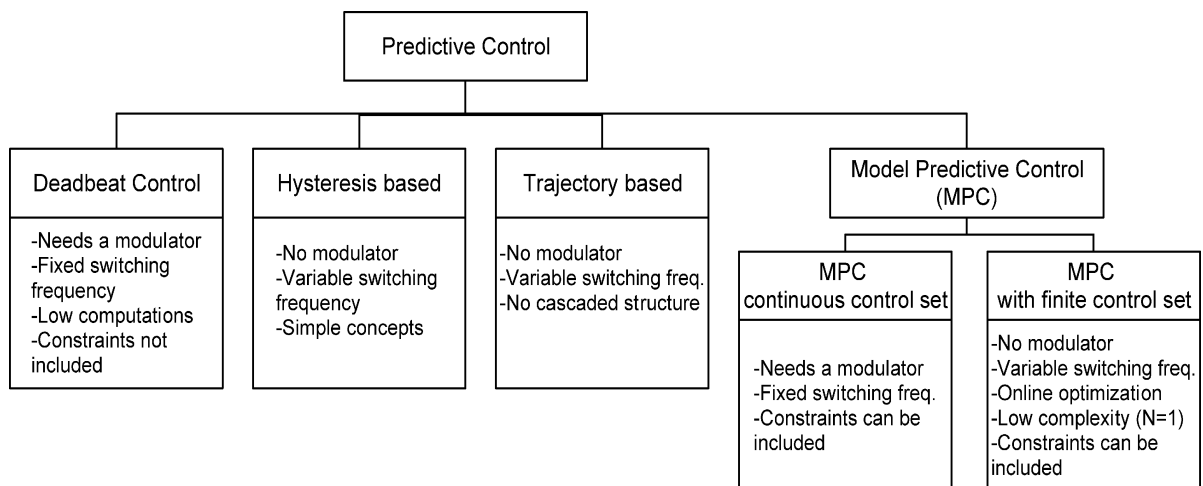


Figure 3.5: Classification of predictive control methods used in power electronics.

The main characteristic of predictive control is the use of the model of the system for the prediction of the future behavior of the controlled variables. This information is used by the controller in order to obtain the optimal actuation, according to a predefined optimization criterion. The optimization criterion in the hysteresis-based predictive control is to keep the controlled variable within the boundaries of a hysteresis area, while

in the trajectory–based, the variables are forced to follow a predefined trajectory. In deadbeat control, the optimal actuation is the one that makes the error equal to zero in the next sampling instant. A more flexible criterion is used in MPC, expressed as a cost function to be minimized.

One advantage of predictive control is that concepts are very simple and intuitive. Depending on the type of predictive control, implementation can also be simple, as with deadbeat control and finite control set MPC (FS-MPC) (particularly for a two–level converter with horizon  $N = 1$ ). However, in general, some implementations of MPC can be more complex. Variations of the basic deadbeat control, in order to make it more robust, can also become very complex and difficult to understand. Using predictive control, it is possible to avoid the cascaded structure, which is typically used in a linear control scheme, obtaining very fast transient responses. An example of this is the speed control using trajectory–based predictive control. Nonlinearities of the system can be included in the model, avoiding the need of linearizing the model for a given operating point and improving the operation of the system for all conditions. It is also possible to include restrictions to some variables when designing the controller. These advantages can be very easily implemented in some control schemes as MPC, but it is very difficult in schemes as deadbeat control.

The basic principle described above is common to all predictive control strategies; the only differences are in the functionality of the block “prediction and calculation”. Because of these differences in prediction and optimization, predictive algorithms can be classified according to different criteria, namely

- the basic functional principle
- the prediction horizon
- the inverter control

If the predictive controllers published so far are classified according to the above criteria, it can be seen that they can further be classified into different families with typical characteristics.

### **3.2.1 Classification Based on Operational Principle**

Considering the functional principles of the different predictive control algorithms, it can be seen that these can be classified into four main groups. A decision can be made between *hysteresis – based*, *trajectory – based*, *deadbeat – based* and *model – based* strategies. Indeed, these families are not clearly separated from each other and sometimes the transition between them is rather floating.

#### **3.2.1.1 Hysteresis–Based Predictive Control**

The principle of hysteresis–based predictive control strategies is to keep the controlled system variables between the boundaries of a hysteresis area or space. The most simple form of this principle is the so–called “bang-bang controller”. Although bang-bang controllers usually are not considered as predictive controllers in literature, they clearly show the characteristics of a typical predictive controller. An improved form of a bang–bang controller is the predictive current controller proposed by Holtz and Stadtfeld [56].

Using predictive current control, the switching instants are determined by suitable error boundaries. As an example, Figure 3.6 shows a circular boundary, the location of which is controlled by the current reference vector is  $i_s^*$ . When the current vector  $i_s$  is touches the boundary line, the next switching state vector is determined by prediction and optimization.

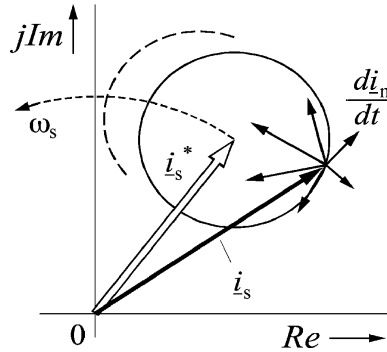


Figure 3.6: Predictive current control, boundary circle, and space vector.

The trajectories of the current vector for each possible switching state are computed, and predictions are made of the respective time intervals required to reach the error boundary again. These events also depend on the location of the error boundary, which is considered moving in the complex plane as commanded by the predicted current reference. The movement is indicated by the dotted circle in Figure 3.6. The predictions of the switching instants are based on mathematical equations of the machine. The switching state vector that produces the maximum on–time is finally selected. This corresponds to minimizing the switching frequency.

The maximum possible switching frequency is limited by the computing time of the algorithms which determines the optimal switching state vector. Higher frequencies can be handled by employing the double prediction method: Well before the boundary is reached, the actual current trajectory is predicted in order to identify the time instant at which the boundary transition is likely to occur. The back emf vector at this time instant is predicted then. It is used for the optimal selection of the future switching state vector using the earlier described procedure. A further reduction of the switching frequency, which may be needed in very high–power applications, can be achieved by defining a current error boundary of rectangular shape, having the rectangle aligned with the rotor flux vector of the machine. Using field–oriented predictive current control, the switching frequency can be reduced more than with a circular boundary area in stator coordinates [60].

Holtz and Stadtfeld optimized their predictive controller for minimum switching frequency. Since 1983, when the algorithm was published, the demand for low switching frequency has decreased. Today different optimizing criteria have more importance, e.g. low current distortion or low electromagnetic interferences (EMI). Modifications of the predictive current control are consequently under consideration.

### 3.2.1.2 Trajectory–Based Predictive Control

The principle of trajectory-based predictive control strategies is to force the system’s variables onto precalculated trajectories. Control algorithms according to this strategy are direct self control by Depenbrock [61] or direct mean torque control by Flach et al.

[62]. Some additional methods like sliding mode control [63] or direct torque control [64] are a combination of hysteresis and trajectory-based strategies, whereas Direct Speed Control (DSPC) by Mutschler [65] can be identified as a trajectory-based control system, although it also has a few hysteresis-based aspects. DSPC will be further explained as an example of trajectory-based predictive controllers. Unlike cascade controllers, predictive control algorithms offer the possibility to directly control the desired system values. Most predictive control methods published so far only deal with stator currents, torque, or flux (linear) directly; the drive speed is controlled by a superimposed control loop. DSPC, in contrast, has no control loop of this type; the switching events in the inverter are calculated in a way where speed is directly controlled in a time-optimal manner. Similar to the methods of Depenbrock [61] and Takahashi and Nogushi [55], the switching states of the inverter are classified as “torque increasing,” “slowly torque decreasing,” or “rapidly torque decreasing.” For small time intervals, the inertia of the system and the derivatives of machine and load torques are assumed as constant values. The behavior of the system leads to a set of parabolas in the speed error versus acceleration area as shown in Figure 3.7.

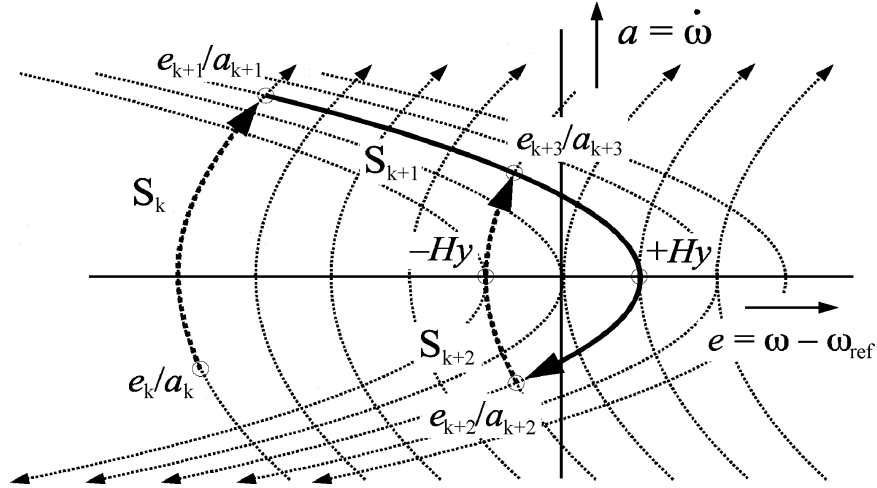


Figure 3.7: DSPC: Trajectories in the  $e/a$ -state plane.

The initial state of the system is assumed to be  $e_k/a_k$ . In this state, a torque increasing voltage vector has to be produced by the inverter, and therefore, the switching state  $S_k$  is chosen. The state now travels along the dotted parabola until the point  $e_{k+1}/a_{k+1}$  is reached. This is the intersection with another parabola for a “torque decreasing” switching state  $S_{k+1}$ , which will pass through the point “ $+H_y$ .” The intersection  $e_{k+1}/a_{k+1}$  has been precalculated as the optimal switching instant to reach the desired state point “ $+H_y$ ” as fast as possible. Therefore, in  $e_{k+1}/a_{k+1}$ , the inverter is commutated into the switching state  $S_{k+1}$ . Then, the state of the system travels along the new parabola until the point  $e_{k+2}/a_{k+2}$  is reached. At this point, the inverter is switched again into a torque increasing state  $S_{k+2}$ . The corresponding trajectory passes the point “ $-H_y$ .” In steady state, the state moves along the path  $+H_y - e_{k+2}/a_{k+2} - H_y - e_{k+3}/a_{k+3} - +H_y$ . Hence, the speed error  $e$  is kept in the hysteresis band between  $-H_y$  and  $+H_y$ . This is the hysteresis aspect of this strategy aforementioned. Of course, the optimal steady-state point would be the point of origin. Since the switching frequency of the inverter is limited, the drive state cannot be fixed to that point. Therefore, the hysteresis band is defined to keep the switching frequency in an acceptable range.

The algorithm of DSPC clearly shows the main principle of predictive control that foreknowledge of the drive system is used to precalculate the optimal switching states instead of trying to linearize the nonlinear parts of the system and then control them by PI controllers. The speed can be controlled directly without a cascade structure.

### **3.2.1.3 Deadbeat–Based Predictive Control**

A well-known type of predictive controller is the deadbeat controller. This approach uses the model of the system to calculate, once every sampling period, the required reference voltage in order to reach the reference value in the next sampling instant. Then, this voltage is applied using a modulator. It has been applied for current control in three phase inverters [60], [66], and [67], rectifiers [26], [68], active filters [69], [27], power factor correctors [70], power factor preregulators [71], [72], uninterruptible power supplies [73], [15], and [29], dc-dc converters [74], and torque control of induction machines [75]. While this method has been used when a fast dynamic response is required, being deadbeat–based, it is often fragile. Indeed, errors in the parameter values of the model, unmodeled delays and other errors in the model often deteriorate system performance and may even give rise to instability. Another disadvantage of these deadbeat control schemes is that non–linearities and constraints of the system variables are difficult to incorporate.

When implemented in a real system, several problems may appear and deteriorate the performance of a deadbeat controller. One of them is the delay introduced by calculation time and modulation. This problem has been solved in [76], [66], and [77] by considering this delay in the model. Another important issue is the sensitivity to plant uncertainties and errors in the model parameter values. This problem has been studied, and several solutions have been proposed, including the use of an adaptive self–tuning scheme [78], a predictive internal model [79], and neural networks [80]. Some results comparing the implementation of the conventional deadbeat current controller implemented in a full digital system without any compensation of the calculation delay, and the modified deadbeat controller proposed in [78].

In some applications, information about the disturbances is needed by the controller, and these include variables which are not measured. In these cases, the use of disturbance observers has been proposed [72], [15]. Other specific applications can require a modified algorithm for reduced switching frequency, as proposed in [81].

### **3.2.1.4 Model Predictive Control**

Another well-known approach of predictive control strategies is the model predictive control (MPC). MPC, also called receding horizon control, is one of the most important advanced control techniques which have been extremely successful in power applications such as inverters. The inputs of the system can be considered continuous, by using a modulator to apply the optimal voltages. This type called MPC with continuous control set, and need to a modulator, in order to generate the required voltage. This will result in having a fixed switching frequency [23].

The other MPC type called MPC with finite control set. Considering the discrete nature of power converters, it is possible to simplify the optimization problem of MPC by avoiding the use of modulators. Taking into account the finite set of possible switching states of the power converter, the optimization problem is reduced to the evaluation of

all possible states and the selection of the one which minimizes the given cost function. In addition to this, if the horizon length is set to  $N = 1$ , the calculation of the optimal actuation is very simple and easy to implement experimentally [23], [32].

Whereas there seems to be a kind of relationship between hysteresis based and trajectory based predictive control strategies, model predictive control (MPC) is founded on totally different ideas. Hysteresis and model based algorithms only use the actual system values to calculate the next switching state of the inverter. MPC uses a discrete-time model of the system to predict the behavior of the variables until a certain horizon of time. Then, a cost function is used as criterion for selecting the optimal future actions. A cost function to be minimized evaluates the error between the output predictions and the reference output. Regarding its structure it seems to have more in common with state control or predictive Kalman filters. Clarke [82] gives a good survey on model based or adaptive predictive control and its historical development. He also proposed Generalized Predictive Control (GPC) [83], [84] as one of many more model based predictive algorithms.

Differences between the various types of MPC mostly can be found in the structure of the models. Some algorithms try to include a disturbance model to improve the stability of the system. Other distinctions can be made regarding the optimizer or the on-line estimation of the model parameters. MPC here is in contrast to trajectory or hysteresis based predictive control strategies, which are especially suited for nonlinear systems. MPC is a very flexible control scheme that allows the easy inclusion of system constraints and nonlinearities in the design stage of the controller. Nevertheless some papers (e.g. [85]) show that a good performance controlling inverter supplied drives can be achieved.

### **3.2.2 Classification Based on Prediction Horizon and Control Principle**

Another classification method for predictive control algorithms based on two others criteria. The first distinctive feature is the depth of the precalculation, which is referred to as *prediction horizon*; another partition can be made according to the type of inverter control, the control principle: While some predictive controllers immediately calculate optimum inverter switching states, i.e. they control the inverter directly. Other strategies determine a value-continuous control signal which must be synthesized by a modulator before it is passed on to the inverter.

Most of the control schemes which have been investigated in drive technology so far have a prediction horizon of only one single sampling cycle. Well known examples with modulator are e.g. Direct Current Control of Induction Motor currents by Mayer/Pfaff [86] or Direct Flux Control proposed by Asher et al. [87]. Nevertheless, the biggest part of the one-step predictive controllers belongs to the group of the predictive schemes with direct inverter control, among them such prominent ones like Direct Torque Control [54], [55] and its derivatives as well as Direct Self Control [88] and Direct Speed Control [89].

Predictive control strategies with a prediction horizon of more than one sampling cycle are exclusively model-based predictive controllers. Thus, they are also referred to as *Long-Range Predictive Control*, abbreviated as *LRPC*. The only scheme of this kind used for drive control as far is Generalized Predictive Control [83], [84]. Its suitability for drive applications has been investigated by Kennel, Linder and Linke in 2001, the results have been published in [90]. Predictive control schemes with a prediction horizon

of more than one sampling cycle and with direct inverter control have not been used for drive control so far. This can, to some extent, be justified by the fact that the whole topic of hybrid systems, which is closely related to these control strategies, is a quite new field of research.

This chapter has provided an overview of the proposed system. The converter and filter models are presented. Moreover, the overview of the most important types of predictive control strategies applied in power electronics and drives are introduced in this chapter. The proposed Model Predictive Control (MPC) considering different prediction steps and the comparison with classical control methods will be explained in the next chapter.

# Chapter 4: The Proposed MPC

This chapter mainly focuses on the proposed Model Predictive Control (MPC) considering a one prediction step  $N = 1$  and two prediction steps  $N = 2$ . Then, a cost function which is used to minimize the error between the output voltage predictions and the reference voltage is presented. Moreover, the proposed predictive control method is compared with hysteresis and PWM control under linear and nonlinear loads. Finally, the detailed inverter system simulation model of each controller is presented.

## 4.1 Model Predictive Control

Another approach of predictive control strategies is the model predictive control (MPC). MPC, also referred to as *receding horizon control*, is the only one among the so-called advanced control techniques which has been extremely successful in practical applications in recent decades, exerting a great influence on research and development directions of industrial control systems. Applications and theoretical results abound; see, e.g., the books [2], [3], and [91] and survey papers [92], [93], [94], and [31]. An attractive feature of MPC is that it can handle general constrained nonlinear systems with multiple inputs and outputs in a unified and clear manner.

It uses a model of the system to predict the behavior of the variables until a certain horizon of time, and a cost function is used as criterion to select the optimal future actions [23], [31], [32], [95], and [33]. MPC is a very flexible control scheme that allows the easy inclusion of system constraints and nonlinearities in the design stage of the controller [10], [23]. In MPC, different formulations of the cost function are possible, considering different norms and including several variables and weighting factors [23]. It is also possible to consider different prediction horizons, as shown in [34]. The inputs of the system can be considered continuous, by using a modulator to apply the optimal voltages, as presented in [31] and [96]. In order to simplify the implementation of MPC, the converter can be modeled as a system with a finite number of switching states, and only one time step horizon can be considered, as presented for a three phase inverter in [6] and [97], an active front-end rectifier in [98], and a multilevel inverter in [99]. All possible switching states can be evaluated online. Then, the one that minimizes the cost function is selected.

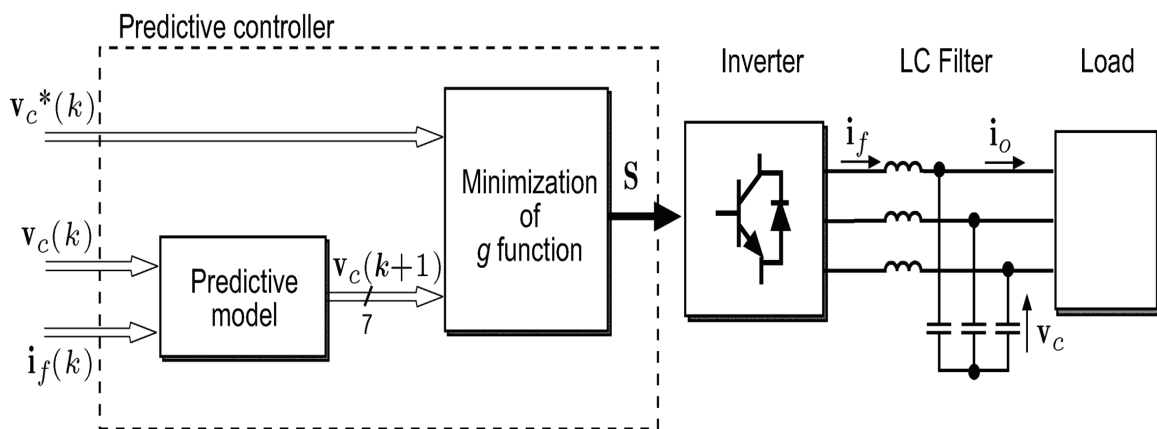


Figure 4.1: The block diagram of MPC with only one prediction step.

The block diagram of the model predictive control (MPC) for a three phase inverter with output  $LC$  filter, considering a one prediction step  $N = 1$ , is shown in Figure 4.1. The control cycle of MPC at sampling time  $k$  is described step by step as follows:

1. Obtain (measure) the value of the output voltage  $v_c(k)$  and the filter current  $i_f(k)$  at sampling time  $k$ .
2. Predict the value of the output voltage at the next sampling instant  $v_c(k+1)$  for all the possible voltage vectors that the inverter generates, as shown in Table 3.1, using (3.20).
3. Estimate the (unmeasured) output current  $i_o(k)$  using (3.13) to obtain the prediction  $v_c(k+1)$  using (3.20).
4. The seven predictions obtained for  $v_c(k+1)$  are compared using a cost function  $g_1$ , as shown in (4.2).
5. The voltage vector  $v_i$  that minimizes this function is then chosen and its corresponding switching state is applied at the next sampling instant.
6. Wait until sampling time  $k+1$  and turn back to step 1..

The simulation model of the voltage vector  $v_i$ , the filter current  $i_f$ , the output voltage  $v_c$ , and the output current  $i_o$ , according to (3.5), (3.7), (3.8), and (3.9), are shown in Figure 4.2, Figure 4.3, Figure 4.4, and Figure 4.5, respectively. The output voltage reference  $v_c^*$  can be expressed as space vector using the same previous method and implemented as shown in Figure 4.6. The detailed inverter system simulation model, for linear and nonlinear loads, using MPC with only one prediction step is shown in Figure 4.7.

The proposed predictive control algorithm is detailed in Figure 4.8 as a flow diagram. As shown in the diagram, the minimization of the cost function can be implemented as a **for** cycle predicting for each voltage vector, evaluating the cost function, and storing the minimum value and the index value of the corresponding switching state which generate the corresponding gate signals for the IGBTs. This control strategy can be summarized in the following steps.

- Define a cost function  $g$ .
- Build a model of the converter and its possible switching states.
- Build a model of the load for prediction.

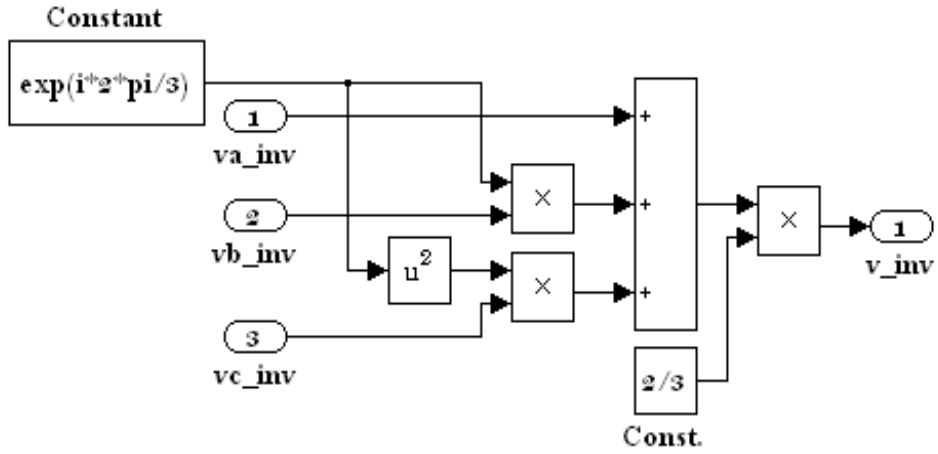


Figure 4.2: The simulation model of the voltage vector  $v_i$ .

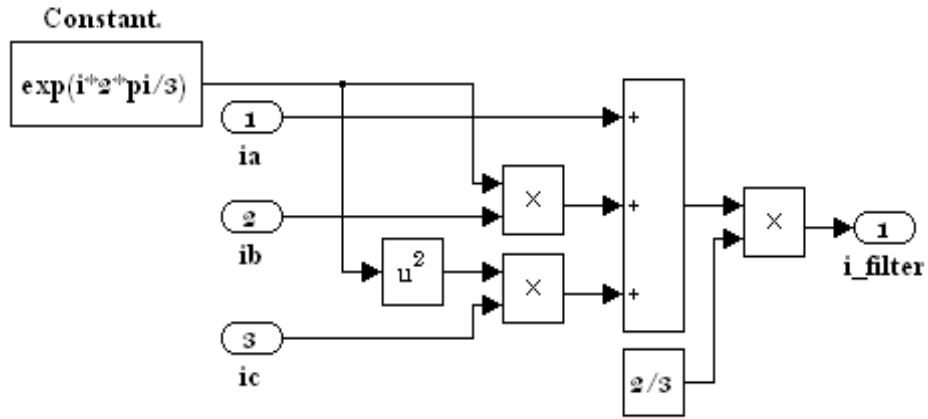


Figure 4.3: The simulation model of the filter current  $i_f$ .

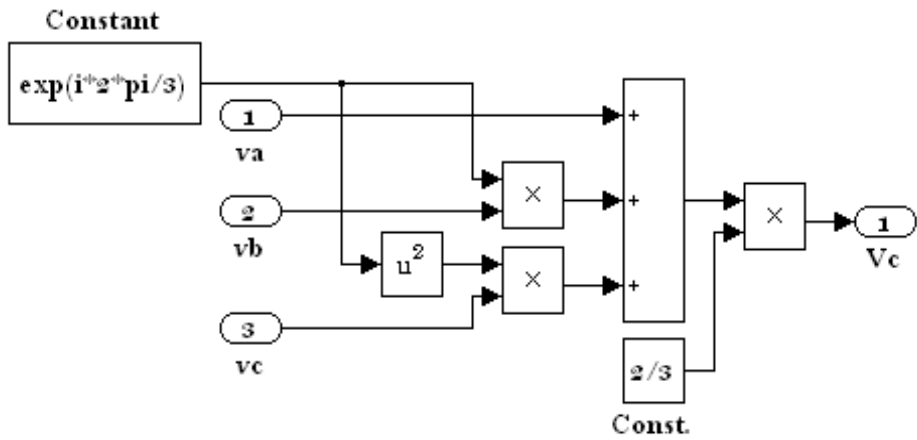


Figure 4.4: The simulation model of the output voltage  $v_c$ .

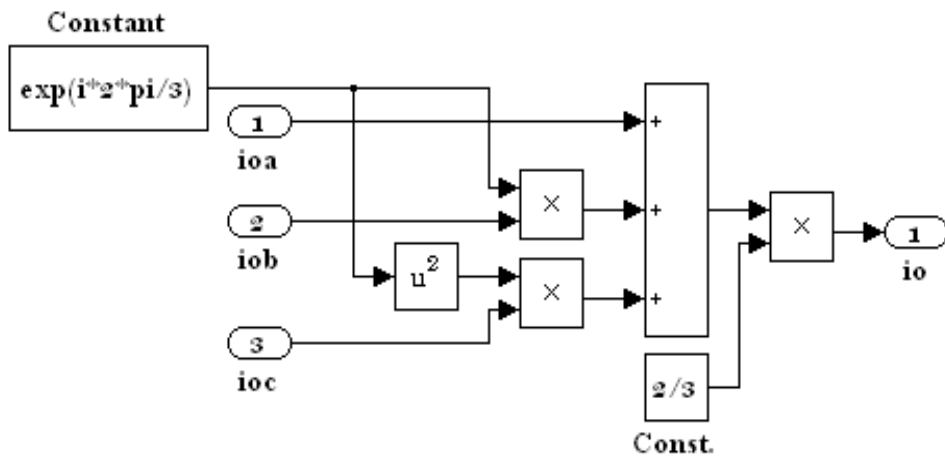


Figure 4.5: The simulation model of the output current  $i_o$ .

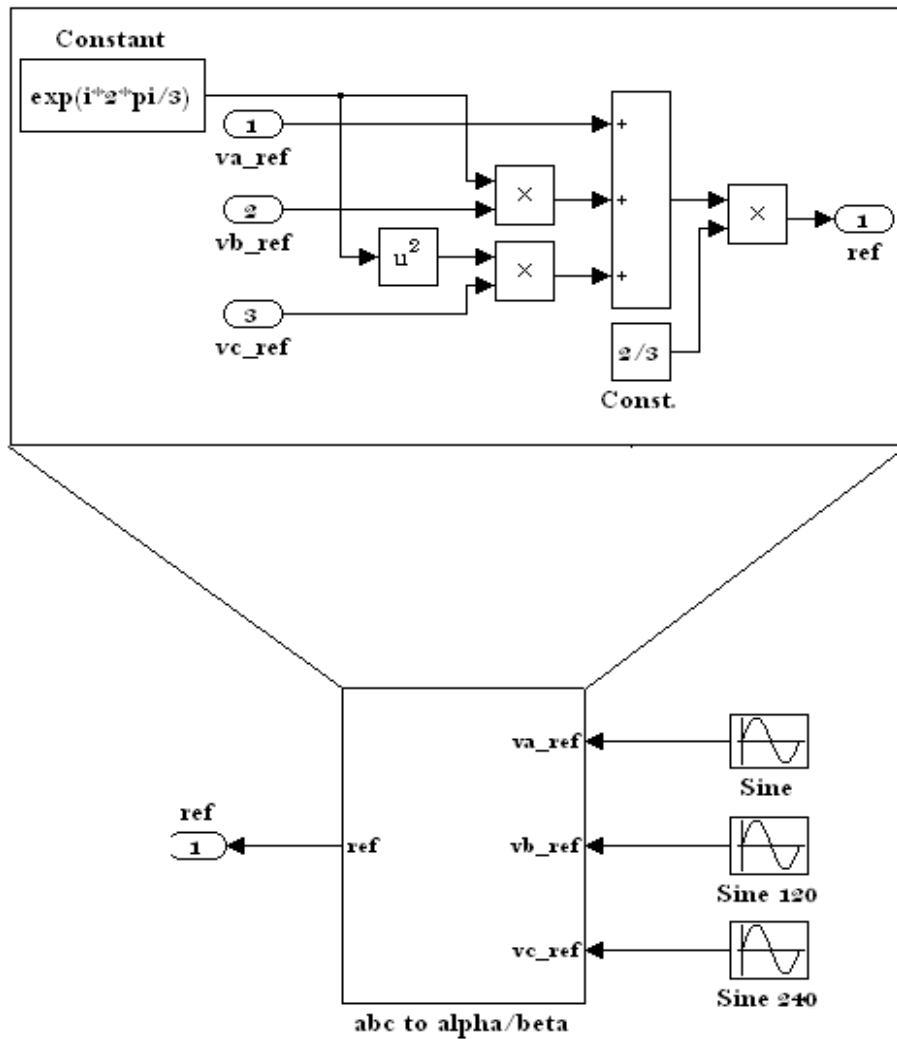


Figure 4.6: The simulation model of the output voltage reference  $v_c^*$ .

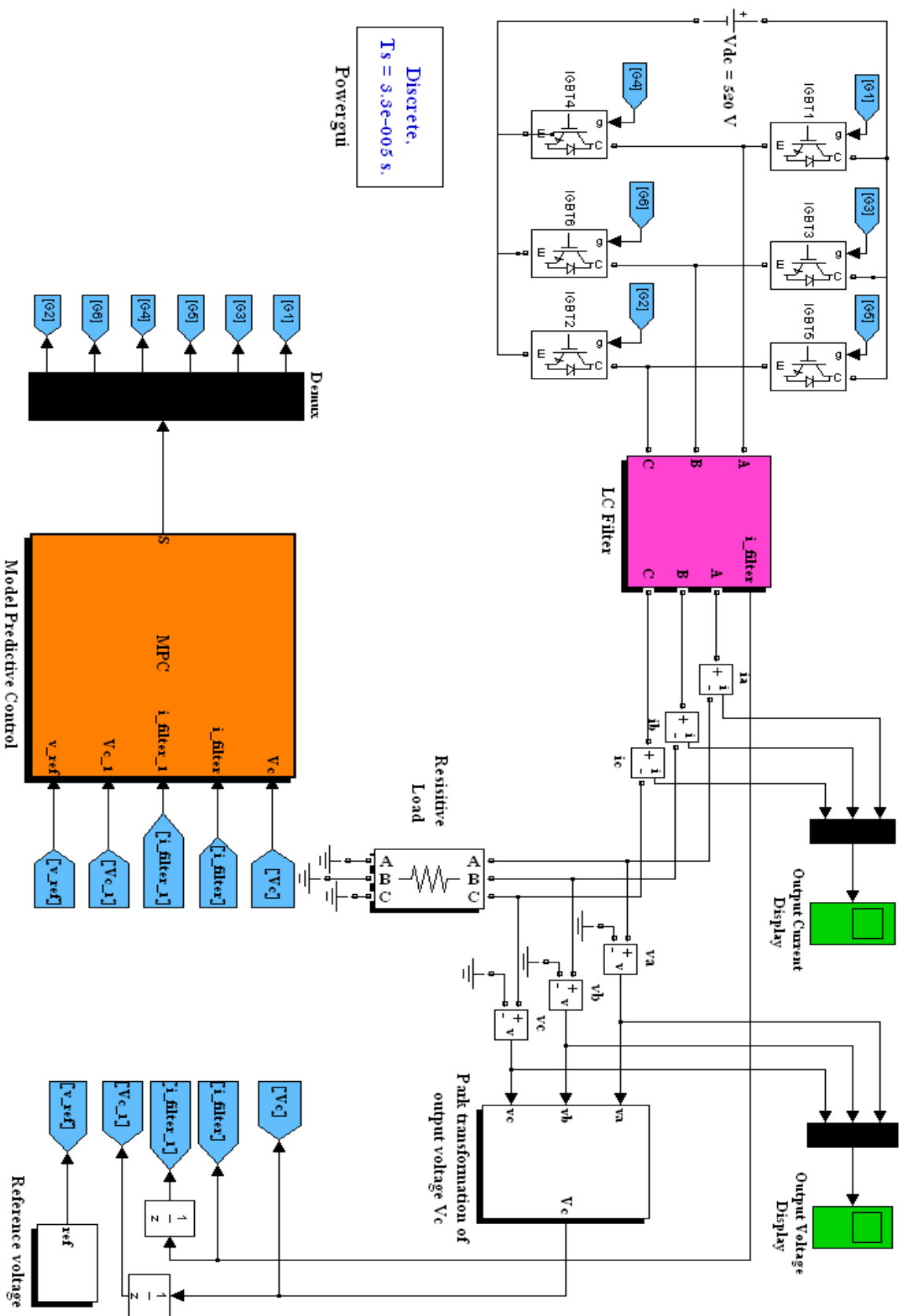


Figure 4.7: The inverter system simulation model using MPC with one prediction step.

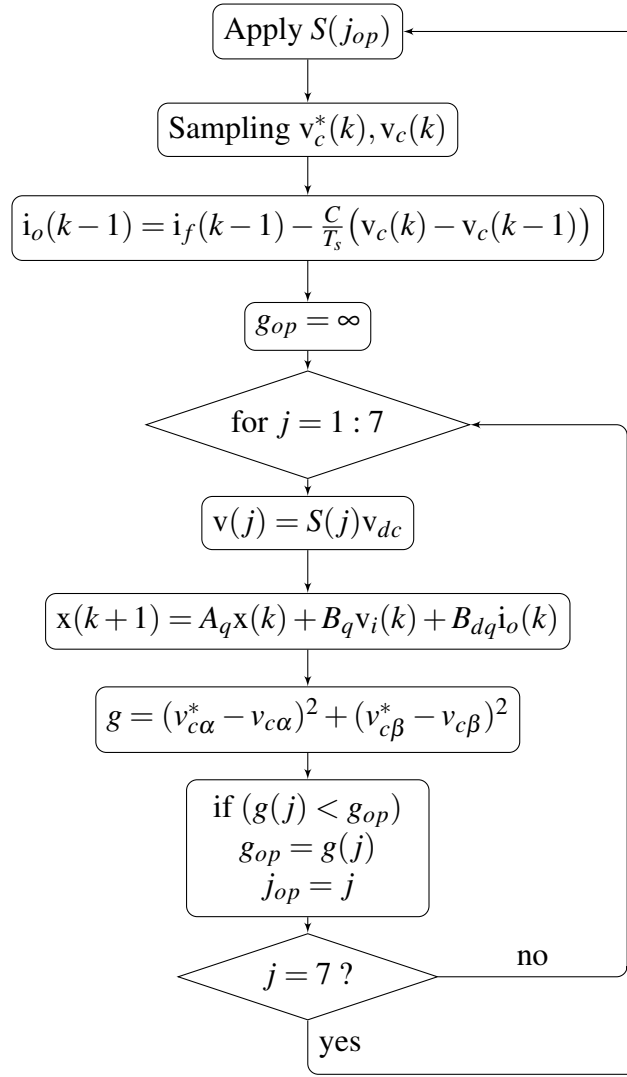


Figure 4.8: The flow chart of the proposed predictive control algorithm.

## 4.2 Improved Model Predictive Control

It is possible to consider different prediction horizons for improving the behavior of the system, but increasing the complexity of the system and the computational cost. When a horizon length  $N$  is used, the number of possible input sequences, considering the possible switching states of the converter, can be quite large. Then, the idea of predicting the behavior of the system for all possible switching state sequences becomes difficult to apply in a real system. A simple solution is the use of  $N = 1$ , reducing the number of calculations to the number of possible switching states of the converter. However, it is also possible to consider different prediction horizons for improving the behavior of the system, but increasing the complexity of the system and the computational cost.

When two steps are considered for prediction, two cases are considered for voltage vectors. First case, one voltage vector is applied during the first sampling period and another voltage vector is applied during the second sampling period. In this case, 49 sequences of two voltage vectors are possible. A total of  $7^N$  possible sequences must be evaluated for  $N$  steps. This requires a high amount of calculations, which can make the

experimental implementation of the algorithm very difficult. Second case, the same voltage vector is applied during two sampling periods to reduce the number of calculations. This approach simplifies the algorithm. It can be observed that in both cases the performance is very similar and considerably better than the case of one step prediction, as presented in [100]. So, in this work the second case is considered.

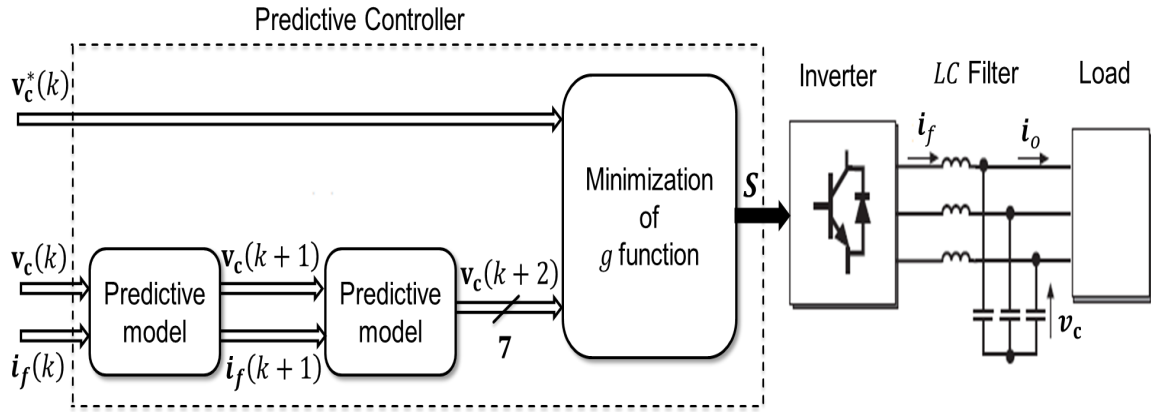


Figure 4.9: The block diagram of the Improved MPC with two prediction steps.

The block diagram of the Improved MPC for a three phase inverter with output  $LC$  filter, considering two prediction steps  $N = 2$ , is shown in Figure 4.9. The control cycle of the improved MPC at sampling time  $k$  is described step by step as follows:

1. Obtain (measure) the value of the output voltage  $v_c(k)$  and the filter current  $i_f(k)$  at sampling time  $k$ .
2. Predict the value of the output voltage and the filter current at the next sampling instant using (3.20),  $v_c(k+1)$  and  $i_f(k+1)$ , considering the voltage that the converter is applying during the present sampling interval.
3. The value of the output voltage  $v_c(k+2)$  is predicted for all the possible voltage vectors that the inverter generates using the values,  $v_c(k+1)$  and  $i_f(k+1)$ , predicted for  $k+1$ .
4. The seven predictions obtained for  $v_c(k+2)$  are compared using a cost function  $g_2$ , as shown in (4.3).
5. The voltage vector  $v_i$  that minimizes this function is then chosen and its corresponding switching state is applied at the next sampling instant  $k+1$ .
6. The output current,  $i_o(k+1)$ , value used for predictions  $k+2$  is estimated using (3.13). Here, in this work the present value of output current  $i_o(k)$  is measured and fed to predict the value of the output voltage and the filter current,  $v_c(k+1)$  and  $i_f(k+1)$ , at the next sampling instant,  $k+1$ , using (3.20).
7. Wait until sampling time  $k+1$  and turn back to step 1..

Here, the inverter applies a voltage vector during a whole sampling period. The proposed predictive control calculates predictions until time  $k + 2$  based on measurements made at time  $k$  and considering that the new voltage vector will be applied in  $k + 1$ . The detailed inverter system simulation model, for linear and nonlinear loads, using Improved MPC is shown in Figure 4.10.

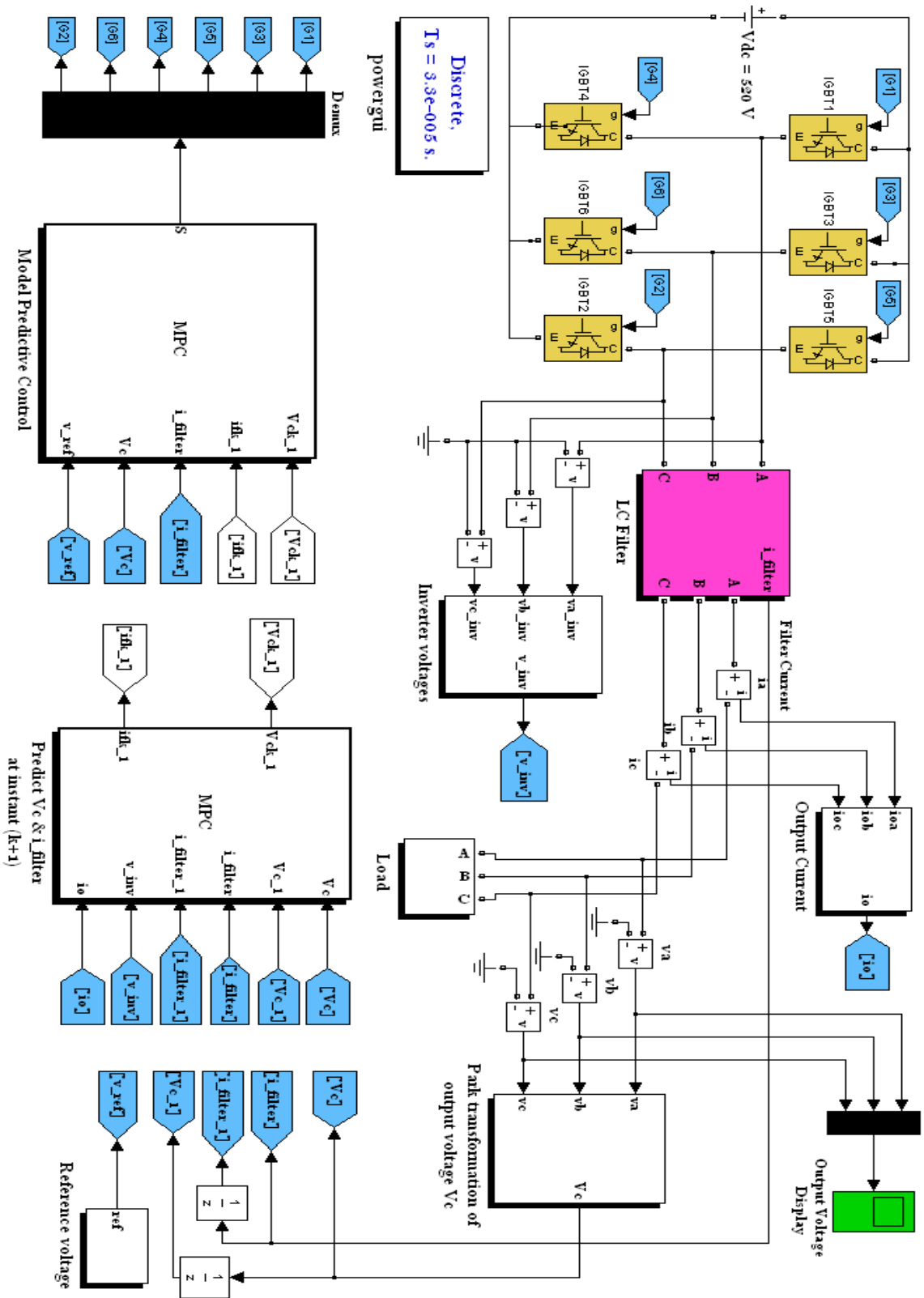


Figure 4.10: The inverter system simulation model using Improved MPC.

### 4.3 The Cost Function

In MPC, at each time instant  $k$  and for a given (measured or estimated) plant state  $x(k)$ , a cost function over a finite horizon of length  $N$  is minimized. A cost function to be minimized evaluates the error between the output voltage predictions and the reference voltage. In this work, a cost function  $g_N$  expressed in orthogonal coordinates and defines the desired behavior of the system: To minimize the error in the output voltage

$$g_N = (v_{c\alpha}^* - v_{c\alpha}(k+N))^2 + (v_{c\beta}^* - v_{c\beta}(k+N))^2 \quad (4.1)$$

where  $v_{c\alpha}^*$  and  $v_{c\beta}^*$  are the real and imaginary parts of the output voltage reference vector  $v_c^*$ , while  $v_{c\alpha}$  and  $v_{c\beta}$  are the real and imaginary parts of the predicted output-voltage vector  $v_c(k+N)$ . This cost function is evaluated for each one of the seven voltage vectors generated by the inverter. In this work, the voltage reference is kept constant until time  $k+N$  and equal to  $v_c^*(k)$ .

For a MPC with only one step prediction  $N = 1$ , it considers the following cost function

$$g_1 = (v_{c\alpha}^* - v_{c\alpha}(k+1))^2 + (v_{c\beta}^* - v_{c\beta}(k+1))^2 \quad (4.2)$$

While for the Improved MPC with two steps prediction  $N = 2$ , it considers the following cost function

$$g_2 = (v_{c\alpha}^* - v_{c\alpha}(k+2))^2 + (v_{c\beta}^* - v_{c\beta}(k+2))^2 \quad (4.3)$$

### 4.4 Classical Control Methods

Several control schemes have been proposed for this converter, including nonlinear methods (like hysteresis control), linear methods (like proportional-integral controllers using pulse-width modulation (PWM)), deadbeat control, multiloop feedback control and repetitive-based controllers. In this work, two types of classical control methods are considered and compared with the proposed predictive control.

#### 4.4.1 Hysteresis Voltage Control

In this control strategy, shown in Figure 4.11, the measured output voltage  $v_c$  is compared with the output voltage reference  $v_c^*$  using hysteresis comparators. The  $abc/\alpha\beta$  transformation provides best performance with the lower number of calculations. Then, the transformation  $\alpha\beta/abc$  is occurred to generate the output error voltages, using (4.4). The output error voltages of each comparator determines the switching state of the corresponding inverter leg ( $S_a$ ,  $S_b$ , and  $S_c$ ) such that the output voltages are forced to remain within the hysteresis band  $H$ .

$$v_{abc} = \frac{3}{2} \begin{bmatrix} \frac{2}{3} & 0 \\ -\frac{1}{3} & \frac{\sqrt{3}}{3} \\ -\frac{1}{3} & -\frac{\sqrt{3}}{3} \end{bmatrix} \begin{bmatrix} v_\alpha \\ v_\beta \end{bmatrix} \quad (4.4)$$

The advantage of this controller lies on its simplicity and the implementation does not require complex circuits or processors. The performance of the hysteresis controller is good, with a fast dynamic response. On the other hand, the disadvantage is that the

switching frequency changes during fundamental period according to variations of the load parameters and operating conditions, resulting in irregular operation of the inverter and can cause resonance problems [9], [52]. As a result the switching losses are increased. Various strategies have been proposed in the literature to control or minimize the switching frequency variation [101].

The simulation model of the transformation  $\alpha\beta/abc$  according to (4.4) is shown in Figure 4.12. The detailed inverter system simulation model for linear and non-linear loads using hysteresis voltage control is shown in Figure 4.13.

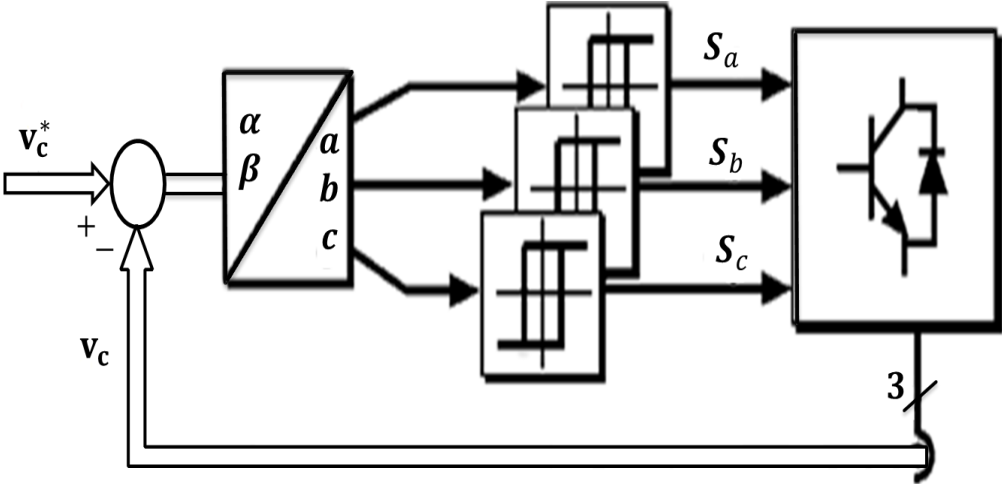


Figure 4.11: The block diagram of hysteresis voltage control.

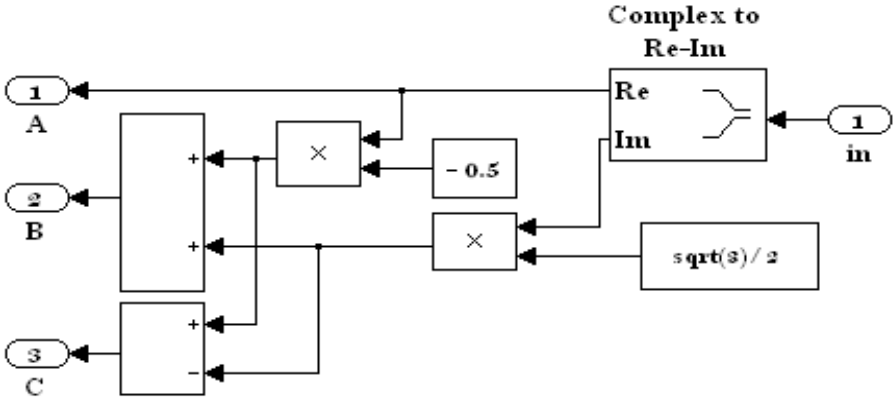


Figure 4.12: The simulation model of the transformation  $\alpha\beta/abc$ .

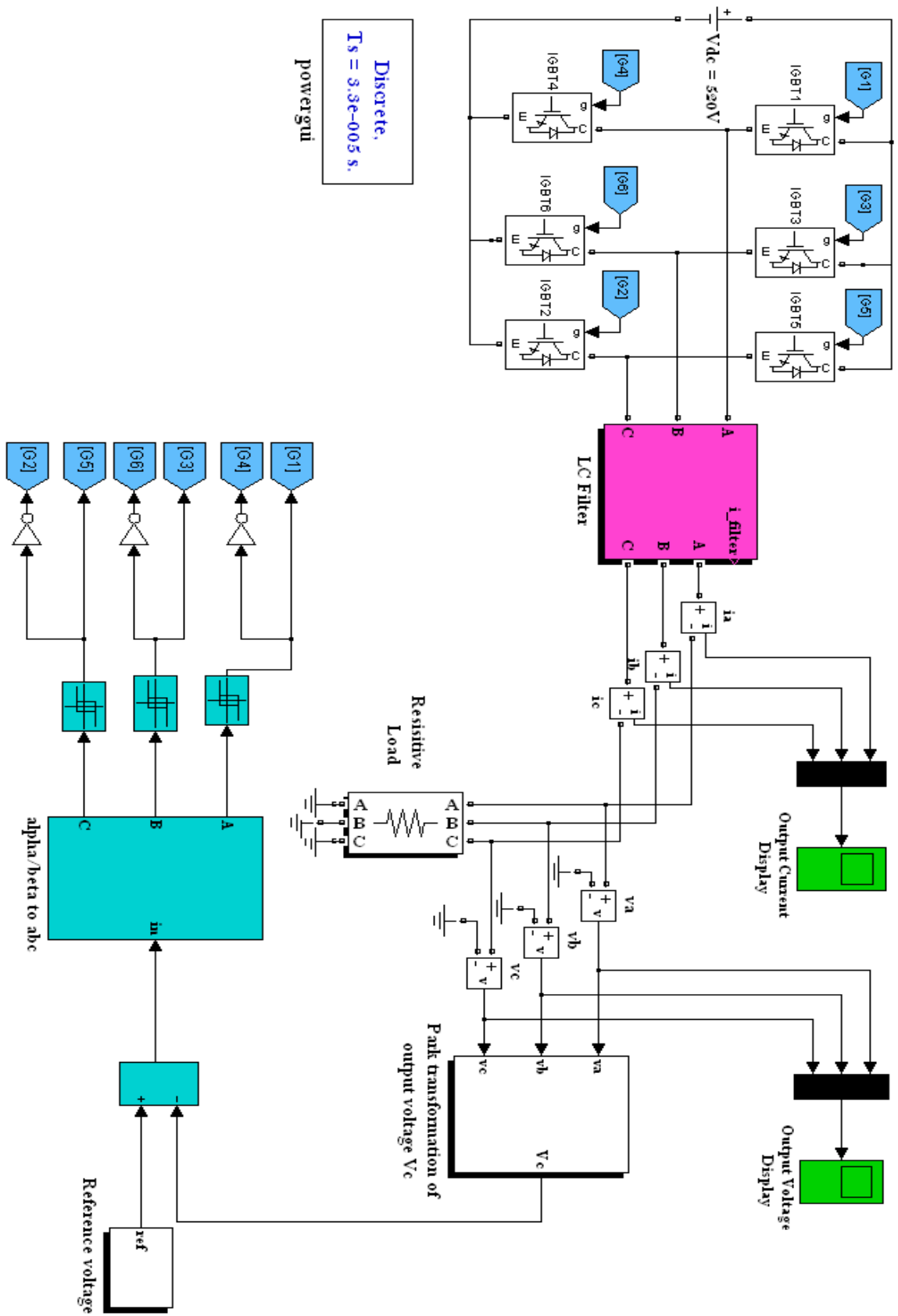


Figure 4.13: The inverter system simulation model using hysteresis voltage control.

## 4.4.2 Linear Voltage Control with PWM

In this control strategy, shown in Figure 4.14, the reference output voltage  $v_c^*$  is compared with the measured output voltage  $v_c$ . This process generates the error voltages, which are fed to the PI controllers for the output voltage regulation. The PI controller minimizes the rise time and the steady-state error of the inverter output voltage for keeping the output voltage as close as possible to the reference voltage. A modulator is needed to generate the drive signals for the inverter switches. The reference load voltages are compared with a triangular carrier signal, and the output of each comparator is used to drive an inverter leg.

The performance of this control scheme depends on the design of the controller parameters, and on the frequency of the reference output voltage. Although the PI controller assures zero steady-state error for continuous reference, it can present such an error for sinusoidal references. This error increases with the frequency of the reference output voltage and may become unacceptable for certain applications.

The detailed inverter system simulation model for linear and non-linear loads using PWM voltage control is shown in Figure 4.15. Note that, the PI controller block does not accept complex numbers. So, it is separated to **PI\_alpha** and **PI\_beta**, as shown in the same figure.

Several control schemes have been proposed for this inverter system. This chapter presented the proposed MPC and some of classical control methods used to control the inverter system. The advantages and disadvantages, and the simulation model of each control method are provided. The simulation results for the previous control methods under linear and non-linear loads are presented in the next chapter to verify the proposed MPC and compare its performance with another control methods.

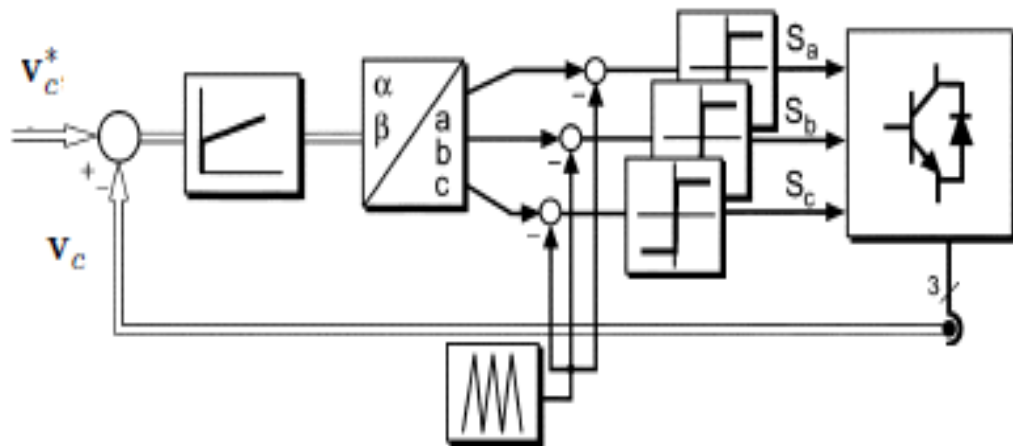


Figure 4.14: The block diagram of PWM voltage control.

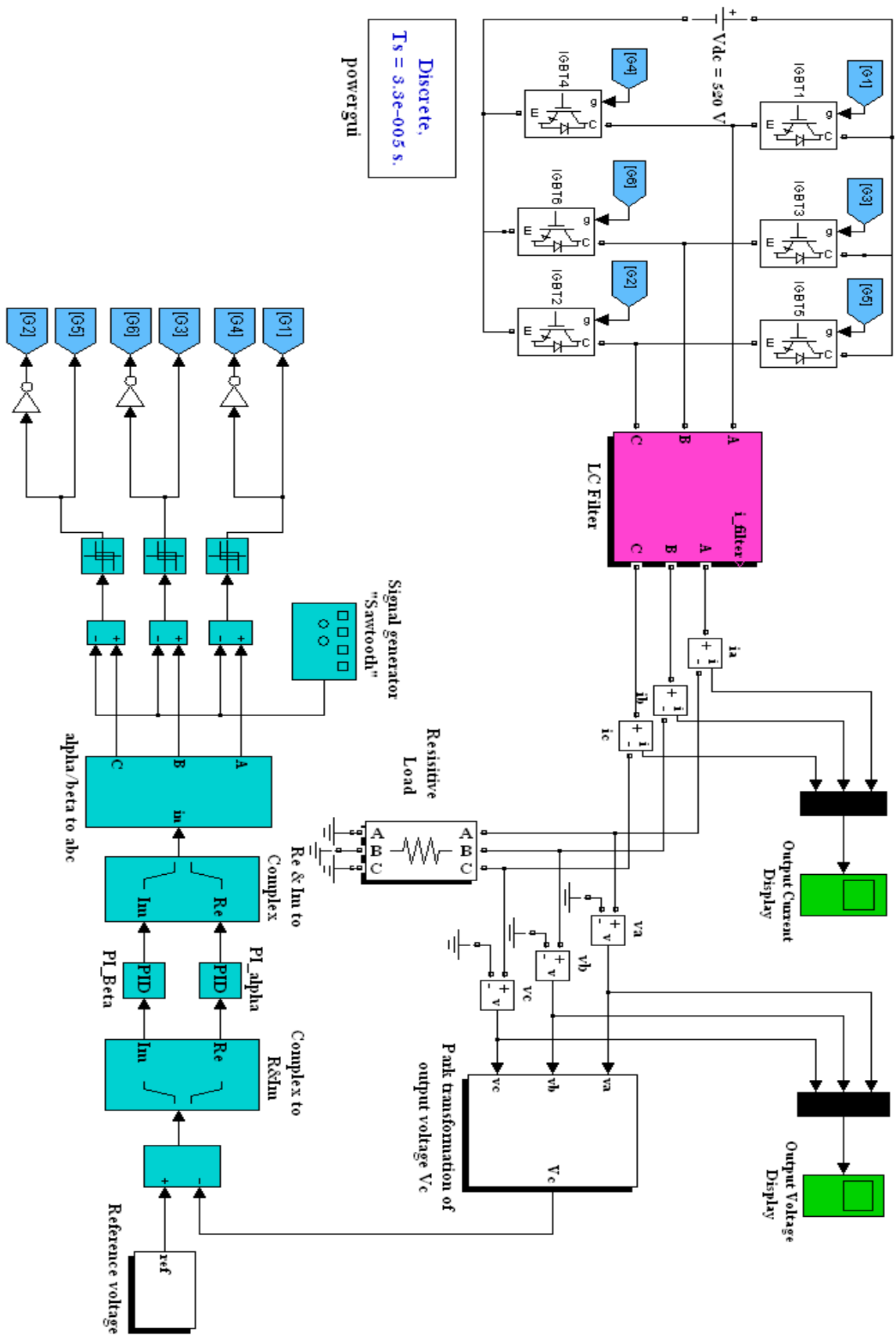


Figure 4.15: The inverter system simulation model using PWM voltage control.

# Chapter 5: Results

This chapter introduces the simulation results for linear and nonlinear loads. This results verify the proposed MPC then compare its performance with the well-known hysteresis and PWM control. It is possible to consider different prediction horizons for improving the behavior of the system [100]. So, the comparison of MPC considering one and two prediction horizons are carried out for different loads. Hardware testing allows you to deploy the design on target and observe the performance of the design under real-life conditions. So, the experimental results, using HIL testing, are carried out for linear and nonlinear loads, to verify the proposed MPC using eZdsp F28335 Kit.

## 5.1 Simulation Results

Simulations of the system shown in Figure 3.1 were carried out for resistive and nonlinear loads, using Matlab/Simulink tools, to verify the proposed control strategy. The parameters of the system are shown in Table 5.1.

Table 5.1: System Parameters

Parameter	Value
DC link voltage $V_{dc}$	520 [V]
Filter capacitor $C$	40 [ $\mu$ F]
Filter inductance $L$	2.4 [mH]
Sampling time $T_s$	33 [ $\mu$ s]

### 5.1.1 MPC

The behavior of the proposed predictive controller in steady-state operation for a resistive load of 3- $\Omega$  is shown in Figure 5.1. Also, the steady-state operation for a resistive load of 20- $\Omega$  is shown in Figure 5.2. The amplitude of the reference voltage is set to 200 V, and the frequency is 50 Hz. It is shown in the figures that the output voltages are sinusoidal with low distortion.

The effect of changing the value of resistive load, e.g.  $R = 3\Omega$ ,  $R = 6\Omega$ , and  $R = 10\Omega$ , with different values of output voltage is shown in Figure 5.3. It is shown in the figure that as the output voltage increases the THD decreases for a given load. It means that, the increase of output voltage value, between 200 and 300 V, and the decrease of resistive load,  $R = 3\Omega$ , leads to improve the performance of the proposed predictive controller.

The transient behavior of the system for a load step from no load to full load is shown in Figure 5.4. Assume that a 3- $\Omega$  load is connected at time of 0.05 s. It can be seen in this result that the output voltage of phase "A" is not affected by this change in the load. But, the output voltage of two other phases is affected by this change in the load for about 0.7 msec. Note that the controller quickly compensates the voltage drop caused by the transient with low distortion.

The diode-bridge rectifier, with values  $R = 20\Omega$  and  $C = 3000\mu F$ , shown in Figure 5.5 was used as nonlinear load. The behavior of the proposed predictive controller in steady-state operation for a nonlinear load is shown in Figure 5.6. Here, the output voltage presents a small distortion, but it is still sinusoidal despite the highly distorted load currents. A noticeable unbalance in the load currents is present in this result due to unbalanced voltages when a nonlinear load is connected. This result could be improved by using a higher sampling frequency,  $T_s = 10 \mu s$ , as shown in Figure 5.7. But in the hardware implementation, this solution may be difficult to implement due to hardware restrictions. It is possible to improve the system performance, without changing the value of sampling frequency, by increasing the filter capacitance value.

The effect of changing the value of resistance, e.g.  $R = 10\Omega$ ,  $R = 40\Omega$ , and  $R = 80\Omega$ , of a nonlinear load with different values of output voltage is shown in Figure 5.8. It is shown that, the THD increases with increasing the output voltage and decreasing the resistance of a nonlinear load. This means that, the increase of output voltage value, between 150 and 200V, and the increase of resistance leads to improve the performance of the controller. The best performance of controller occurs at  $v_c = 150V$  and  $R = 40\Omega$  because the THD equal to 1.84%.

Considering that the performance of the predictive controller highly depends on the parameters of the model used for prediction, some tests considering changes in the parameter values are presented. A change in the capacitor value, -50% ( $C = 20\mu F$ ) and +150% ( $C = 100\mu F$ ) of the real value, was introduced in the predictive model. When the converter is connected to a resistive load, the change in the model have little effect, as shown in Figure 5.9 and Figure 5.10. However, when connected to a nonlinear load, distortion in the output voltage is noticeable but the performance of controller still good, as shown in Figure 5.11 and Figure 5.12. Furthermore, it is possible to improve the system performance, for linear and nonlinear loads, by increasing the filter capacitance value. Table 5.2 presents the effect of varying the filter capacitance value on the performance of the predictive controller. The performance of the proposed MPC is improved when the value of the filter capacitance increased by +150% of the real value for different loads.

Table 5.2: The effect of varying the filter capacitance value on the performance of MPC.

Different loads	THD % (real value $C$ )	THD % (+150%)	THD % (-50%)
Resistive load $R = 20\Omega$	1.71	1.01	2.60
Resistive load $R = 100\Omega$	2.74	1.49	3.69
Nonlinear load $R = 50\Omega$	3.50	2.05	3.82
Nonlinear load $R = 100\Omega$	2.24	1.87	3.48
Nonlinear load $R = 200\Omega$	2	1.41	2.91

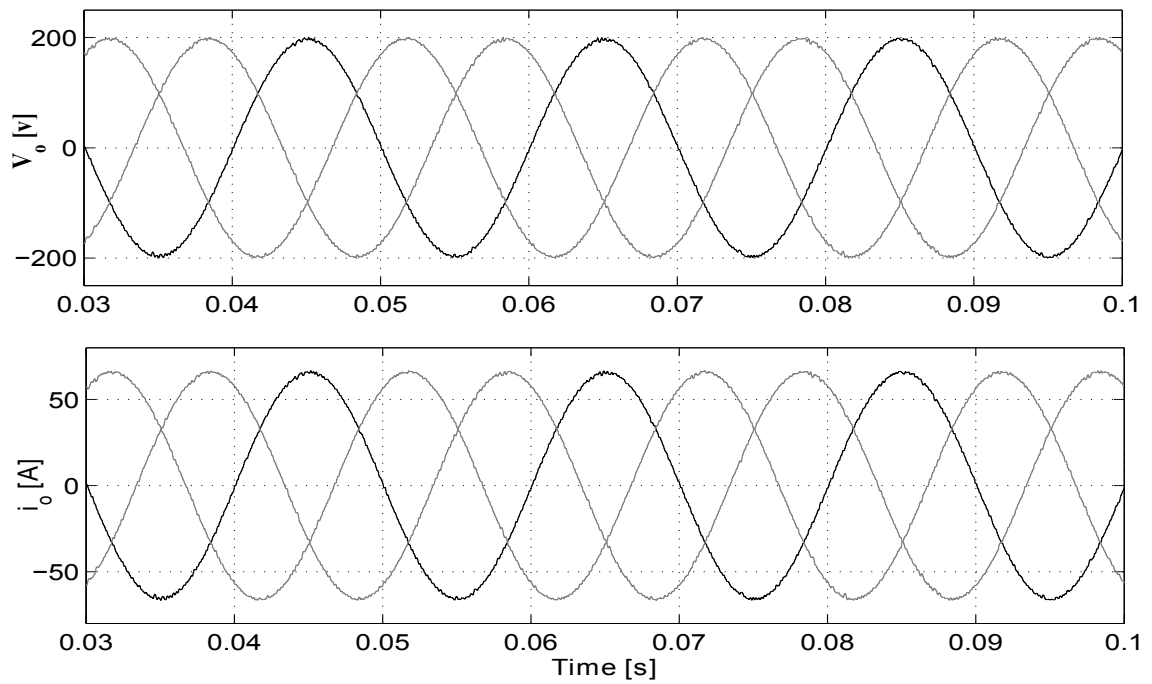


Figure 5.1: The simulated three phase output voltages and currents at steady state for a resistive load of  $3\text{-}\Omega$ . Voltage THD: 0.71%.

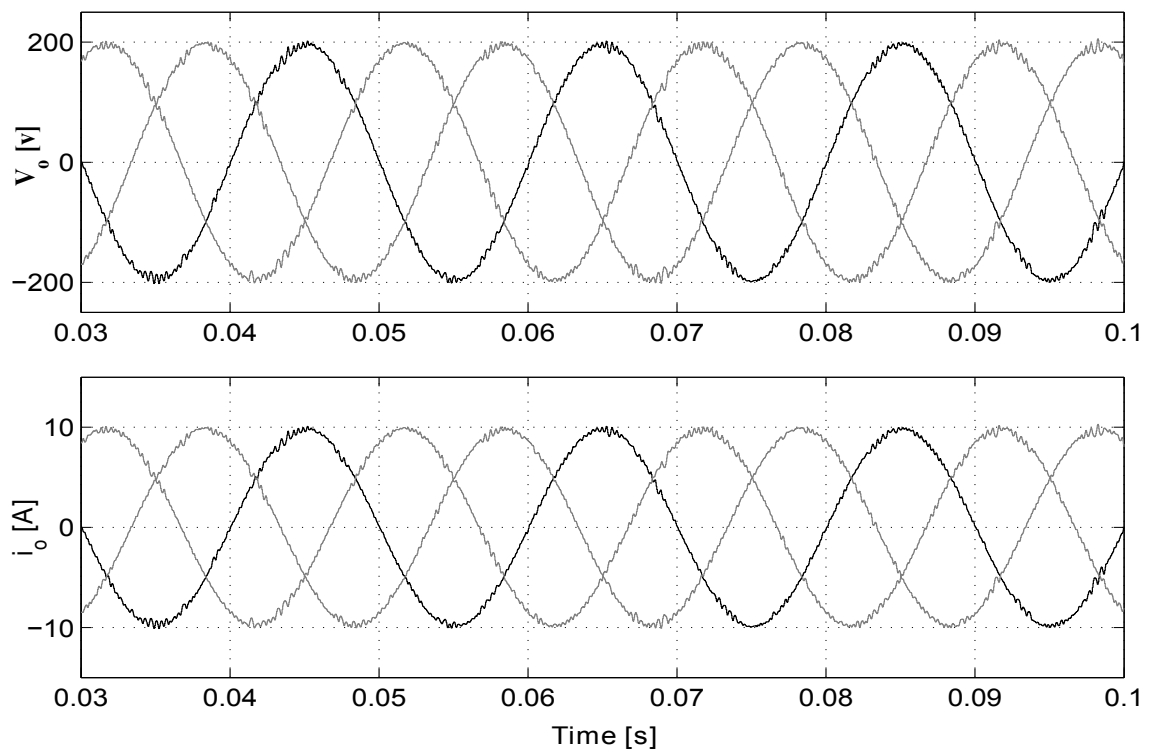


Figure 5.2: The simulated three phase output voltages and currents at steady state for a resistive load of  $20\text{-}\Omega$ . Voltage THD: 1.71%.

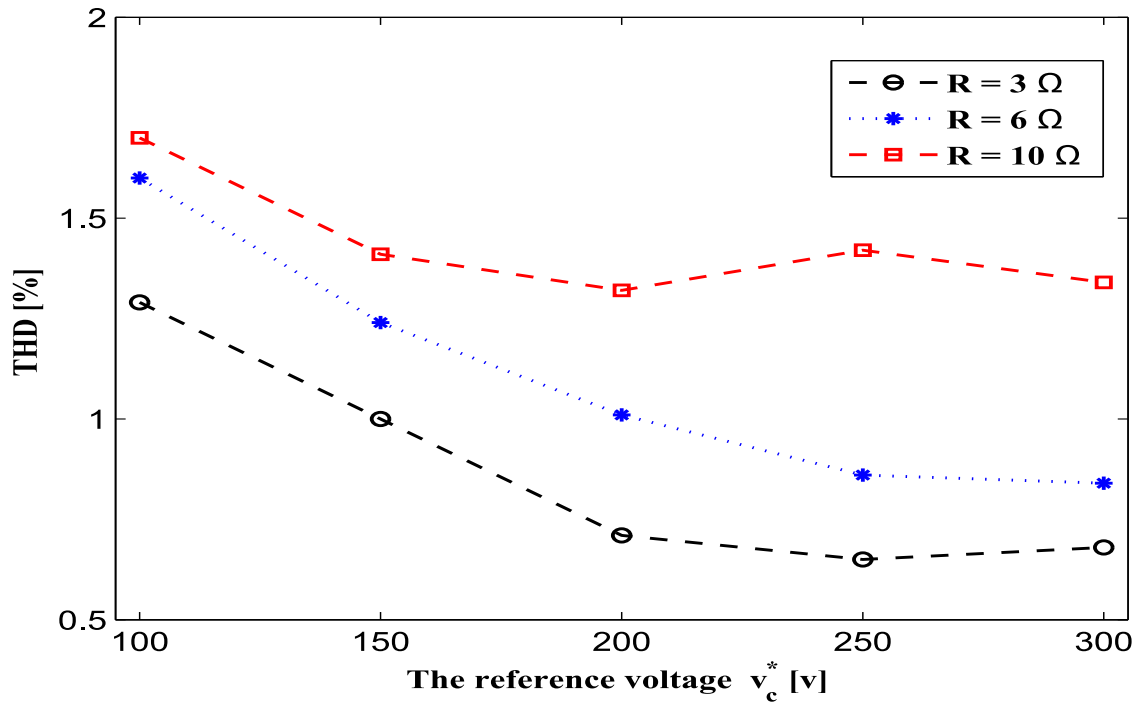


Figure 5.3: The effect of varying the inverter output voltage reference value on the THD at different resistive loads.

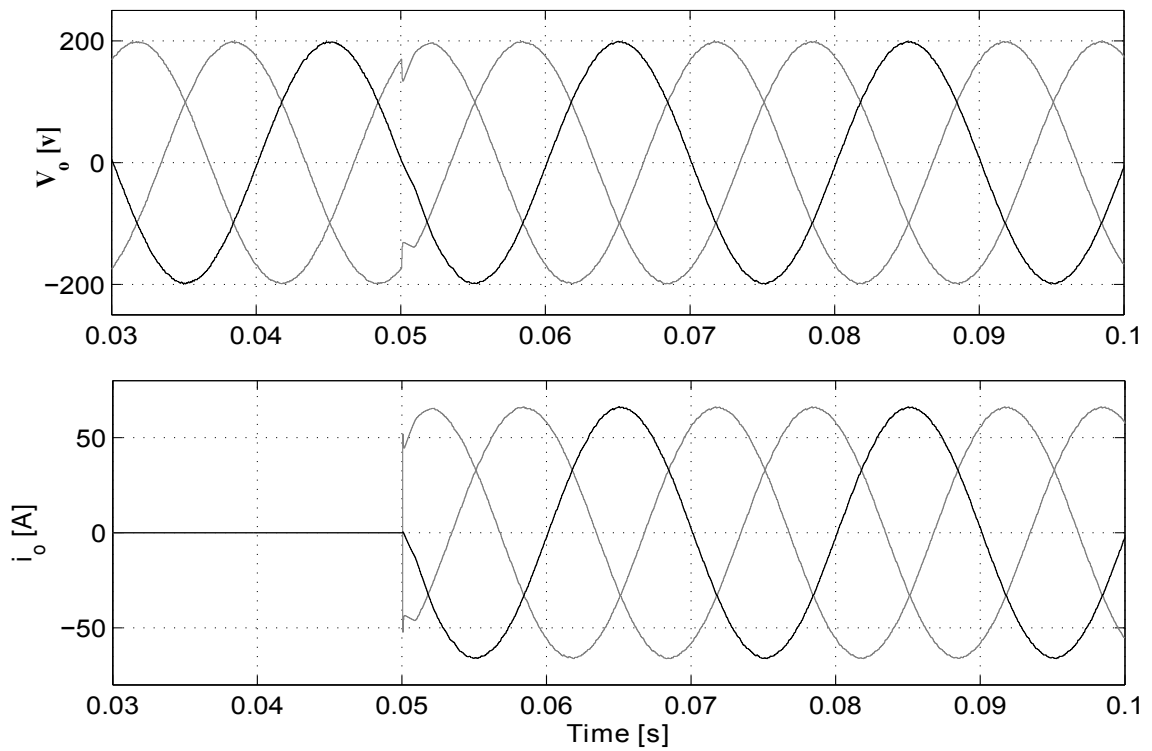


Figure 5.4: The simulated output voltages and currents according to full load step change at  $t = 0.05sec$ .

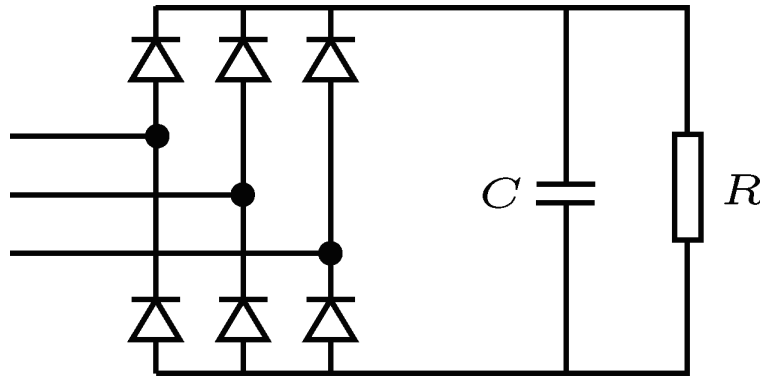


Figure 5.5: The inverter nonlinear load.

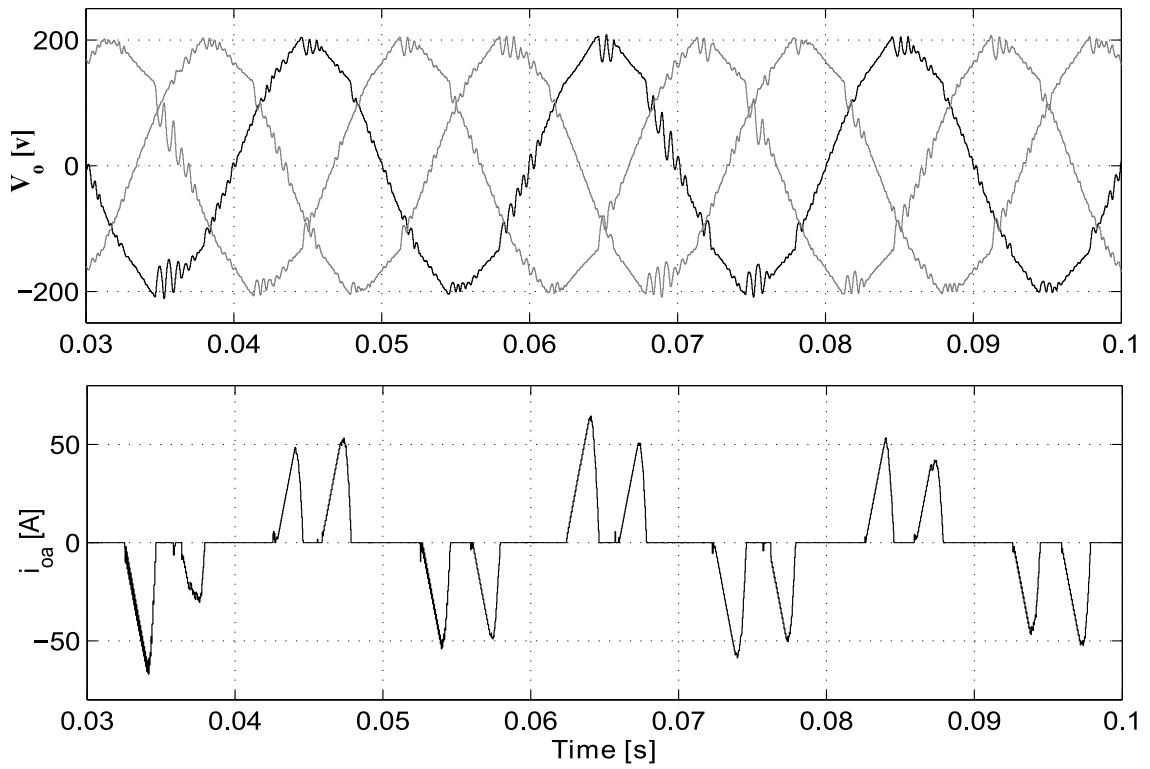


Figure 5.6: The simulated three phase output voltages and currents at steady state for a nonlinear load. Voltage THD: 4.75%.

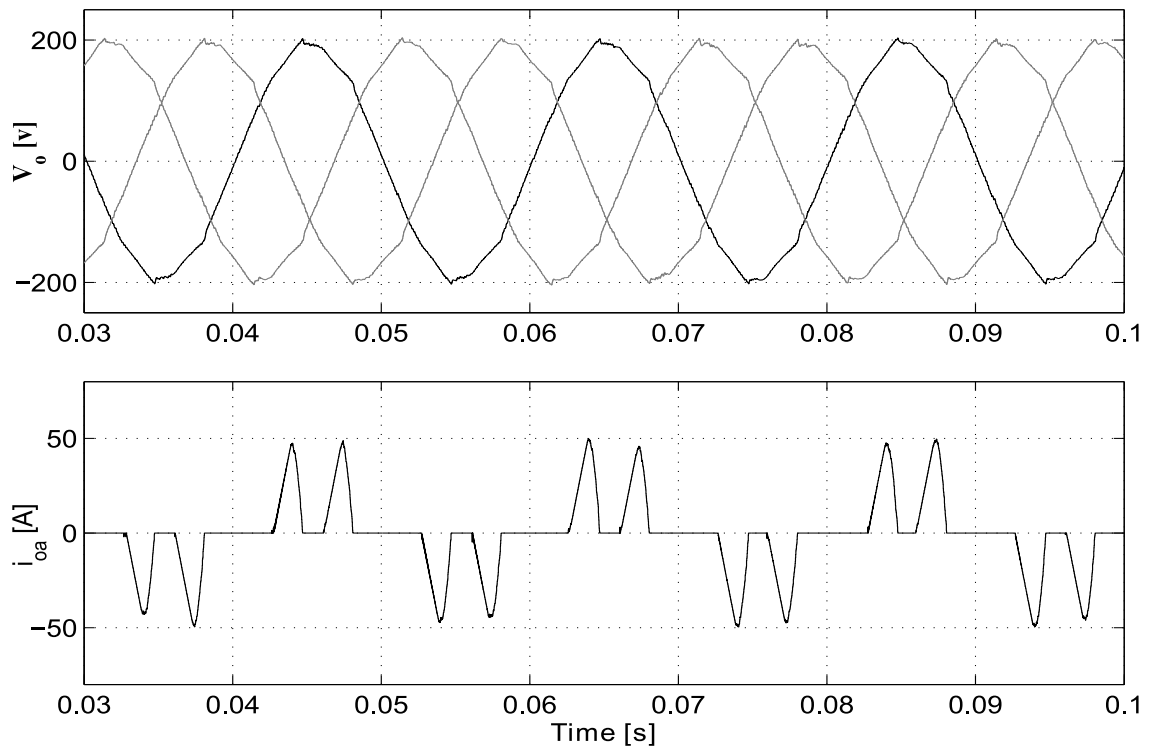


Figure 5.7: The simulated three phase output voltages and currents at steady state for a nonlinear load with a sampling time of  $T_s = 10 \mu s$ . Voltage THD: 2.18%.

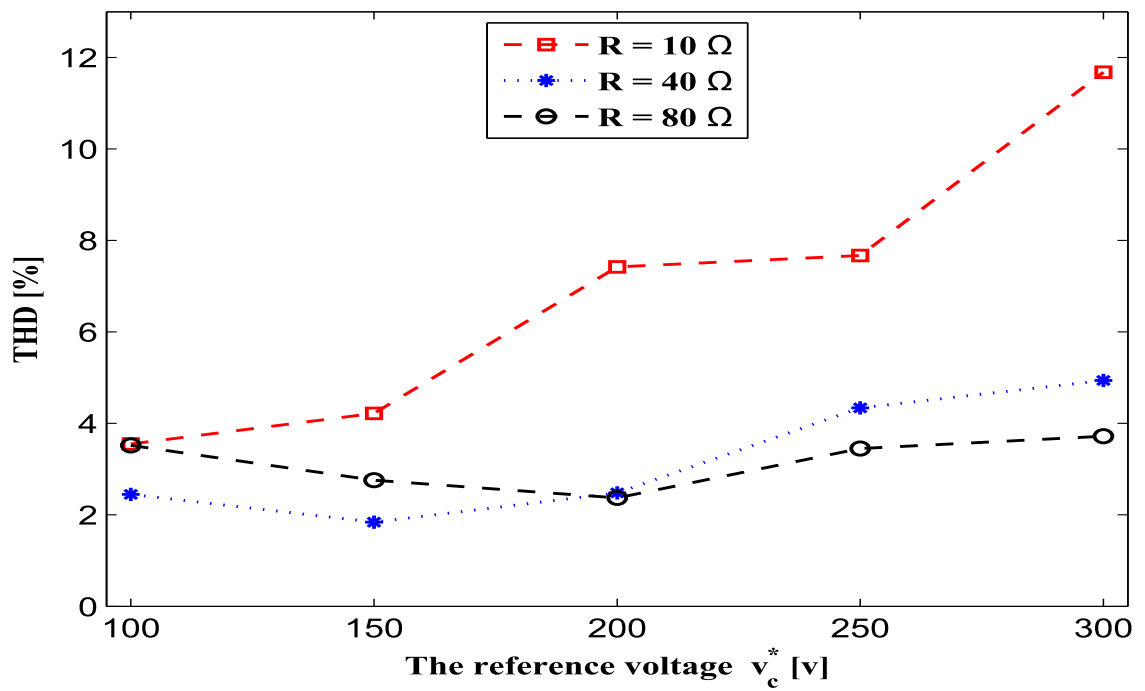


Figure 5.8: The effect of varying the inverter output voltage reference value on the THD at different nonlinear loads.

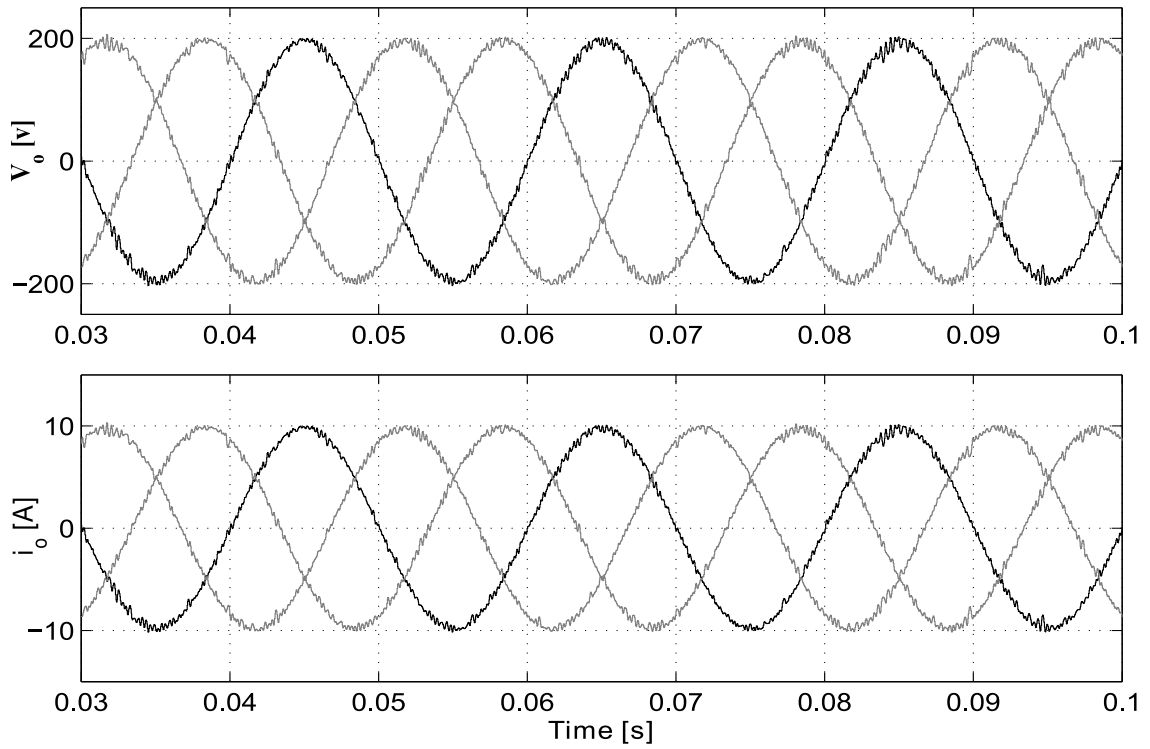


Figure 5.9: The simulated three phase output voltages and currents at steady state for a resistive load of  $20\text{-}\Omega$  with the filter capacitance of  $20\mu\text{F}$  (-50%). Voltage THD: 2.60%.

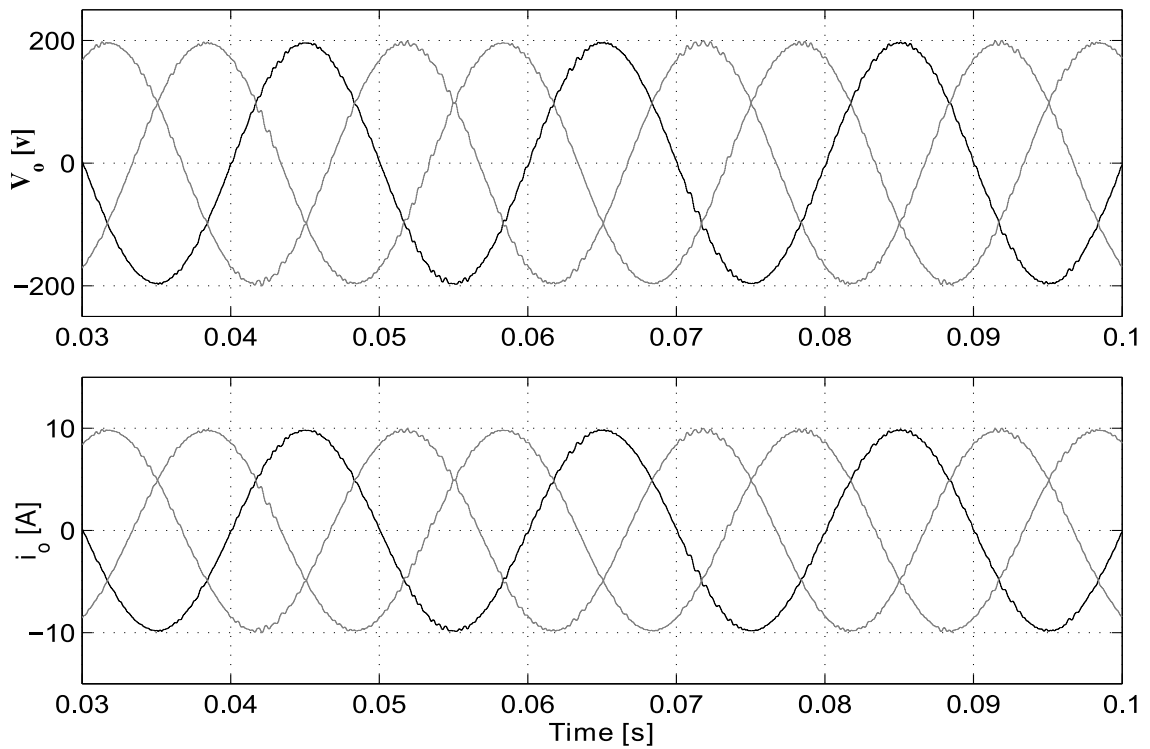


Figure 5.10: The simulated three phase output voltages and currents at steady state for a resistive load of  $20\text{-}\Omega$  with the filter capacitance of  $100\mu\text{F}$  (+150%). Voltage THD: 1.01%.

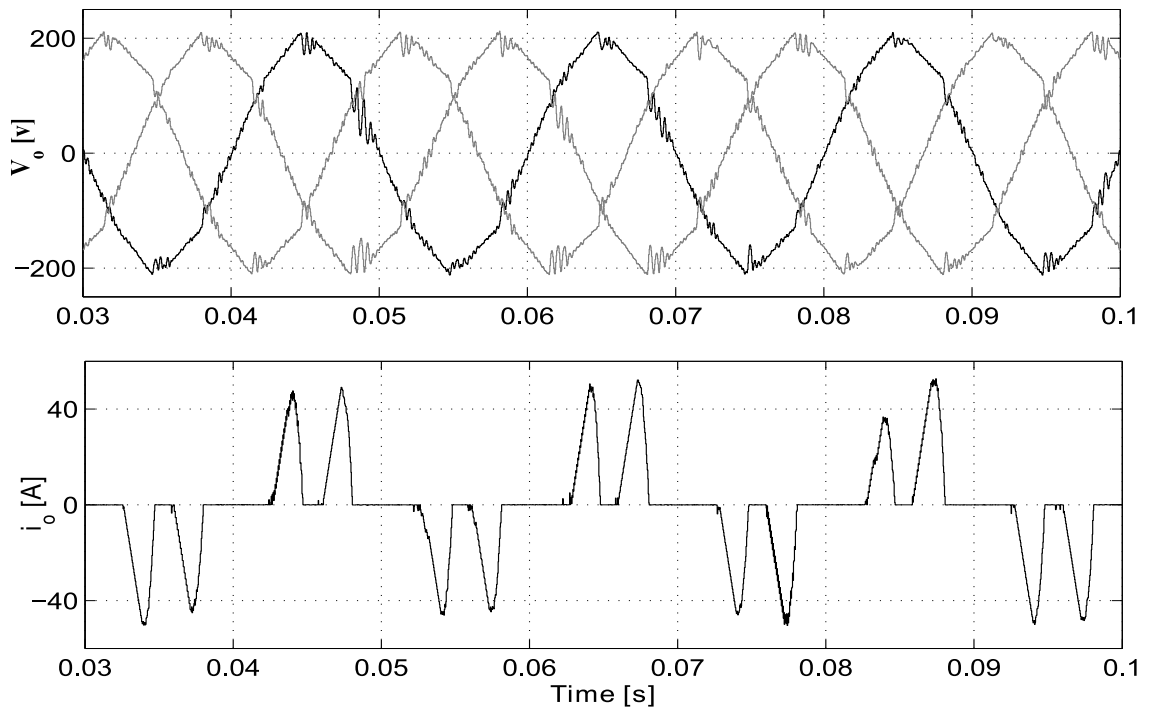


Figure 5.11: The simulated three phase output voltages and currents at steady state for a nonlinear load with the filter capacitance of  $20\mu F$  (-50%). Voltage THD: 4.53%.

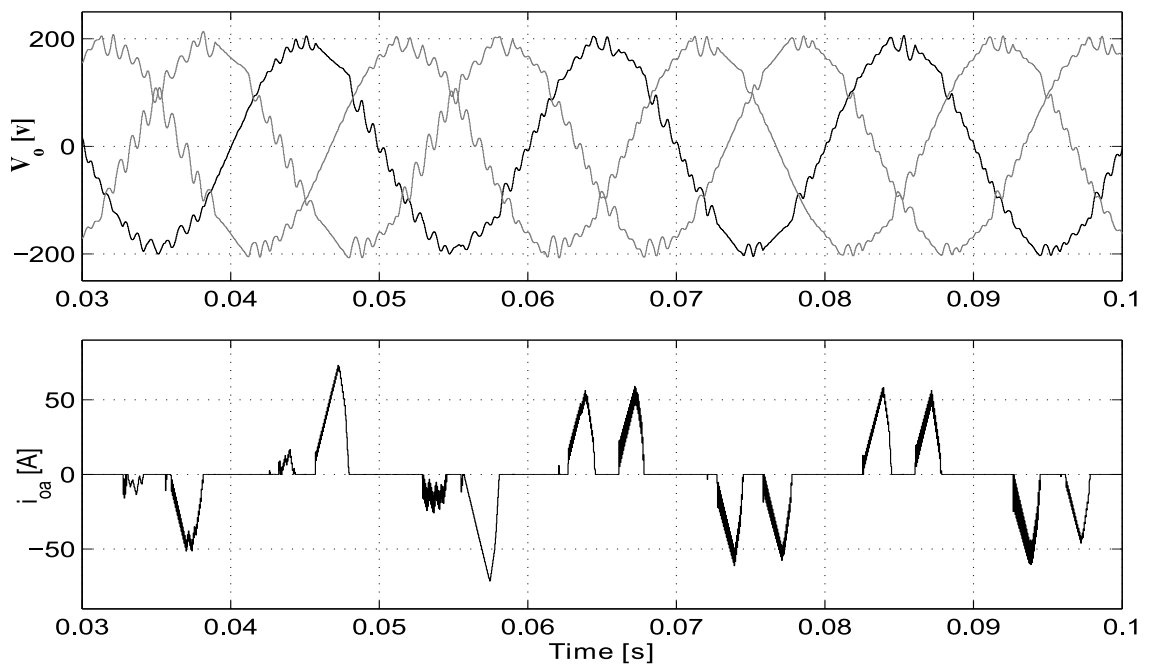


Figure 5.12: The simulated three phase output voltages and currents at steady state for a nonlinear load with the filter capacitance of  $100\mu F$  (+150%). Voltage THD: 4.66%.

### 5.1.2 MPC and Classical Methods

Simulations of the system shown in Figure 3.1 are carried out for resistive and nonlinear loads, using Matlab/Simulink tools, to verify the proposed predictive control strategy for a three phase inverter and compare its performance with well-known hysteresis and PWM control. The parameters of the system are shown in Table 5.1. For comparison purposes, controller parameters of the classical methods considered in this work are designed to obtain comparable average switching frequencies. Namely, a hysteresis width of  $H = \pm 0.3V$  and a PWM carrier frequency of 10 KHz.

The behavior of the proposed predictive controller in steady-state operation for a resistive load of  $3 \Omega$  is compared with the classical methods, as shown in Figure 5.13, Figure 5.14, and Figure 5.15. The amplitude of the reference voltage is set to 200 V (RMS), and the frequency is 50 Hz. It is shown in the figures that the output voltages are sinusoidal with low distortion, especially in MPC, which satisfies the IEEE 915-1992 standard.

Also, the steady-state operation for a resistive load of  $20\text{-}\Omega$  in case of MPC is shown in Figure 5.16. It is shown in the figure that the output voltages are sinusoidal with low distortion. Unlike classical methods, the output voltages are sinusoidal with very high distortion. THD is equal to 25.76% and 26.24% for hysteresis and PWM control, respectively. These values do not achieve the IEEE 915-1992 standard. Moreover, the UPS does not work well for a higher THD value. For this reason, the controller may be fail to control the output voltage.

The transient behavior of the system for a load step from no load to full load for three types of control is shown in Figure 5.17, Figure 5.18, and Figure 5.19. Assume that a  $3\text{-}\Omega$  load is connected at time of 0.05 s. It can be seen in this result that the output voltage of phase "A" is not affected by this change in the load. But, the output voltage of two other phases is affected by this change in the load for about 0.7 msec, 0.9 msec, and 1.2 msec in the case of MPC, hysteresis, and PWM control, respectively. Note that the MPC quickly compensates the voltage drop caused by the transient with low distortion.

The diode-bridge rectifier, with values  $R = 50\Omega$  and  $C = 3000\mu F$ , shown in Figure 5.5 was used as nonlinear load. The behavior of the proposed predictive controller, hysteresis, and PWM control in steady-state operation for a nonlinear load is shown in Figure 5.20, Figure 5.21, and Figure 5.22. Here for a MPC, the output voltage presents a low distortion, but it is still sinusoidal despite the highly distorted load currents. Unlike classical methods, the output voltage presents a very high distortion. Therefore, a higher THD value makes the controller fail to control the output voltage, and the UPS does not work. A noticeable unbalance in the load currents is present in these results due to unbalanced voltages when a nonlinear load is connected.

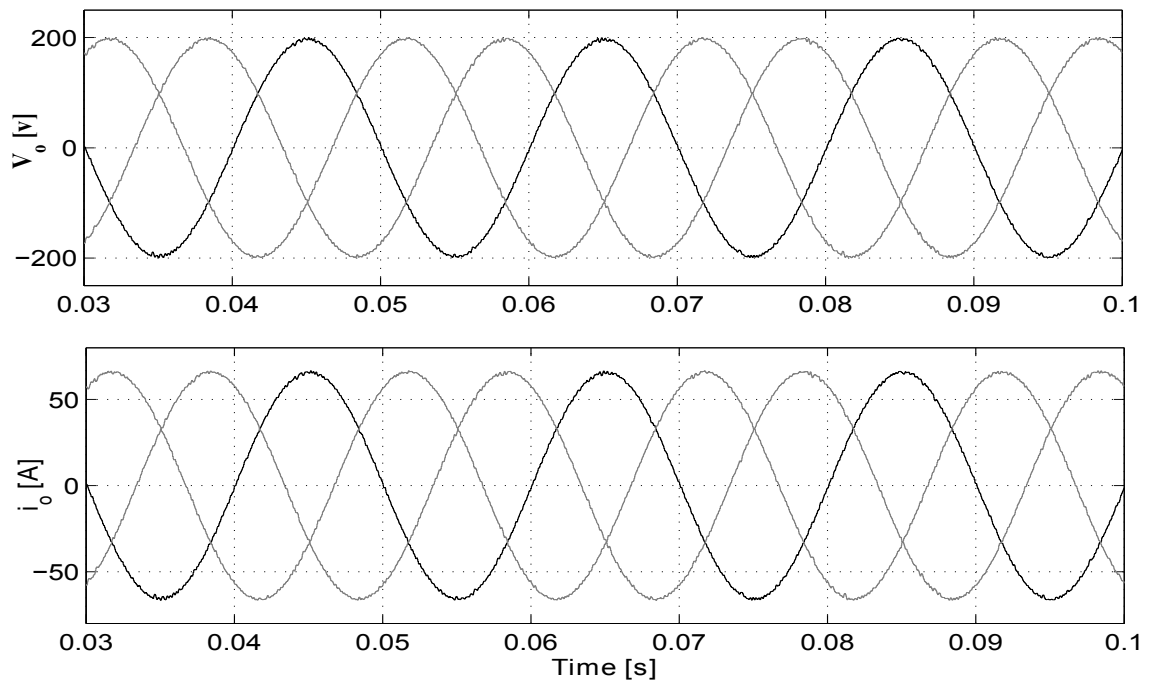


Figure 5.13: The simulated three phase output voltages and currents at steady state for a resistive load of  $3\text{-}\Omega$  in case of MPC. Voltage THD: 0.71%.

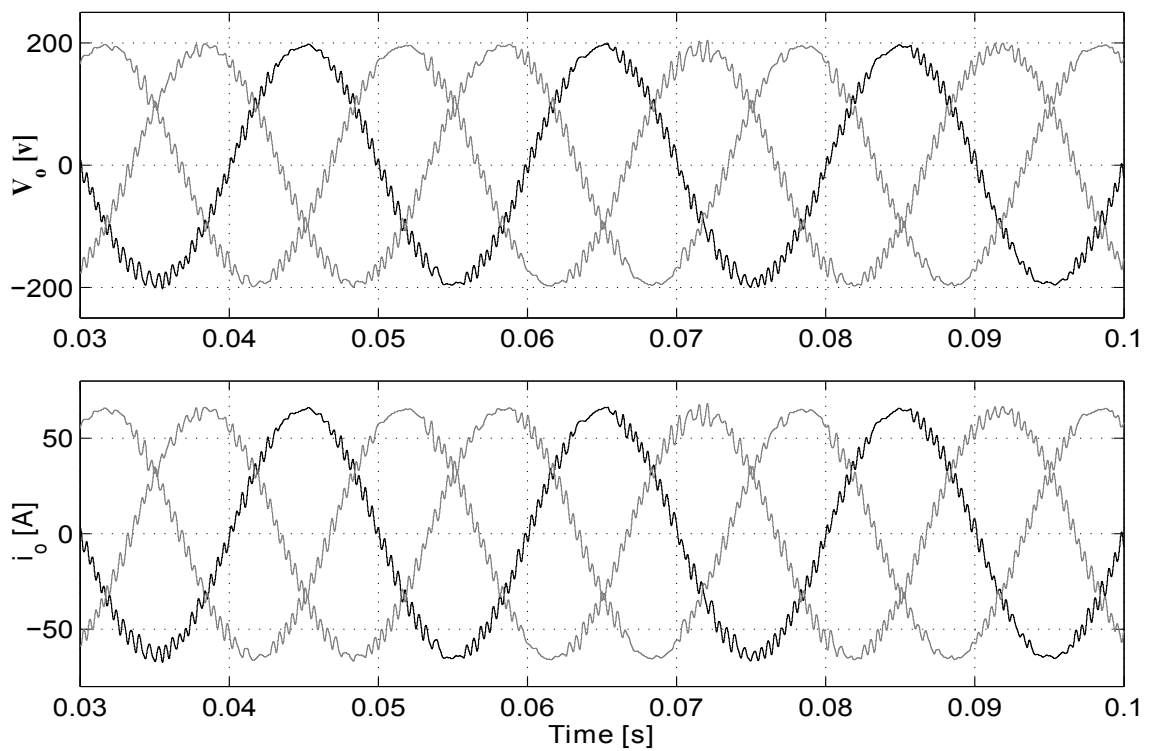


Figure 5.14: The simulated three phase output voltages and currents at steady state for a resistive load of  $3\text{-}\Omega$  in case of PWM control. Voltage THD: 3.13%.

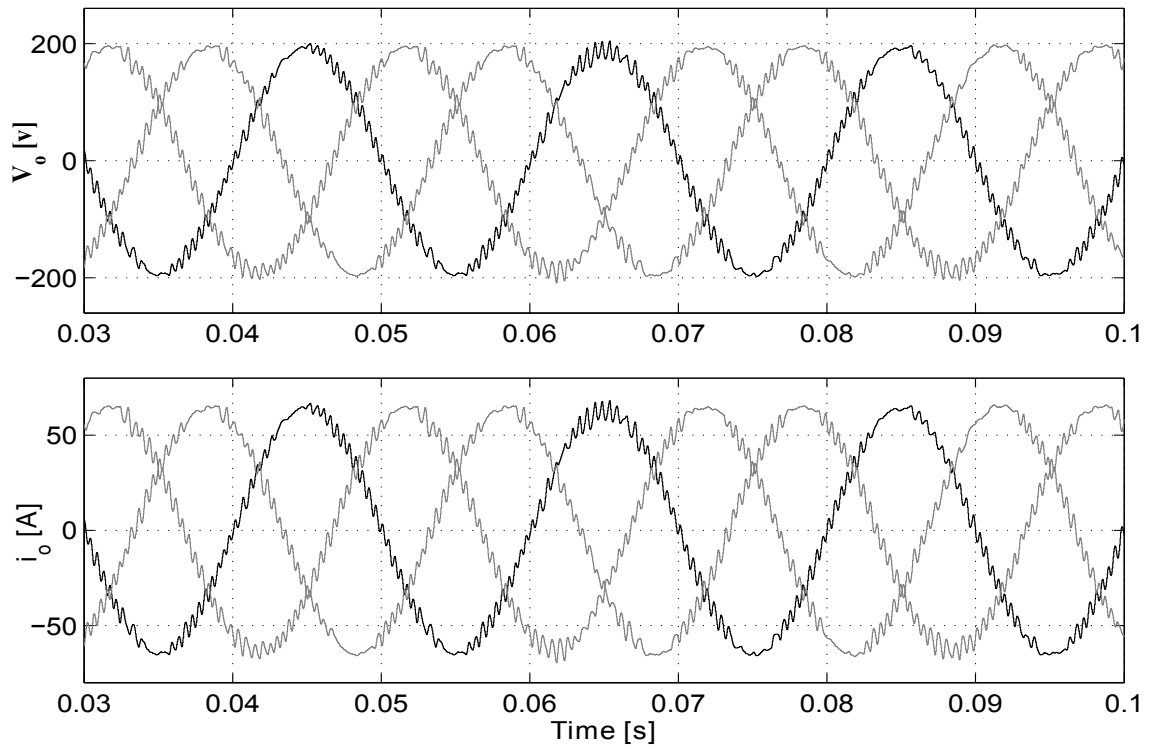


Figure 5.15: The simulated three phase output voltages and currents at steady state for a resistive load of  $3\text{-}\Omega$  in case of hysteresis control. Voltage THD: 4.21%.

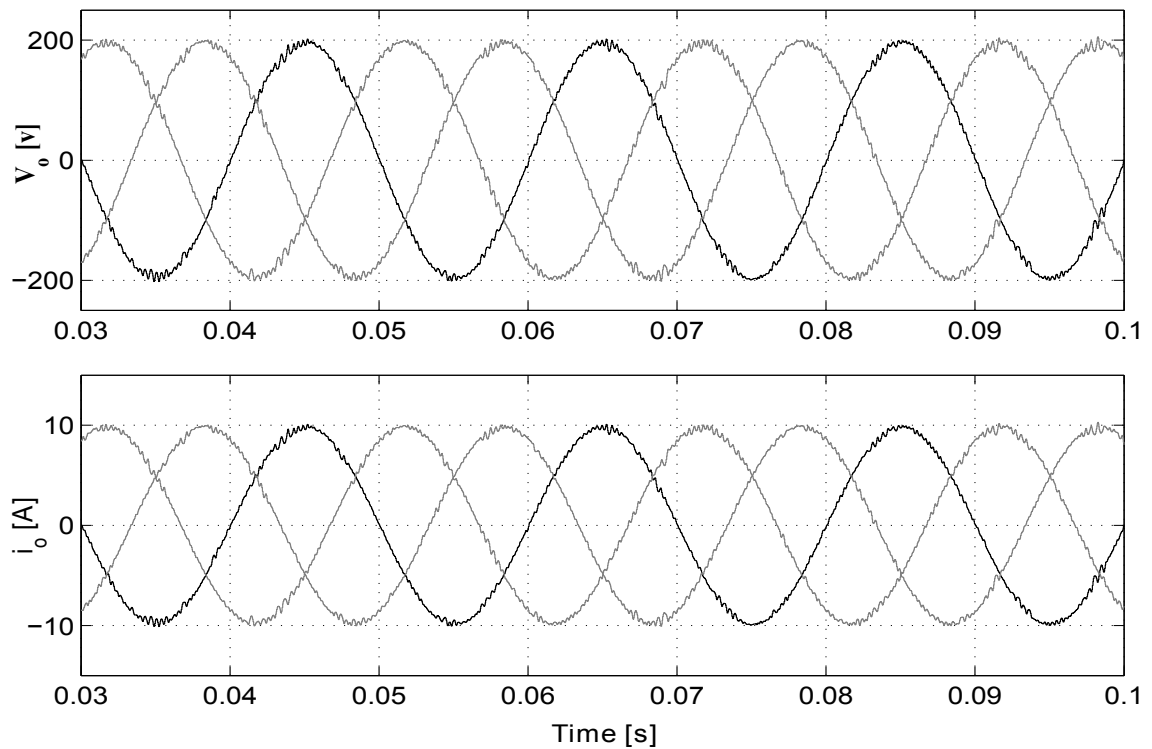


Figure 5.16: The simulated three phase output voltages and currents at steady state for a resistive load of  $20\text{-}\Omega$  in case of MPC. Voltage THD: 1.71%.

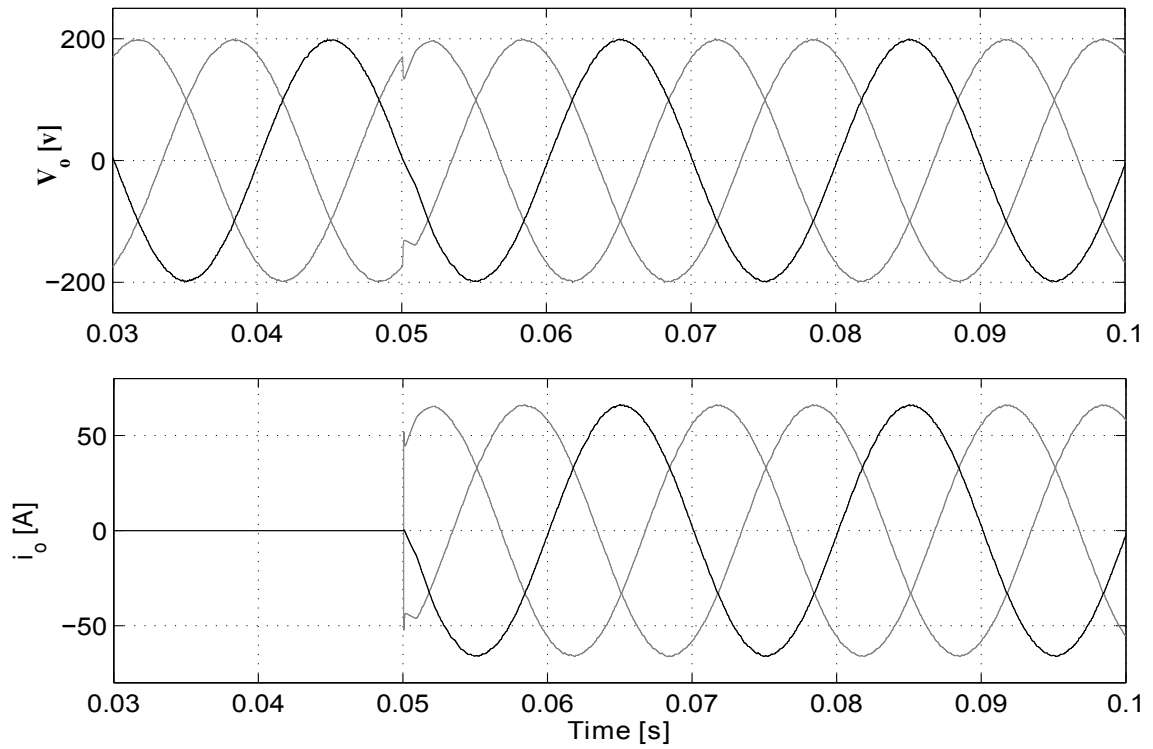


Figure 5.17: The simulated output voltages and currents according to full load step change at  $t = 0.05$ sec for a MPC.

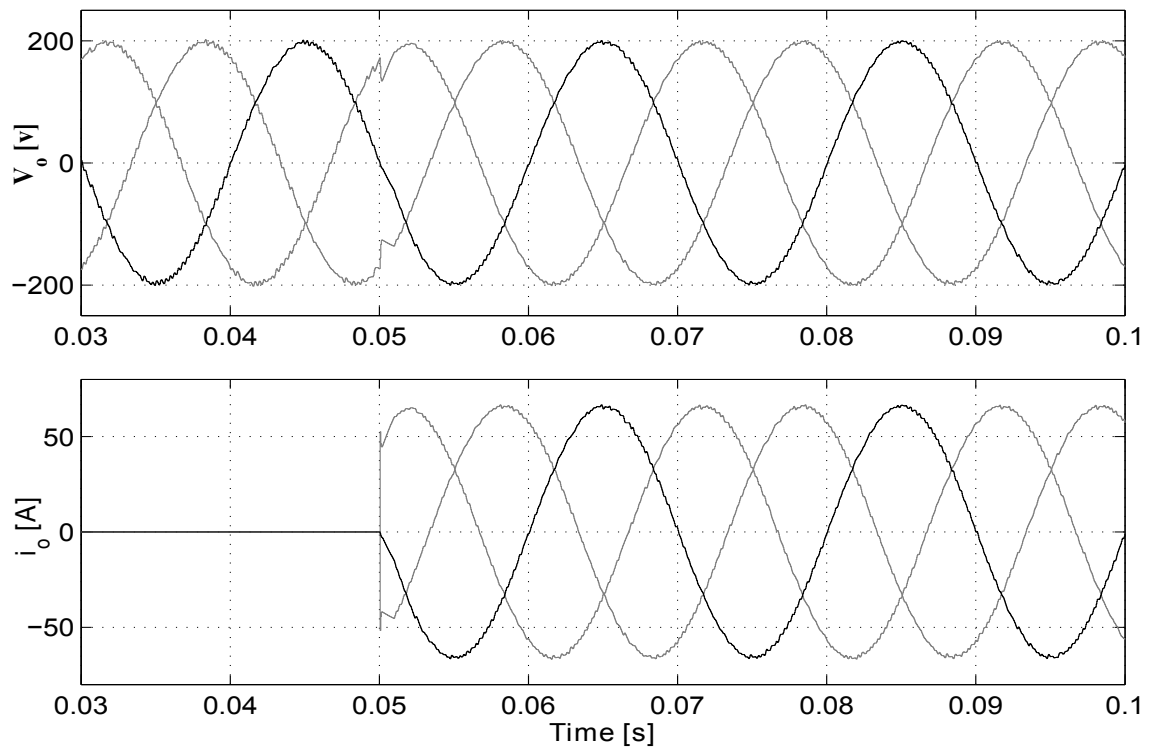


Figure 5.18: The simulated output voltages and currents according to full load step change at  $t = 0.05$ sec for a PWM control.

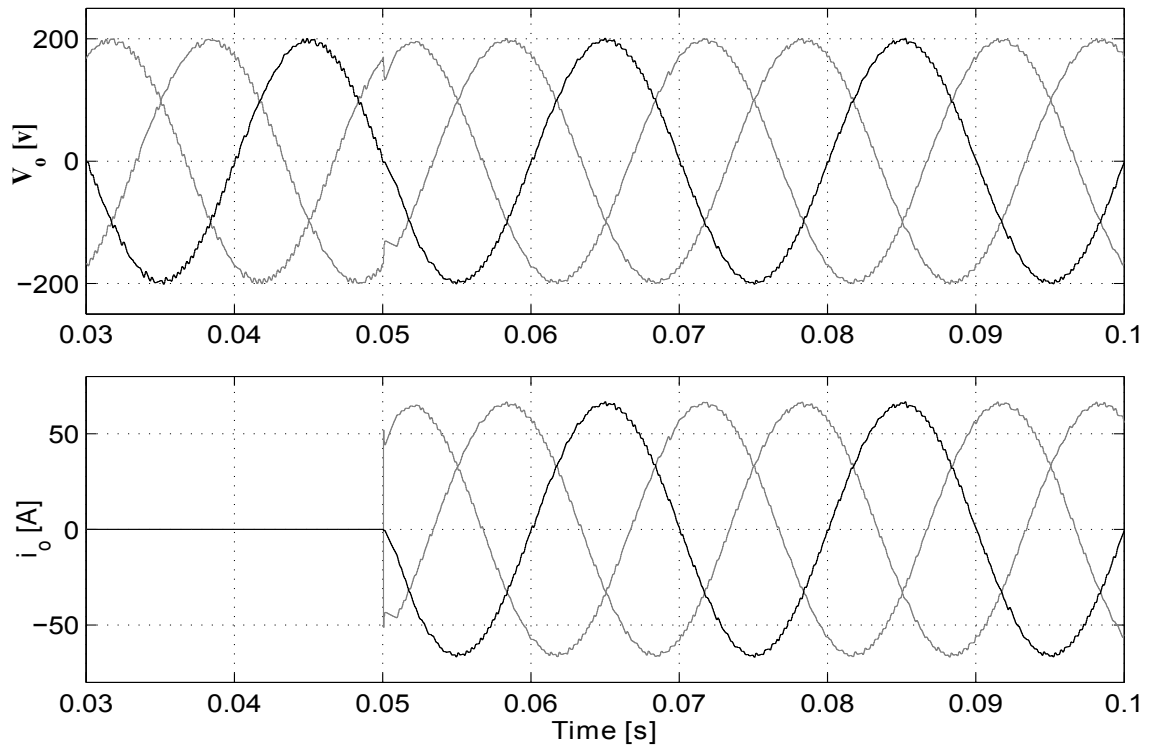


Figure 5.19: The simulated output voltages and currents according to full load step change at  $t = 0.05\text{sec}$  for a hysteresis control.

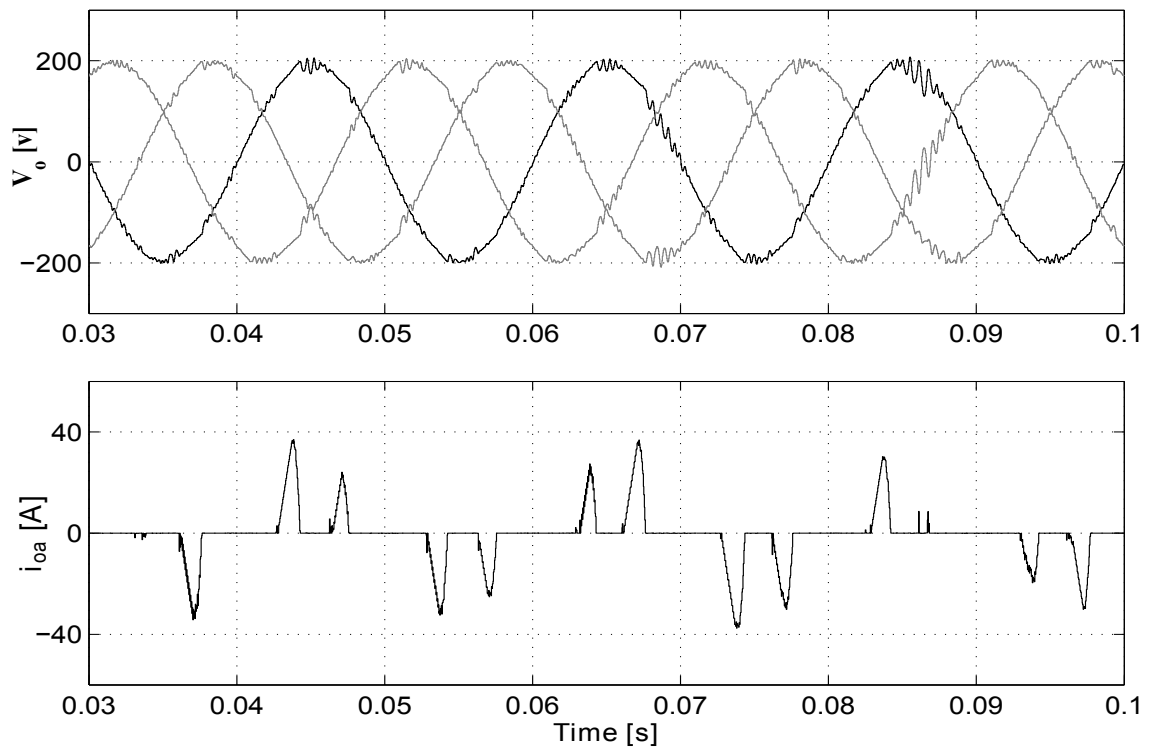


Figure 5.20: The simulated three phase output voltages and currents at steady state for a nonlinear load for a MPC. Voltage THD: 3.02%.

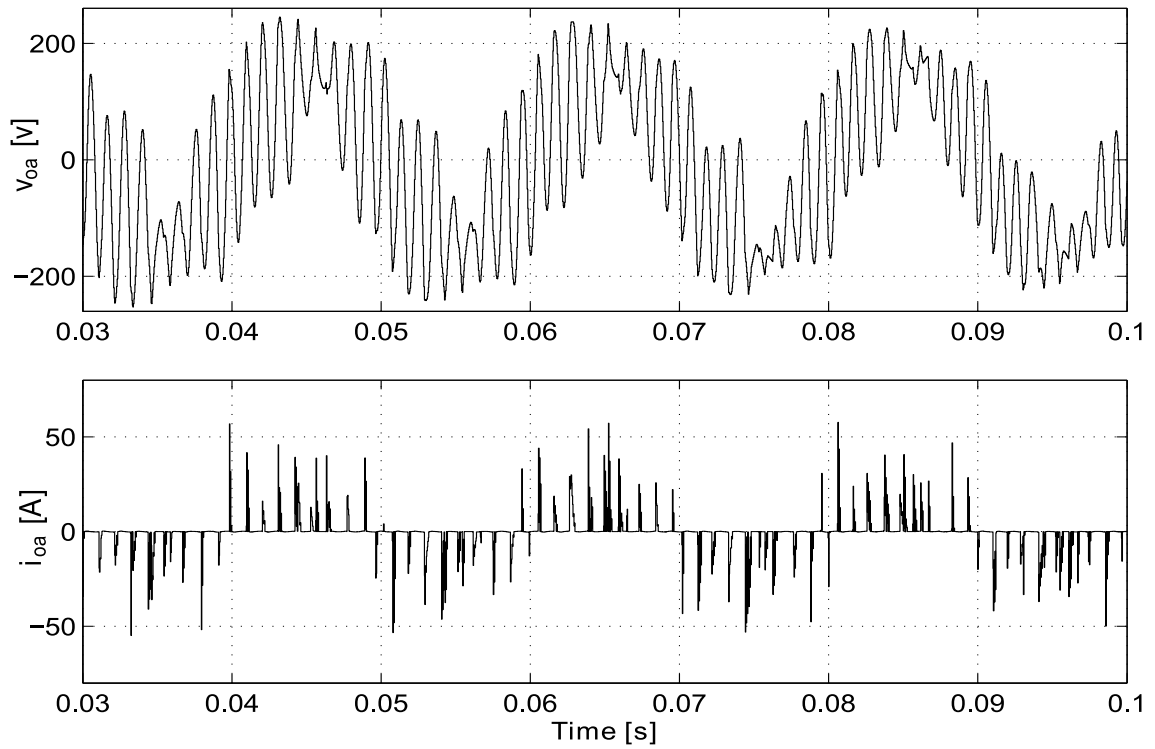


Figure 5.21: The simulated three phase output voltages and currents at steady state for a nonlinear load for a hysteresis control. Voltage THD: 50.66%.

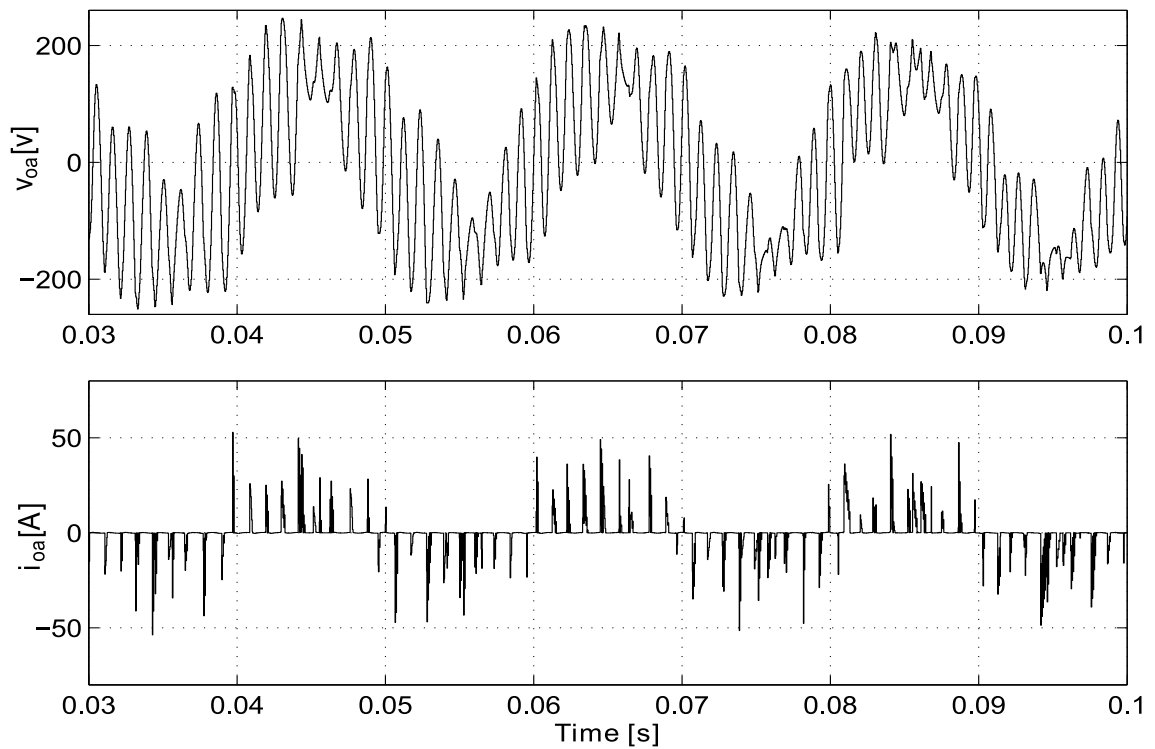


Figure 5.22: The simulated three phase output voltages and currents at steady state for a nonlinear load for a PWM control. Voltage THD: 40.75%.

### 5.1.3 Improved MPC

Simulation of the system shown in Figure 3.1 were carried out for resistive and nonlinear loads, using Matlab/Simulink tools, to verify the proposed control strategy for a three phase inverter. Behavior of the system is evaluated and compared for one and two prediction steps. The parameters of the system are shown in Table 5.1.

The behavior of the MPC, with only one prediction step, for resistive loads of 50- $\Omega$ , 2-k $\Omega$ , and 4-M $\Omega$  are shown in Figure 5.23, Figure 5.24, and Figure 5.25. The amplitude of the reference voltage is set to 200V, and the frequency is 50 Hz. It is observed that, the output voltages in the steady state operation are sinusoidal with low distortion. Moreover, the settling time “the time to reach steady state operation” changes with the resistive loads. It takes about 5 msec ( $\frac{1}{4}$  cycle), 35 msec (1.75 cycles), and 40 msec (2 cycles) to reach steady state operation for resistive loads of 50- $\Omega$ , 2-k $\Omega$ , and 4-M $\Omega$ , respectively.

The behavior of the Improved MPC, with two prediction steps, for the same previous resistive loads are shown in Figure 5.26, Figure 5.27, and Figure 5.28. It can be observed that in these cases the performance is very similar and considerably better than the case of one step prediction. It means that, the output voltage THD can be considered constant (about 0.76%) and the settling time can be considered constant with very small value (2 msec). Simulation results of different resistive loads for both cases of MPC are shown in Table 5.3. It is observed that the changing of resistive load value leads to change the value of output voltage THD and settling time, in the case of MPC. Unlike in the Improved MPC, the THD and settling time can be considered constant due to the small variation and very better than the first case.

The diode-bridge rectifier, with values  $R = 60\Omega$  and  $C = 3000\mu F$  or with values  $R = 1000\Omega$  and  $C = 3000\mu F$ , shown in Figure 5.4 was used as nonlinear load. The behavior of the MPC for the previous nonlinear loads are shown in Figure 5.29 and Figure 5.30. Here, distortion in the output voltage in the steady state operation is noticeable but the performance of controller still good, despite the highly distorted load currents. Moreover, the settling time changes with the load. It takes about 20 msec (*one cycle*) and 55 msec (2.5 cycles) to reach the steady state operation for the diode-bridge rectifier with values  $R = 60\Omega$  and  $C = 3000\mu F$  and with values  $R = 1000\Omega$  and  $C = 3000\mu F$ , respectively.

The behavior of the Improved MPC for the same previous nonlinear loads are shown in Figure 5.31 and Figure 5.32. It is observed that, the output voltage presents a small distortion, but it is still sinusoidal despite the highly distorted load currents. Moreover, the settling time in both cases less than 10 msec ( $< 0.5$  cycle). Simulation results for non linear load with different values of  $R$  and  $C$  for both cases of MPC are shown in Table 5.4. It is observed that the performance of the Improved MPC is better than the case of MPC. This improvement can be noticed in the lower THD and in less settling time, at most 10 msec, in the output voltage. The meaning of inrush current is the current peak at the moment of switching on the circuit. Power converters often have inrush currents much higher than their steady state currents, due to the charging current of the capacitance of the nonlinear load, as shown in Figure 5.29, Figure 5.30, Figure 5.31, and Figure 5.32.

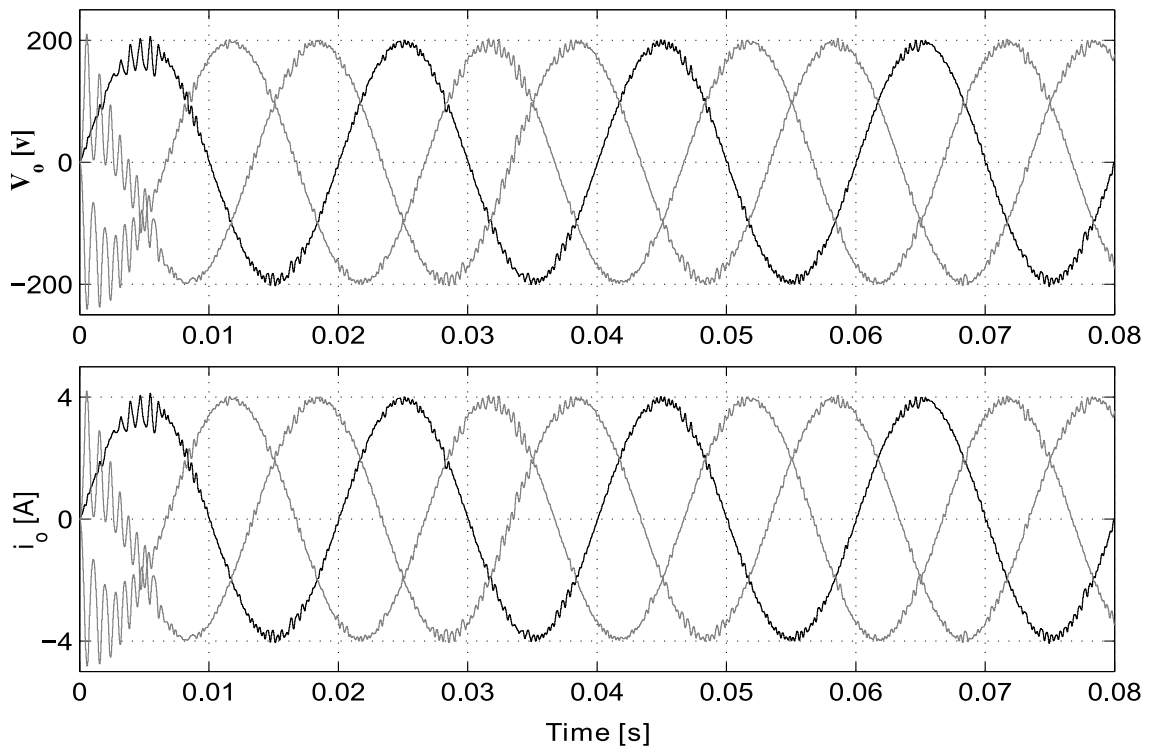


Figure 5.23: The simulated three phase output voltages and currents for a MPC with 50- $\Omega$  load. Voltage THD: 2.30%.

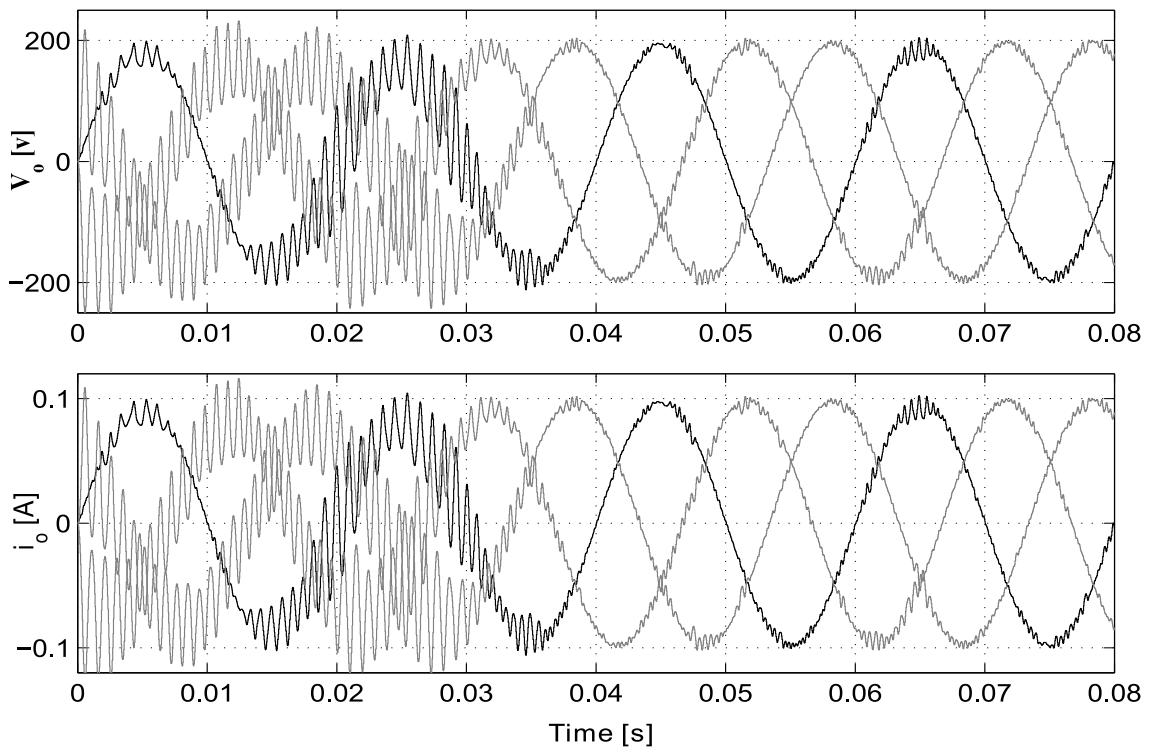


Figure 5.24: The simulated three phase output voltages and currents for a MPC with 2-k $\Omega$  load. Voltage THD: 3.84%.

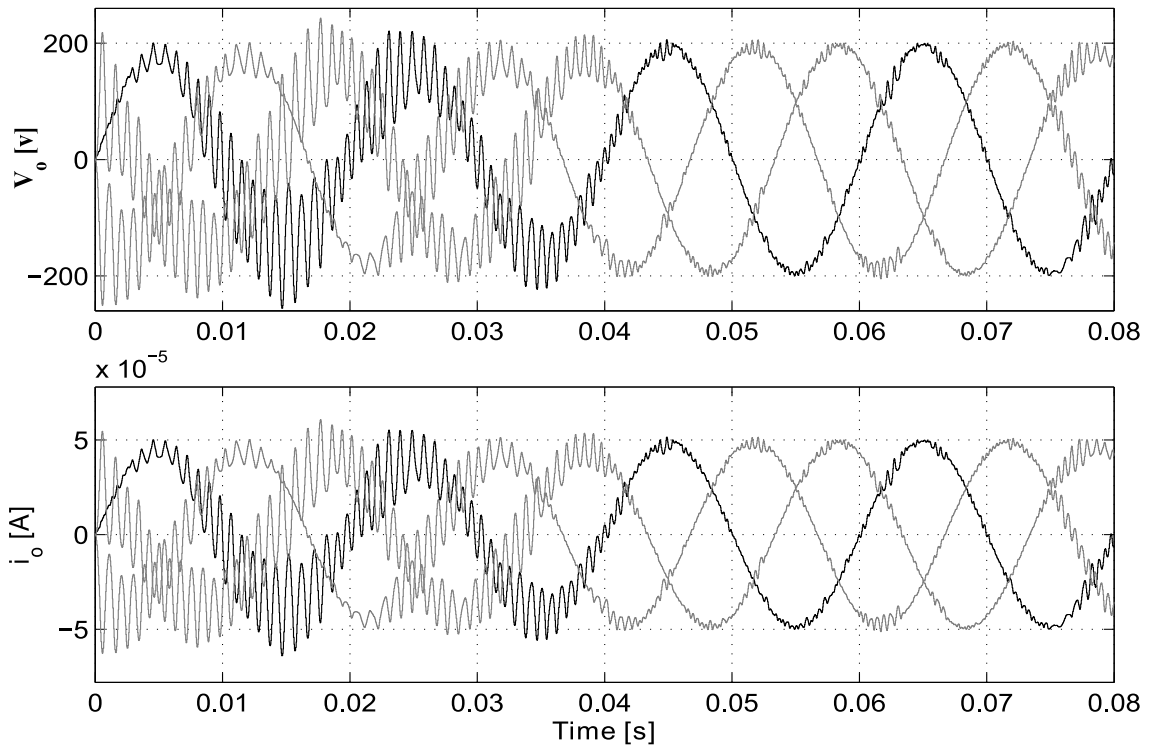


Figure 5.25: The simulated three phase output voltages and currents for a MPC with 4-M $\Omega$  load. Voltage THD: 6.12%.

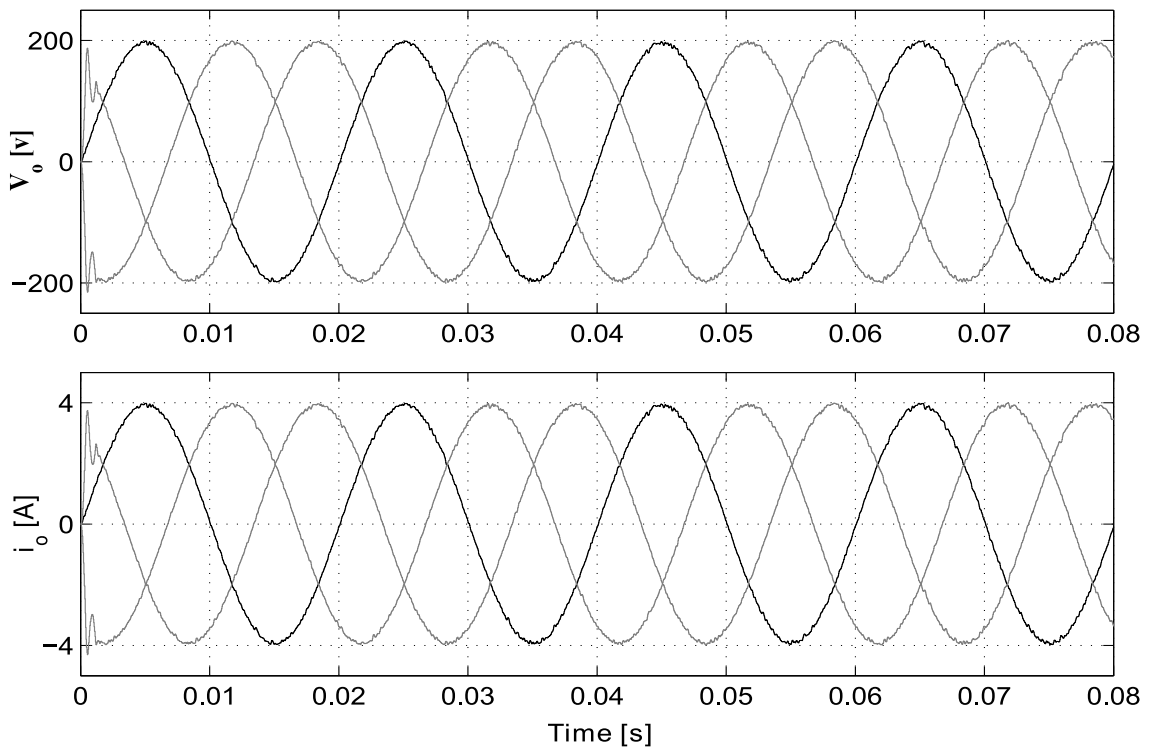


Figure 5.26: The simulated three phase output voltages and currents for the Improved MPC with 50- $\Omega$  load. Voltage THD: 0.74%.

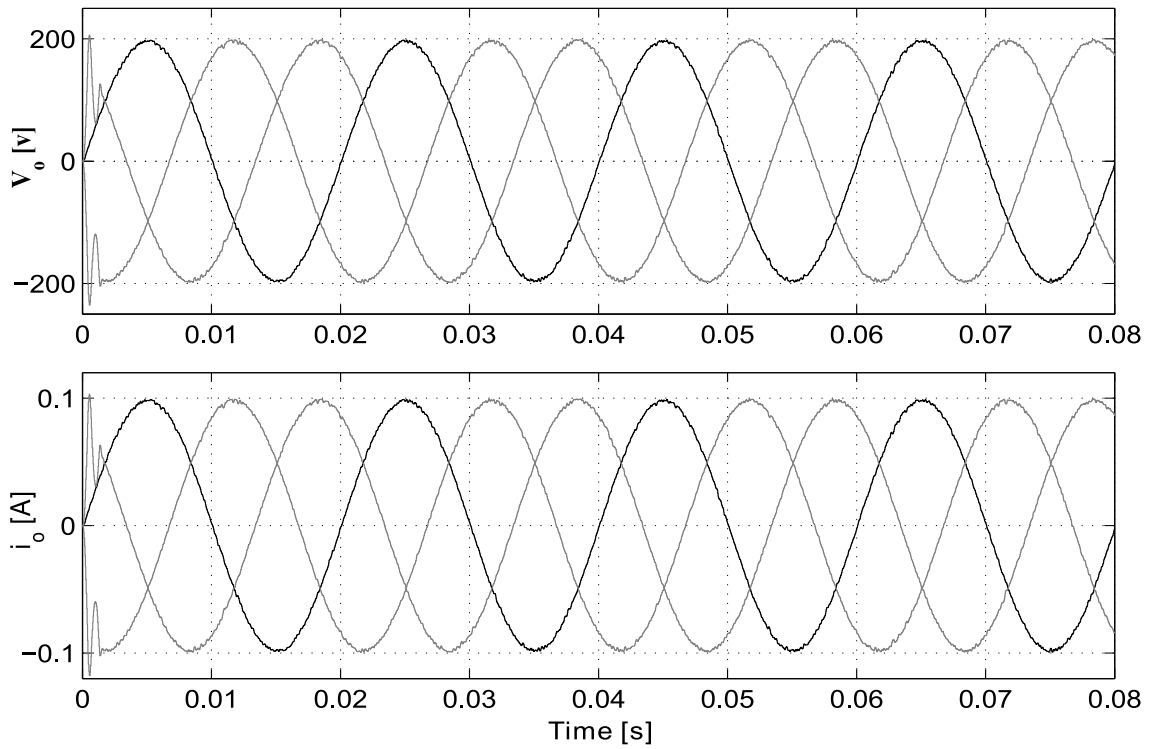


Figure 5.27: The simulated three phase output voltages and currents for the Improved MPC with 2-k $\Omega$  load. Voltage THD: 0.76%.

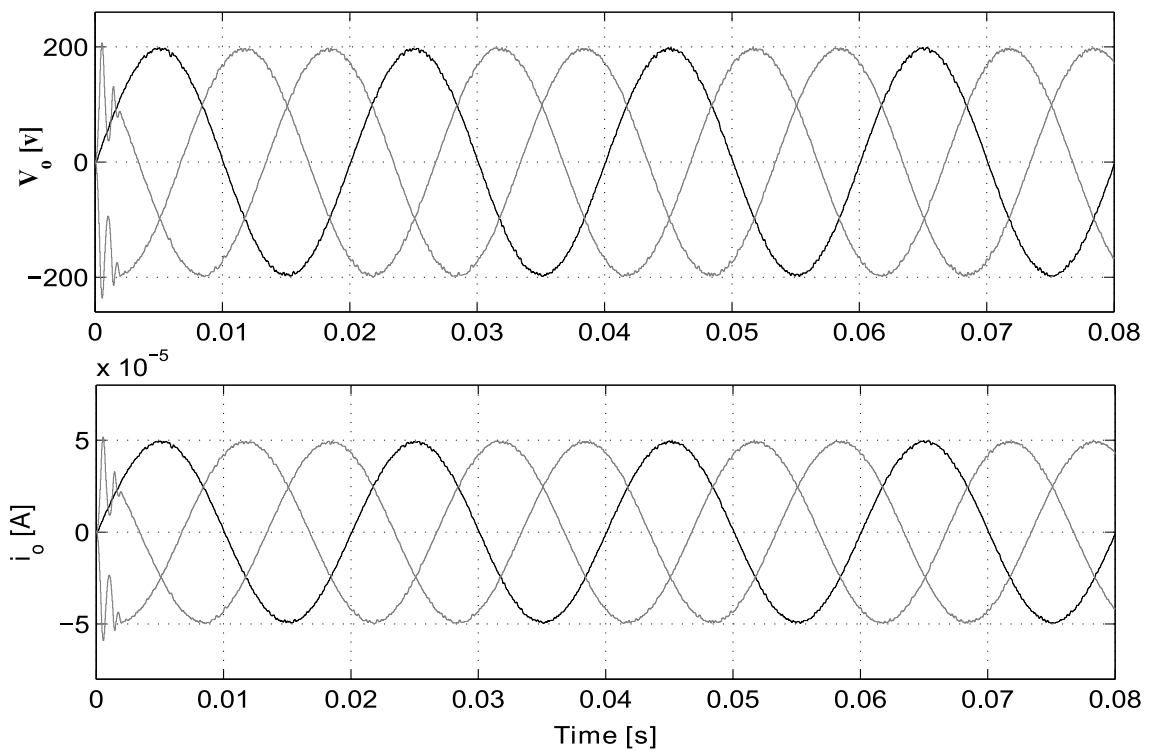


Figure 5.28: The simulated three phase output voltages and currents for the Improved MPC with 4-M $\Omega$  load. Voltage THD: 0.77%.

Table 5.3: A summary for different values of a resistive load

Resistive Load	Improved MPC		MPC	
$R$	THD %	$t_{settling}$ [msec]	THD %	$t_{settling}$ [msec]
20- $\Omega$	0.74	2	1.71	3
50- $\Omega$	0.74	2	2.30	5
0.1-k $\Omega$	0.74	2	2.74	11
0.5-k $\Omega$	0.74	2	3.16	16
1-k $\Omega$	0.74	2	3.32	20
2-k $\Omega$	0.76	2	3.84	35
4-M $\Omega$	0.77	2	6.12	40

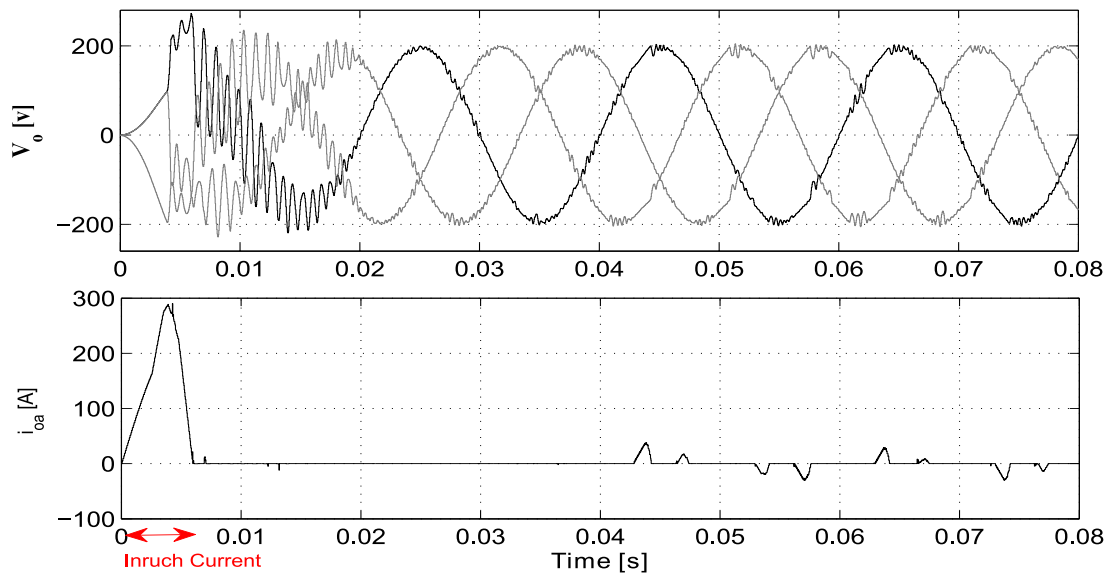


Figure 5.29: The simulated three phase output voltages and currents for a MPC with a nonlinear load of  $R = 60\Omega$  and  $C = 3000\mu F$ . Voltage THD: 2.34%.

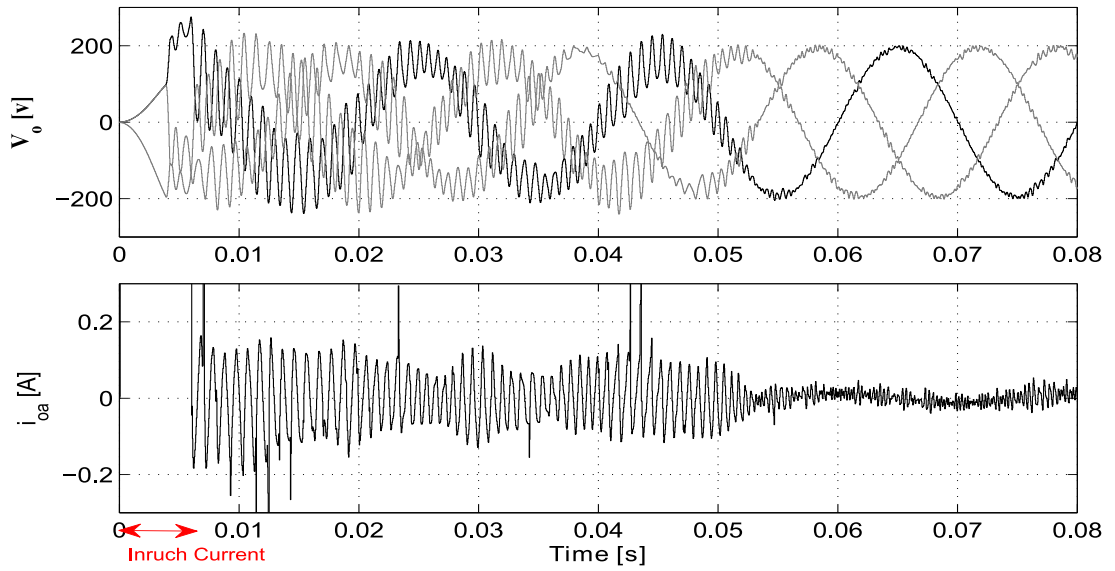


Figure 5.30: The simulated three phase output voltages and currents for a MPC with a nonlinear load of  $R = 1000\Omega$  and  $C = 3000\mu F$ . Voltage THD: 3.06%.

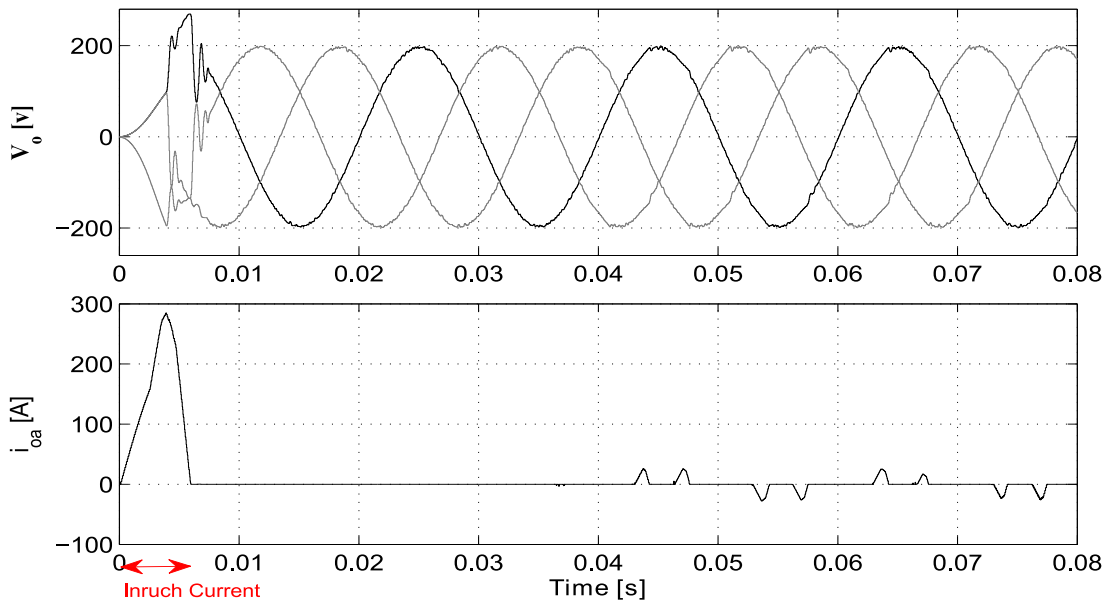


Figure 5.31: The simulated three phase output voltages and currents for the Improved MPC with a nonlinear load of  $R = 60\Omega$  and  $C = 3000\mu F$ . Voltage THD: 1.06%.

Table 5.4: A summary for the nonlinear load with different values of  $R$  and  $C$

Nonlinear Load	Improved MPC		MPC	
Change only the value of $R$ and $C = 3000\mu F$				
Value	THD %	$t_{settling}$ [msec]	THD %	$t_{settling}$ [msec]
30- $\Omega$	1.81	7	3.43	15
60- $\Omega$	1.06	9	2.34	20
100- $\Omega$	1	9	2.24	30
800- $\Omega$	0.71	8.8	3.93	38
1-k $\Omega$	0.75	8.8	3.06	55
Change only the value of $C$ and $R = 60\Omega$				
100 $\mu F$	1.18	3	1.41	9
500 $\mu F$	1.57	4	2.63	16
1000 $\mu F$	1.43	6	2.62	20
5000 $\mu F$	1.17	9	3.45	23

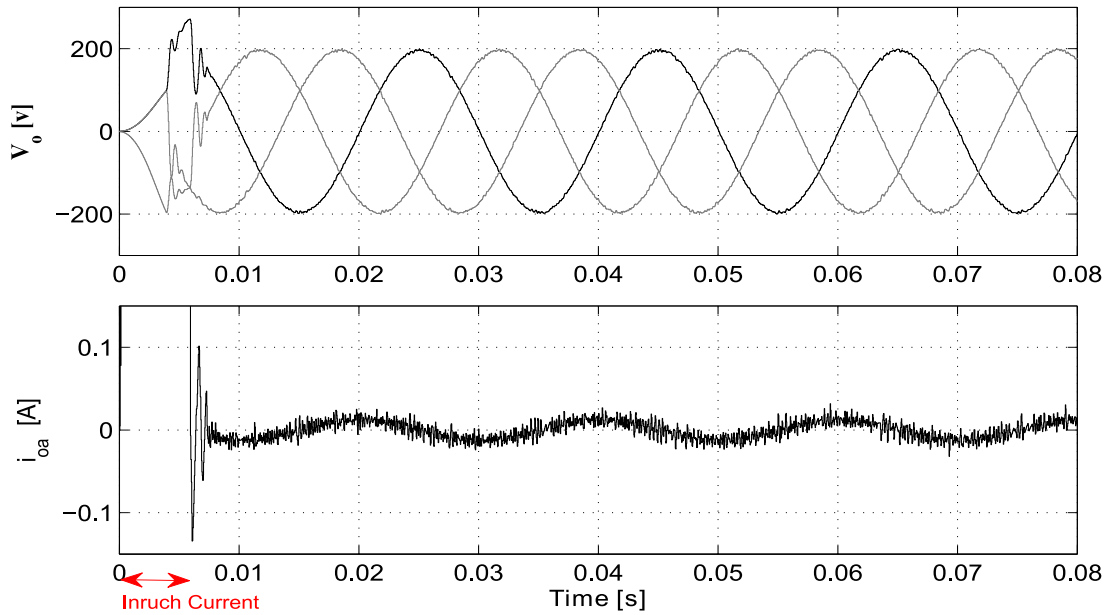


Figure 5.32: The simulated three phase output voltages and currents for the Improved MPC with a nonlinear load of  $R = 1000\Omega$  and  $C = 3000\mu F$ . Voltage THD: 0.75%.

## 5.2 Hardware Testing

Today there are various methodologies for developing digital systems. These methodologies include the processes for tuning, validating, and verifying systems. System development testing is mainly done using two approaches. First, the functionality and performance of the system is observed and tuned using software simulation tools. Second, the design is deployed on a target platform to verify the functionality and measure the performance under more realistic conditions. This approach is also known as “hardware testing”. In this section, we will present the HIL methodology as complementary approach to software simulation and hardware testing. The example in this section focus mainly on the proposed system as shown in Figure 3.1.

### 5.2.1 System Verification Using Software Simulation

Software simulation offers a flexible approach to system verification. It allows you to run through a variety of system behavior and scenarios. However, this approach is limited and is not sufficient for a real system due to the following reasons:

- System design runtime can be extremely long when simulations are performed on a reasonably big system. For example, in electro-mechanical systems, the time constants of a mechanical system can be measured in seconds while the digital computation rate is measured in nanoseconds.
- Significant inaccuracies might occur due to the uncertainties of a system model. The system model might not be known or completely characterized. It might contain different nonlinear components and environment disturbances that are very difficult to measure and characterize.
- A complementary verification flow might still be needed to verify the design to obtain reliability certification. This is especially true with modern flows that involve high-level synthesis tools [102].

### 5.2.2 System Verification Using Hardware Testing

Hardware testing allows you to deploy the design on target and observe the performance of the design under real-life conditions. However, this approach, too, has its own challenges, as highlighted below:

- Usually only the desired scenario is tested. It is difficult to observe the system behavior in “something went wrong” scenarios because the complete hardware test involves external system components that are pre-defined as well. Other system components do not always allow flexibility in the stimulus that can be applied to the design under test (DUT).
- The availability of a hardware platform is also a concern. The final implementation platform is not always available during the initial design phases.
- The cost of verification is a direct result of final hardware availability. The test time on a hardware platform can be expensive, so it may be shared between multiple

users, departments, or divisions. However, this method might eventually cause less verification coverage.

- Safety is another critical aspect of hardware testing, especially during the initial phases of the design when there are uncertainties in multiple system components. Hardware testing on multiple system components puts significant burden on designers as it requires careful test planning and damage mitigation [103], [104], [102].

### 5.2.3 Hardware-in-the-Loop (HIL) Simulation

Hardware-in-the-loop (HIL) simulation or HIL testing is a technique that is used in the development and test of complex process systems. HIL simulation provides an effective platform by adding the complexity of the plant under control to the test platform. The complexity of the plant under control is included in test and development by adding a mathematical representation of all related dynamic systems. These mathematical representations are referred to as the “plant simulation”. The HIL process has existed for no more than 15 years. The use of a HIL process is becoming more prevalent in all industries is driven by two major factors: time to market and complexity.

HIL simulation is a kind of real-time simulation that the input and output signals shows the same time dependent values as the real process. The HIL require cooperation between the host and target. It is usually used in a laboratory environment on the ground to test the prototype controller under different working loads and conditions conveniently and safely. Compared with numerical simulation, HIL simulation is more reliable and credible because numerical simulation is often operated in ideal circumstances, without considering noise, disturbance, and some practical problems often ignored which might result in fatal failure. HIL simulation has the advantages of reducing the risk, shortening the developing time, and being well suitable for critical and hazardous applications [104], [102].

The main purpose of the HIL Simulation is to test the hardware device on a simulator before we implement it on the real process. You may want to test the different part of the system individually to make sure it works as planned and HIL simulation is important in design and testing of the different systems. It may be very useful, e.g., to test a controller function with a simulated process before the controller is applied to the real (physical) process. Another benefit of HIL is that testing can be done without damaging equipment or endangering lives. HIL simulation is more efficient and required [103]. When perform testing, we have a lot of challenges:

- Cost to test and cost of failure
- Availability
- System variation
- Repeatability

In these situations HIL simulation is a powerful technique. With HIL Testing we will reduce cost and risk. With HIL Testing cost and risk will be reduced due to the following reasons:

- Increased reliability and quality
- More efficient development
- Lower cost to innovate

The main steps in HIL Simulation are as follows:

**1. Develop a mathematical or simulation model**

First step is to simulate your system in software make sure that it works as planned. Then, create a mathematical model of the real environment where the hardware device is meant to be used.

**2. HIL Simulation (Software + Hardware)**

Test your system on a simulated process such as HIL simulation to verify the functionality and measure the performance under more realistic conditions.

**3. Implement your hardware on the Real Process (Hardware only)**

If everything is OK, you may want to implement your hardware system in the real environment where it meant to be used.

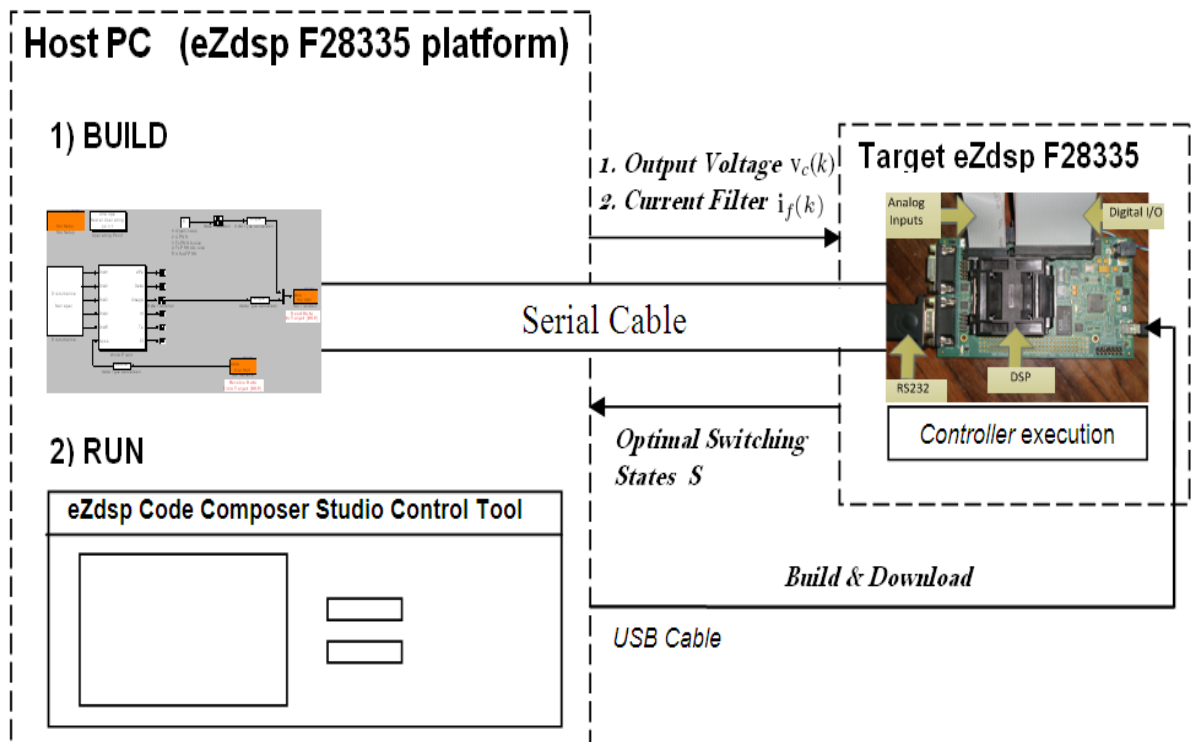


Figure 5.33: The schematic diagram of the proposed HIL platform.

## 5.2.4 Experimental Results

In this section, On-target rapid prototyping technique was used to implement the proposed MPC for three phase inverter with *LC* filter. Hardware-in-the-loop testing (HIL) was used

to verify and validate the proposed MPC for the proposed system. Figure 5.33 illustrates the basic components and signal flows of the HIL simulation for the proposed system. For a typical HIL simulation, the proposed MPC is implemented on eZdsp F28335, as shown in Figure 5.36, and the three phase inverter with  $LC$  filter and its different loads are simulated on the Host-PC as shown in Figure 5.35. However, the system is flexible in that each component can be implemented on eZdsp F28335. The system requirements, Code Composer Studio installation, and connection to PC are shown in [105].

The HIL simulator is programmed using Matlab, Simulink, Target Support Package, and C++. Figure 5.33 illustrates the flow of information during the setup and execution of the proposed system. To setup a HIL simulation, we first configure the Host PC-Target connection. Next, we build a model using standard Simulink blocks, and add a combination of the data conversions, rate transition, send data, receive data and host setup blocks from the Target support package toolbox into the Simulink model. These Target blocks provide the link between the Simulink model and real world devices.

Once the Simulink model has been created, the model is executed from the Matlab Simulink window. This tool provides the interface between the Host-PC and target during both build and run time. The real-time C-code is generated with the Build button, which automates the compiling and uploading process. Since the entire build-and-upload sequence is automated and executed with a single click of the Build button, rapid prototyping and re-compiling of control algorithms is fast, easy, and does not require any knowledge of C programming. After building the model on the target, we get the following linking error as shown in Figure 5.34. This screen indicates that the Build complete and refers to errors, if they exist.

To run a simulation, the Host-PC is first running which containing the plant system. Once the Target is running, the C code is built in the Host-PC and uploaded to memory in the target. The HIL simulation require co-operation between the Host-PC and target and the interaction is done using serial port such as RS232 cable. As a result, the Host-PC transmits, using SCI Transmit block, the output voltage  $v_c$  and the filter current  $i_f$  to the eZdsp F28335. The eZdsp F28335 receives, using SCI Receive block, these signals and the proposed MPC selects the optimal switching state which applied in the next instant. After thus, the Host-PC receives the optimal switching state  $S$  to fed the IGBTs. This procedure will repeat every sampling time  $T_s$ . No software runs on the target other than the target operating system and target application at run time, eliminating interruptions and subroutines typical of windows operating systems which would hamper real-time processing and control. The target application can be controlled from either the Host-PC or the target software, and data can be logged while the application is running or after it stops. Model parameters can be modified in real time without stopping the program execution. This allows for tuning system performance on the fly, which can make control design a quick, efficient, and relatively pain-free process. To sum up, we can conclude the HIL design procedures in the following steps:

1. Install hardware such as CCS and system requirements.
2. Connect electrical power and signals.
3. Setup host-target communication such as RS232 cable.

4. Open the Host Simulink program and Target model after adding the required blocks from the Target support package toolbox.
5. Build the Target model and running the Host program.

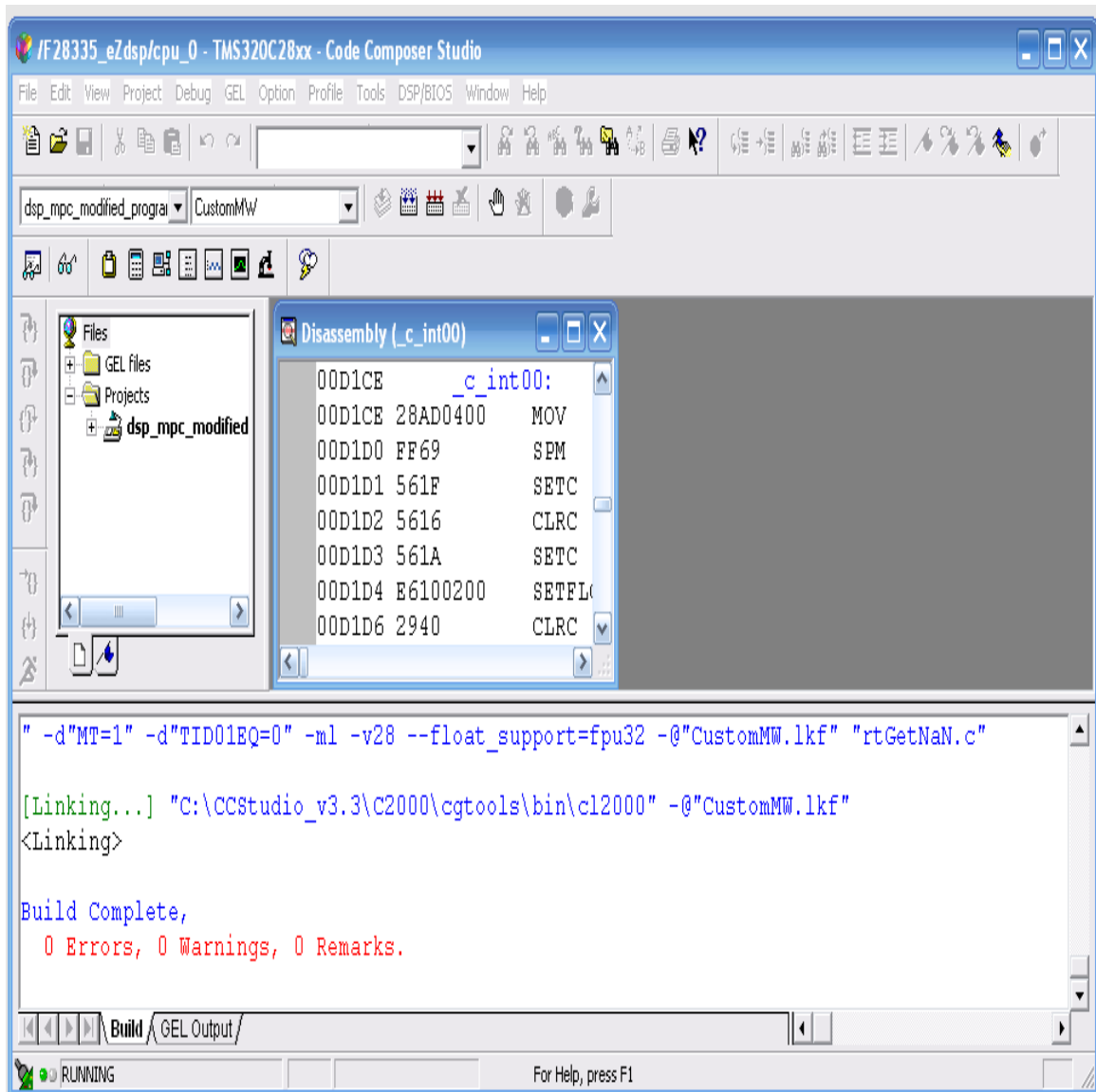


Figure 5.34: The Code Composer Studio (CCS) screen.

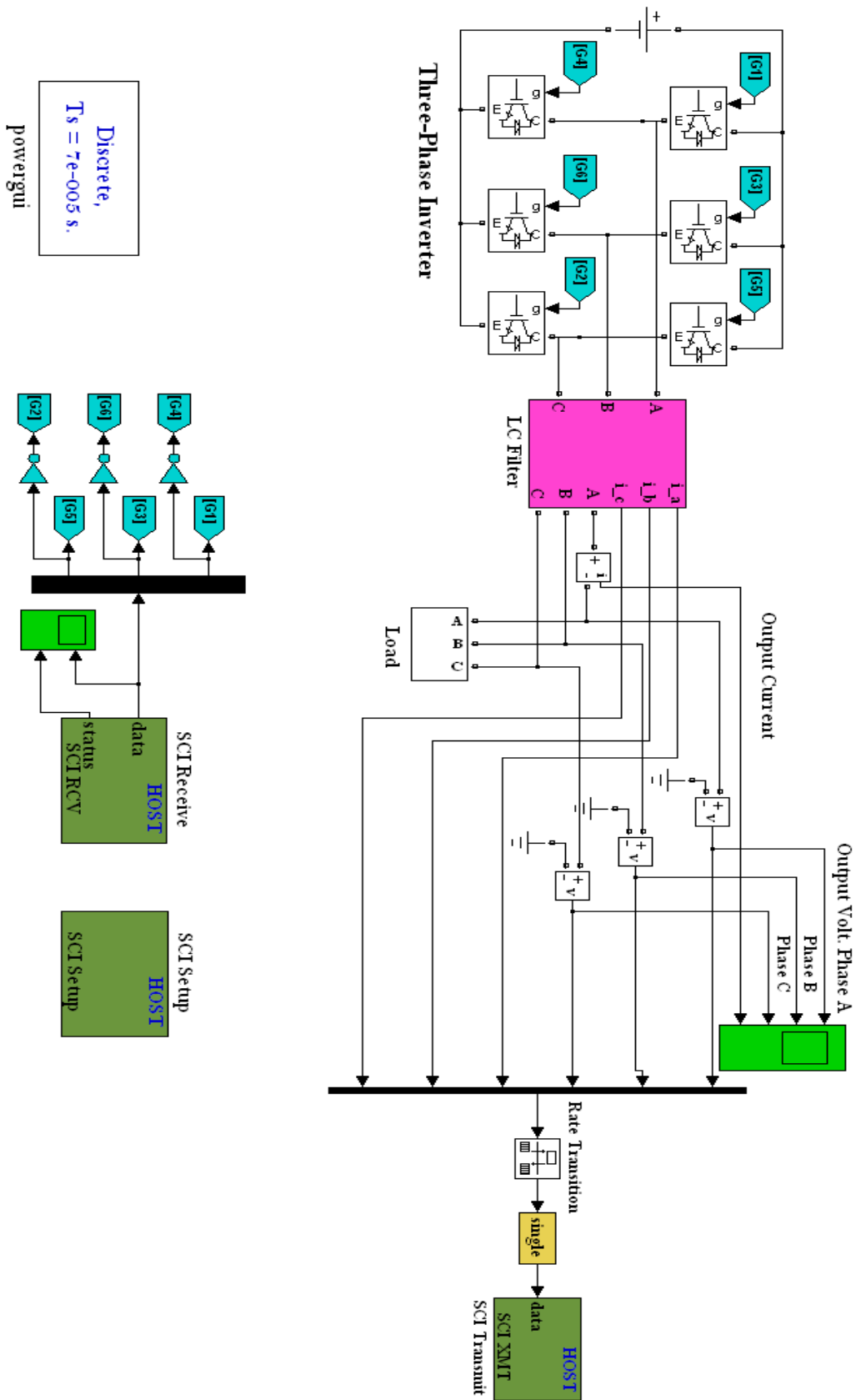


Figure 5.35: The Host-PC program for a three phase inverter with *LC* filter using HIL simulation.

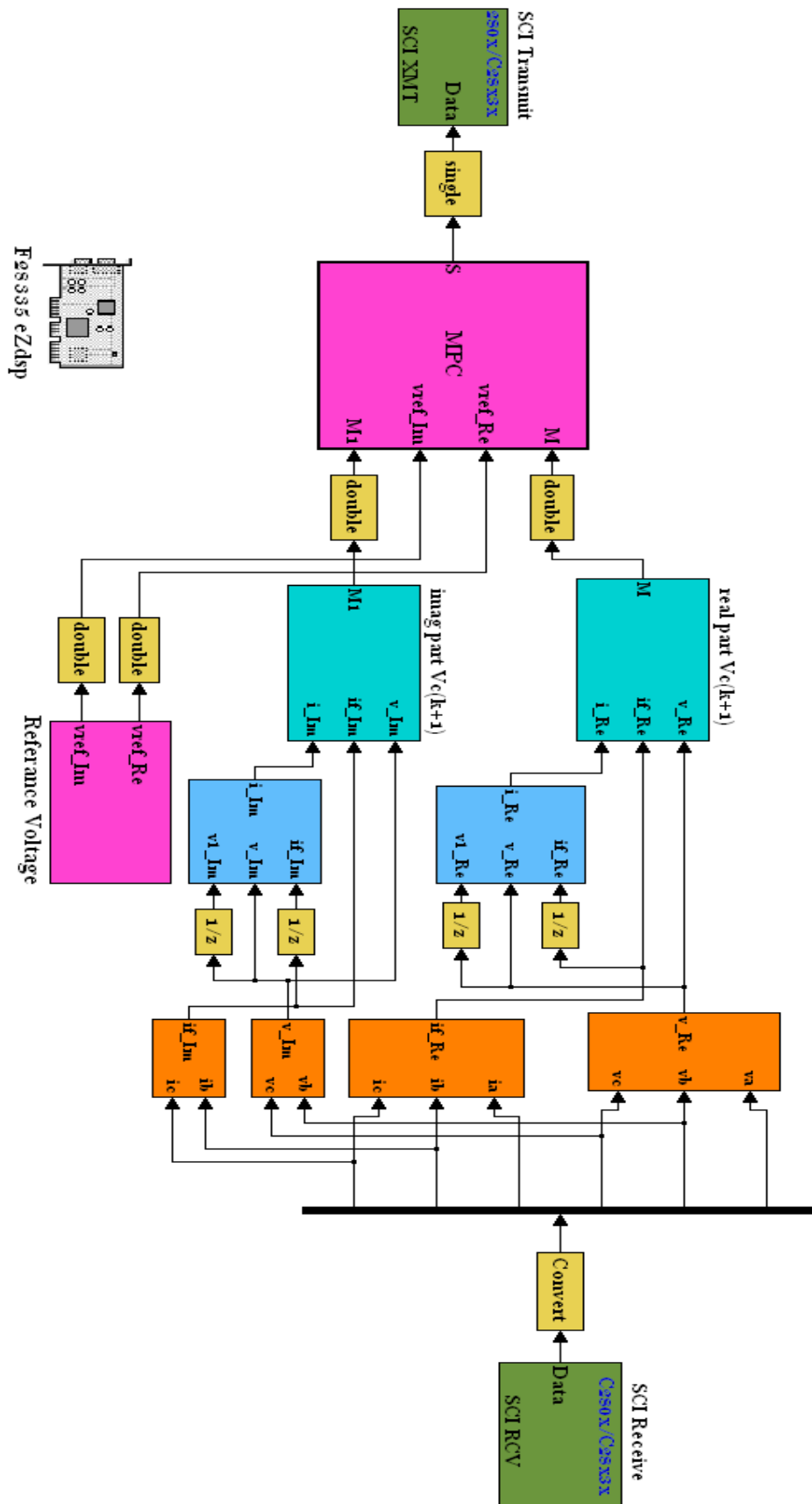


Figure 5.36: The implementation of the proposed MPC on eZdsp F28335 Kit.

Experimental results of the system shown in Figure 3.1 were carried out for resistive and nonlinear loads, using HIL testing, to verify the proposed MPC for a three phase inverter. The parameters of the system are shown in Table 5.5.

Table 5.5: System Parameters

Parameter	Value
DC link voltage $V_{dc}$	520 [V]
Filter capacitor $C$	500 [ $\mu$ F]
Filter inductance $L$	50 [mH]
Sampling time $T_s$	70 [ $\mu$ s]
Reference voltage amplitude	200 [V]
Reference voltage frequency	50 [Hz]

The behavior of the proposed MPC for a resistive load of 20- $\Omega$  using simulation and HIL testing are shown in Figure 5.37 and Figure 5.38, respectively. It is observed that, the output voltages are sinusoidal with low distortion. Also, the behavior of the proposed MPC for a resistive load of 100- $\Omega$  using simulation and HIL testing are shown in Figure 5.39 and shown in Figure 5.40, respectively. It is observed that, the output voltages reach to the steady state operation after 0.3sec (15cycles) in two cases. A comparison between the simulation and experimental results for different values of resistive load using MPC are shown in Table 5.6. It is observed that, the THD can be considered constant due to the small variation in experimental results. Moreover, the proposed MPC was stable and generated output voltage with minimum THD till  $R = 1k\Omega$  due to the selected values of  $L$  and  $C$  of  $LC$  filter.

The diode-bridge rectifier, with values  $R = 35\Omega$  and  $C = 30\mu$ F, shown in Figure 5.5 was used as nonlinear load. The behavior of the proposed MPC for a nonlinear load using simulation and HIL testing are shown in Figure 5.41 and Figure 5.42, respectively. Here, the output voltages and the filter currents, as shown in Figure 5.43 and Figure 5.44, are sinusoidal with low distortion, despite the highly distorted load currents, with the same THD.

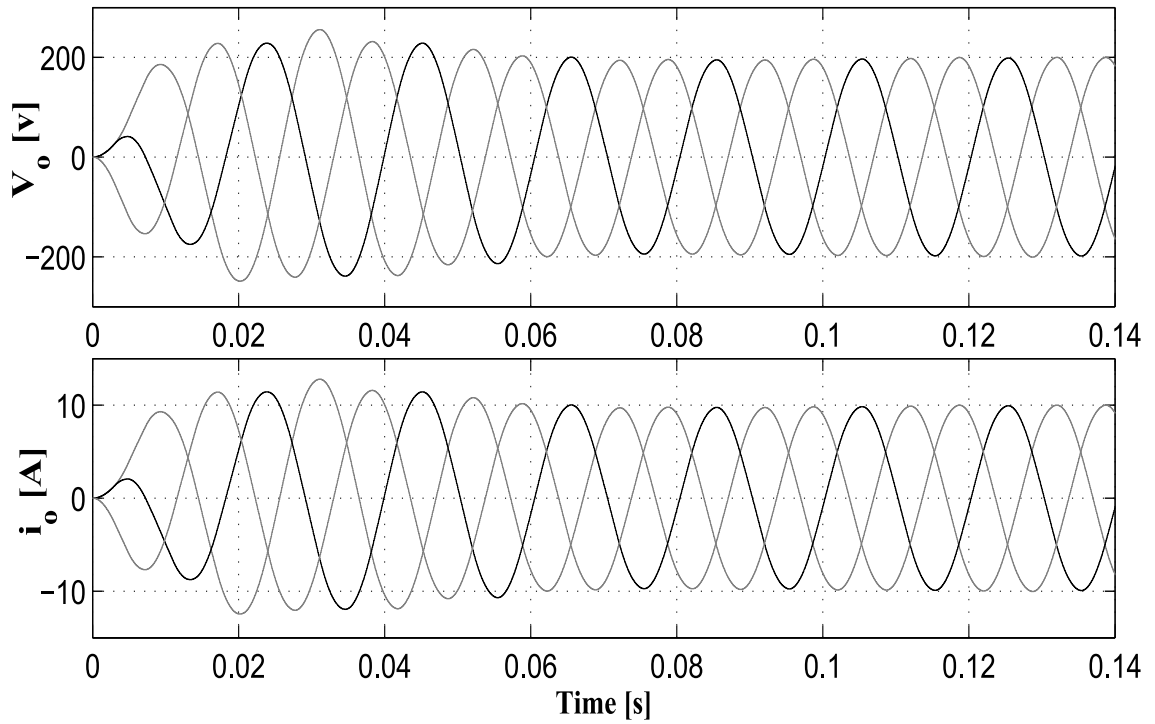


Figure 5.37: The simulated three phase output voltages and currents for a MPC with resistive load of  $20\text{-}\Omega$  load. Voltage THD: 0.57%.

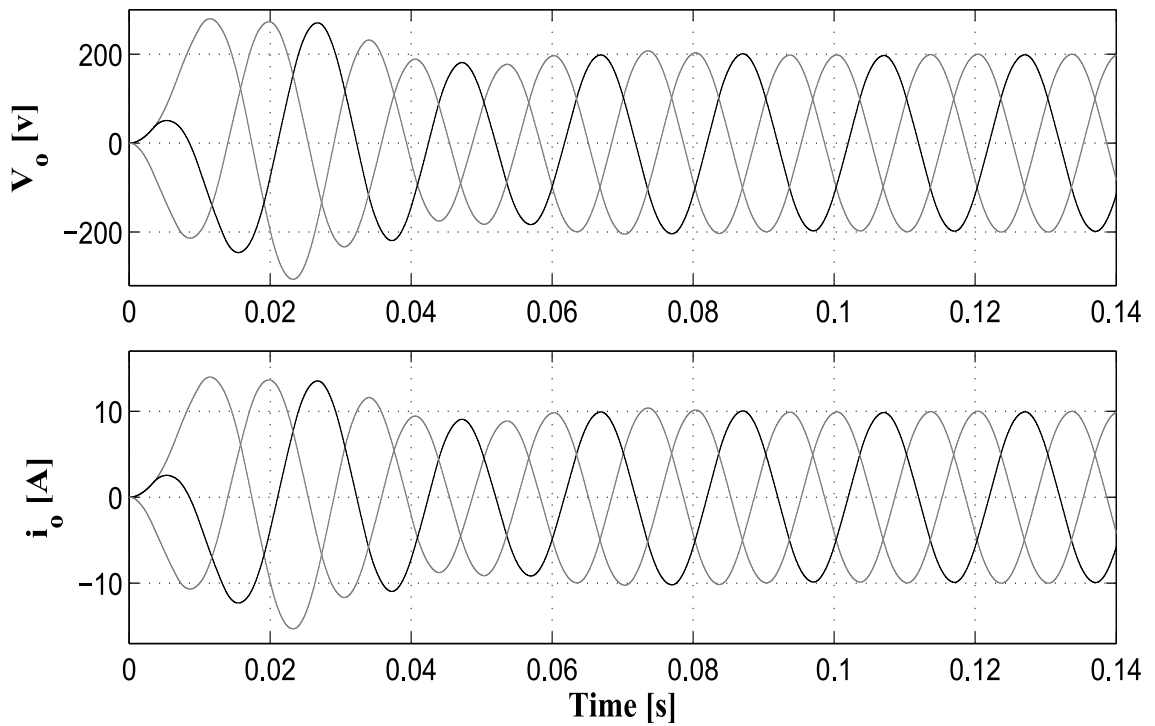


Figure 5.38: The experimental three phase output voltages and currents for a MPC with resistive load of  $20\text{-}\Omega$  load. Voltage THD: 0.7%.

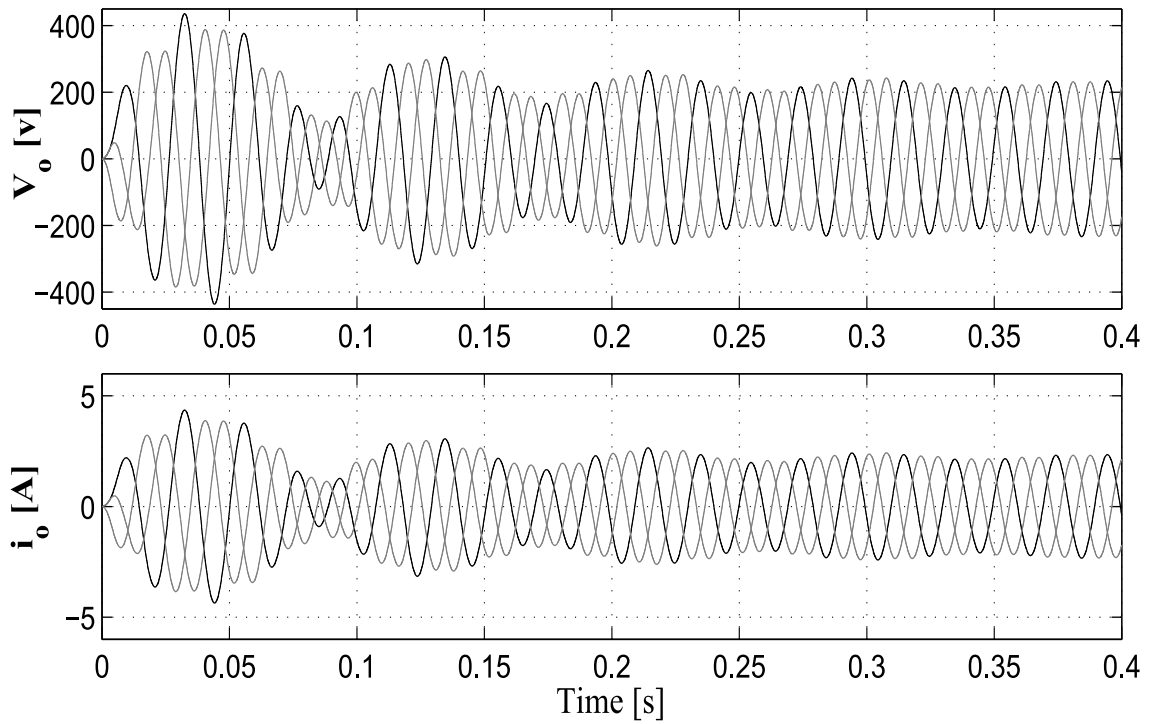


Figure 5.39: The simulated three phase output voltages and currents for a MPC with resistive load of  $100\text{-}\Omega$  load. Voltage THD: 1.44%.

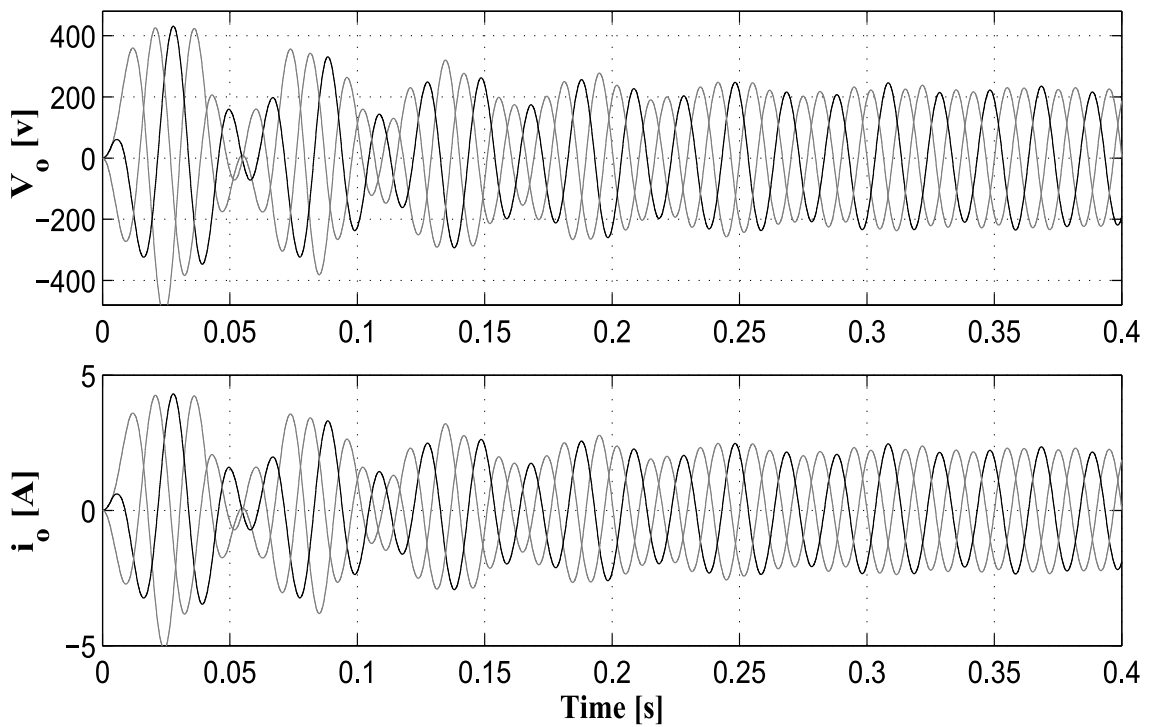


Figure 5.40: The experimental three phase output voltages and currents for a MPC with resistive load of  $100\text{-}\Omega$  load. Voltage THD: 1.7%.

Table 5.6: A comparison between simulation and experimental results for different values of a resistive load

Resistive Loads	Simulation Results (THD %)	Experimental Results (THD %)
20- $\Omega$	0.57	0.7
50- $\Omega$	0.6	0.8
100- $\Omega$	1.44	1.7
200- $\Omega$	2.36	2.43

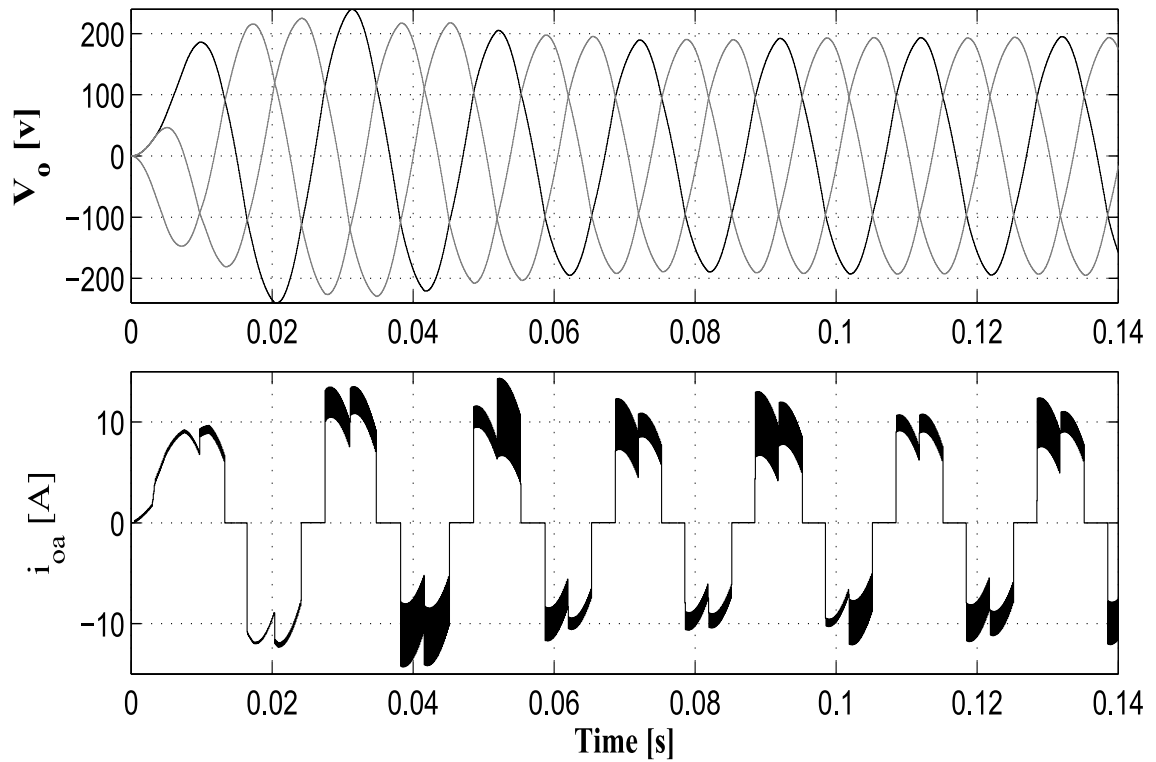


Figure 5.41: The simulated three phase output voltages and currents for a MPC with a nonlinear load. Voltage THD: 1.9 %.

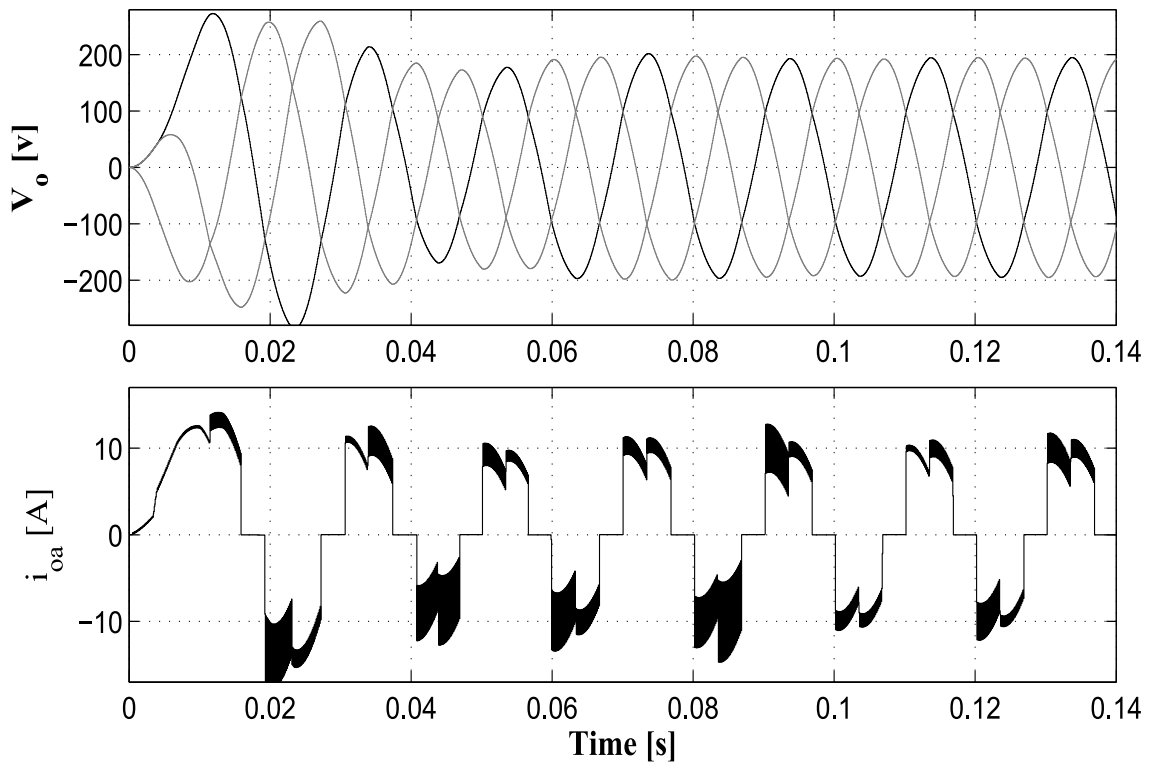


Figure 5.42: The experimental three phase output voltages and currents for a MPC with a nonlinear load. Voltage THD: 1.98 %.

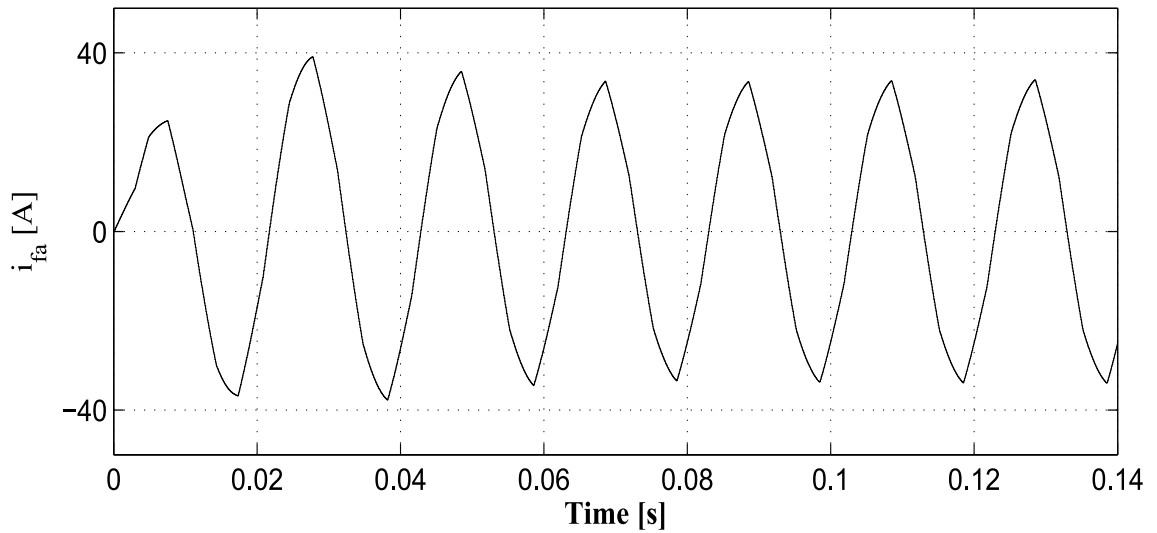


Figure 5.43: The simulated filter current for a MPC with a nonlinear load. Current THD: 3.07%.

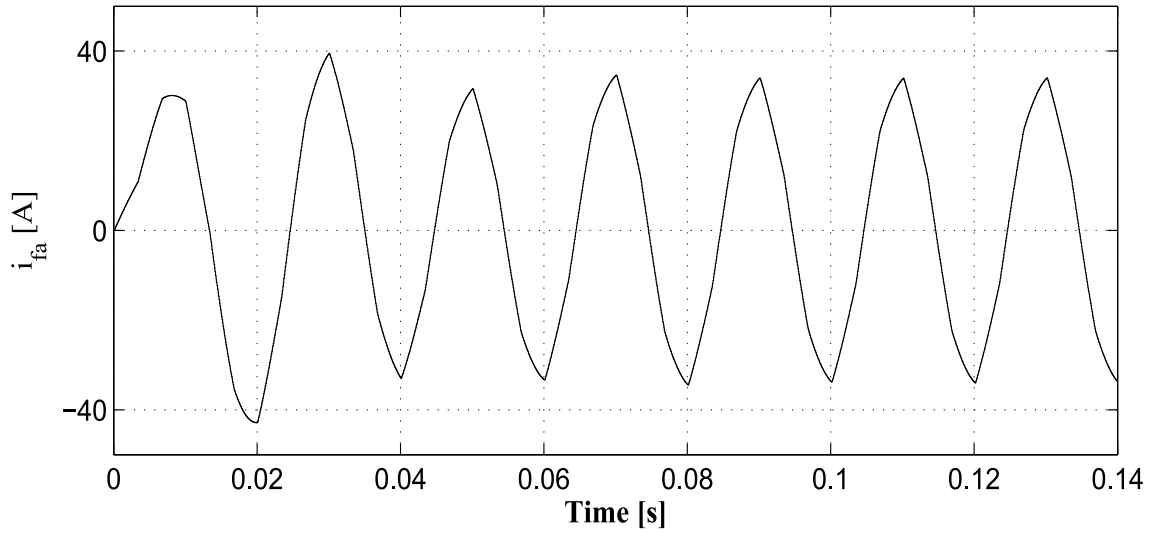


Figure 5.44: The experimental filter current for a MPC with a nonlinear load. Current THD: 3.07%.

Some of modifications are carried out on the previous simulation program, as shown in Chapter 4, of the proposed MPC to improve the performance of the system with DSP in HIL tsetting such as:

1. Change the sampling time from  $T_s = 33\mu s$  to  $T_s = 70\mu s$  to speed up the simulation process and reduce data loss during transmission and reception through serial port.
2. Use the Optimized Blocks (such as C28x IQmath) from Simulink Library Browser to optimize the performance of MPC with DSP.

After these modifications it is observed that the previous simulation values,  $L = 2.4mH$  and  $C = 40\mu F$ , of the  $LC$  filter, as shown in Table 5.1, are unacceptable for the experimental work because the THD of the output voltages increased, so we used the modified values as shown in Table 5.5. For example, the simulated THD for a resistive load of  $20-\Omega$  with  $T_s = 70\mu s$ ,  $L = 2.4mH$ ,  $C = 40\mu F$ , and according to the previous modifications is 6%, as shown in Figure 5.45.

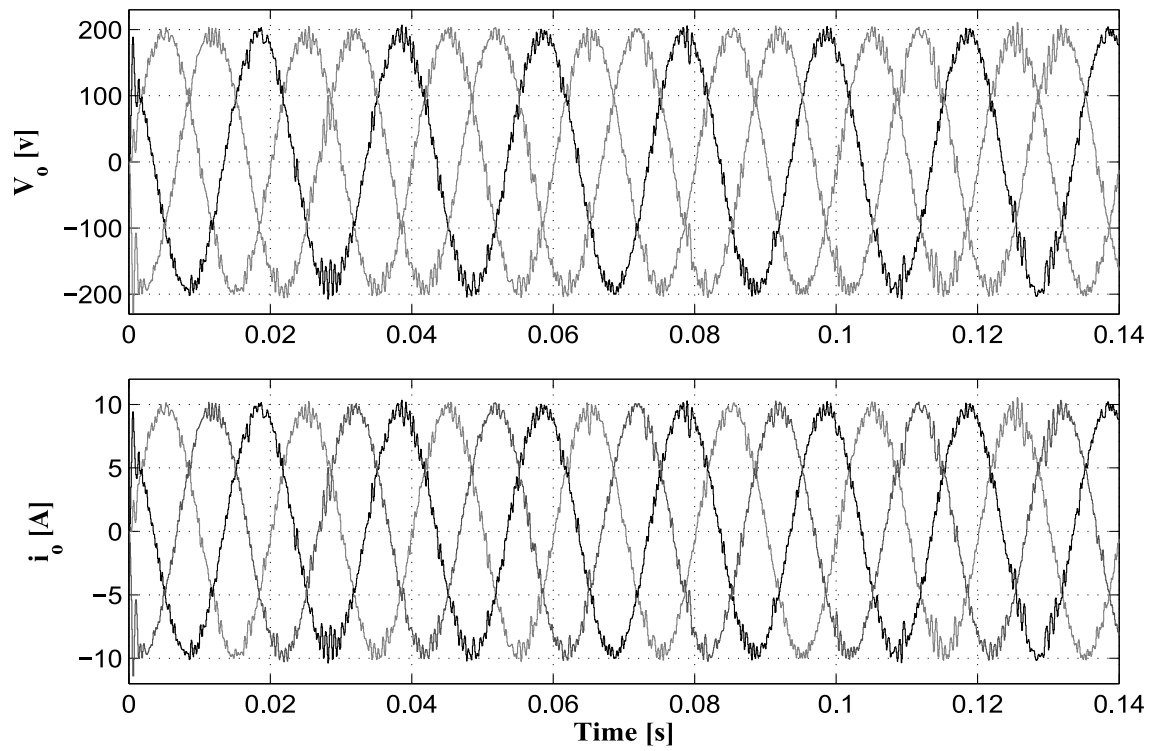


Figure 5.45: The simulated three phase output voltages and currents for a MPC with resistive load of  $20\text{-}\Omega$  and according to the previous modifications. Voltage THD: 6%.

# Chapter 6: Conclusions and Future Work

In this work, a new and simple control scheme was presented for a three phase inverter with output *LC* filter. Results show that the proposed scheme achieves a good voltage regulation with linear loads as well as with nonlinear loads. The proposed controller has no parameters to adjust; it needs a model of the system for calculating predictions of the controlled variables. The gate-drive signals are generated directly by the controller, so a modulator is not needed. The output voltage is directly controlled, without using a cascaded control structure, with an inner current-control loop. This allows for a fast dynamic response of the voltage control. The effect of changing the system parameters values has been studied by means of simulation, achieving a good voltage regulation, with linear loads and nonlinear loads, even with changes of  $-50\%$  and  $+150\%$  in the capacitor value. It is observed that, the performance of the proposed MPC is improved when the value of the filter capacitance increased.

The performance of the proposed predictive control method is compared with hysteresis and PWM control under linear and nonlinear loads. Results show that the proposed scheme achieves a good voltage regulation with linear loads as well as with nonlinear loads compared with classical methods. Also, results show that the classical methods failed to control the output voltage, and the UPS does not work for a nonlinear loads due to a higher distortion. Furthermore, the performance for a linear loads is very bad.

The Improved MPC for an UPS system considering two prediction steps is presented and is compared with MPC with one prediction step. It is observed that, the behavior of the system improves when a higher number of prediction steps is considered. On the other hand, the number of calculations increases exponentially. The problem of high number of calculations can be simplified by considering the same voltage vector is applied during several sampling periods.

The simulation results show that the performance of the Improved MPC is better than the case of MPC. It is observed, for different values of resistive load, that the changing of resistive load value leads to change the value of output voltage THD and settling time, in the case of MPC. On the other hand, the THD and settling time for the Improved MPC can be considered constant due to the small variation and are not changed with different values of resistive load. For different values of non linear load, the improvement of the Improved MPC can be noticed in the lower THD and in less settling time. The output voltage takes almost 10 msec to reach steady state operation for different values of non linear load.

Hardware testing allows you to implement the design on target and observe the performance of the design under real-life conditions. So, the experimental results, using HIL testing, are carried out for linear and nonlinear loads, to verify the proposed MPC using ezdsp F28335 Kit. It is observed that, the performance of the proposed MPC is very close to that in the simulation. Finally, the proposed MPC is applicable for systems with different frequencies and can be applied without major changes to any type of converter and variables to be controlled.

The future work will take into consideration the delay of calculations for MPC and its solution. Moreover, it will take into consideration the design of the *LC* filter and its optimal values. The three phase inverter will be built in laboratory using ezdsp F28335

Kit, totally, to verify the proposed MPC and the Improved MPC. It is possible to design an observer to estimate the output current  $i_o(k)$ . This observer will improve the system performance.

# References

- [1] M. Nikolaou, *Model predictive controllers: A critical synthesis of theory and industrial needs*, *Advances in Chemical Engineering*, vol. 26. Academic Press, 2001.
- [2] E. F. Camacho and C. Bordons, *Model Predictive Control*. New York: Springer-Verlag, 1999.
- [3] J. M. Maciejowski, *Predictive Control With Constraints*. Englewood Cliffs, NJ: Prentice-Hall, 2002.
- [4] M. Masten and I. Panahi, “Digital signal processors for modern control systems,” *Control Eng. Practice*, vol. 5, no. 4, pp. 449–458, 1997.
- [5] IEEE std 519-1992, “IEEE recommended practices and requirements for harmonic control in electric power systems,” in *Institute of Electrical and Electronics for Engineerings*, Inc. 1993.
- [6] J. Rodriguez, J. Pontt, C. A. Silva, P. Correa, P. Cortes, and U. Ammann, “Predictive current control of a voltage source inverter,” *IEEE Trans. Ind. Electron.*, vol. 54, pp. 495–503, Feb. 2007.
- [7] J. M. Carrasco, L. G. Franquelo, J. T. Bialasiewicz, E. Galvan, R. C. PortilloGuisado, M. A. M. Prats, J. I. Leon, and N. Moreno-Alfonso, “Power–electronic systems for the grid integration of renewable energy sources: A survey,” *IEEE Trans. Ind. Electron.*, vol. 53, pp. 1002–1016, Jun. 2006.
- [8] F. Blaabjerg, R. Teodorescu, M. Liserre, and A. V. Timbus, “Overview of control and grid synchronization for distributed power generation systems,” *IEEE Trans. Ind. Electron.*, vol. 53, pp. 1398–1409, Oct. 2006.
- [9] I. S. Mohamed, S. A. Zaid, M. F. Abu-Elyazeed, and H. M. Elsayed, “Model predictive control –a simple and powerful method to control UPS inverter applications with output LC filter,” in *Saudi International Electronics, Communications and Photonics Conference (SIECPC’13)*, (Riyadh), pp. 1–6, 27-30 Apr. 2013.
- [10] P. Cortes, G. Ortiz, J. I. Yuz, J. Rodriguez, S. Vazquez, and L. G. Franquelo, “Model predictive control of an inverter with output LC filter for UPS applications,” *IEEE Trans. Ind. Electron.*, vol. 56, pp. 1875–1883, Jun. 2009.
- [11] J. Holtz, “Pulsewidth modulation electronic power conversion,” *Proc. IEEE*, vol. 82, pp. 1194–1214, Aug. 1994.
- [12] N. Mohan, T. M. Undeland, and W. P. Robbins, *Power Electronics*. New York: Wiley, 2nd ed., 1995.
- [13] O. Kukrer, “Deadbeat control of a three–phase inverter with an output LC filter,” *IEEE Trans. Power Electron.*, vol. 11, pp. 16–23, Jan. 1996.

- [14] M. Kojima, K. Hirabayashi, Y. Kawabata, E. C. Ejiogu, and T. Kawabata, "Novel vector control system using deadbeat-controlled PWM inverter with output LC filter," *IEEE Trans. Ind. Appl.*, vol. 40, pp. 162–169, Jan./Feb. 2004.
- [15] P. Mattavelli, "An improved deadbeat control for UPS using disturbance observers," *IEEE Trans. Ind. Electron.*, vol. 52, pp. 206–212, Feb. 2005.
- [16] P. C. Loh, M. J. Newman, D. N. Zmood, and D. G. Holmes, "A comparative analysis of multiloop voltage regulation strategies for single and three-phase UPS systems," *IEEE Trans. Power Electron.*, vol. 18, pp. 1176–1185, Sep. 2003.
- [17] P. C. Loh and D. G. Holmes, "Analysis of multiloop strategies for *LC/CL/LCL*-filtered voltage-source and current-source inverters," *IEEE Trans. Ind. Appl.*, vol. 41, pp. 644–654, Mar./Apr. 2005.
- [18] S. Buso, S. Fasolo, and P. Mattavelli, "Uninterruptible power supply multiloop control employing digital predictive voltage and current regulators," *IEEE Trans. Ind. Appl.*, vol. 37, pp. 1846–1854, Nov./Dec. 2001.
- [19] A. Kulka, T. Undeland, S. Vazquez, and L. G. Franquelo, "Stationary frame voltage harmonic controller for standalone power generation," in *Proc. Eur. Conf. Power Electron. Appl.*, pp. 1–10, Sep. 2007.
- [20] M. N. Marwali and A. Keyhani, "Control of distributed generation systems-part I: Voltages and currents control," *IEEE Trans. Power Electron.*, vol. 19, pp. 1541–1550, Nov. 2004.
- [21] G. Escobar, A. A. Valdes, J. Leyva-Ramos, and P. Mattavelli, "Repetitive based controller for a UPS inverter to compensate unbalance and harmonic distortion," *IEEE Trans. Ind. Electron.*, vol. 54, pp. 504–510, Feb. 2007.
- [22] G. Willmann, D. F. Coutinho, L. F. A. Pereira, and F. B. Libano, "Multiple-loop H-infinity control design for uninterruptible power supplies," *IEEE Trans. Ind. Electron.*, vol. 54, pp. 1591–1602, Jun. 2007.
- [23] P. Cortes, M. P. Kazmierkowski, R. M. Kennel, D. E. Quevedo, and J. Rodriguez, "Predictive control in power electronics and drives," *IEEE Trans. Ind. Electron.*, vol. 55, Dec. 2008.
- [24] G. Bode, P. C. Loh, M. J. Newman, and D. G. Holmes, "An improved robust predictive current regulation algorithm," *IEEE Trans. Ind. Appl.*, vol. 41, pp. 1720–1733, Nov./Dec. 2005.
- [25] S.-M. Yang and C.-H. Lee, "A deadbeat current controller for field oriented induction motor drives," *IEEE Trans. Power Electron.*, vol. 17, pp. 772–778, Sep. 2002.
- [26] L. Malesani, P. Mattavelli, and S. Buso, "Robust dead-beat current control for PWM rectifier and active filters," *IEEE Trans. Ind. Appl.*, vol. 23, pp. 613–620, May/Jun. 1999.

- [27] J. Mossoba and P. W. Lehn, "A controller architecture for high bandwidth active power filters," *IEEE Trans. Power Electron.*, vol. 18, pp. 317–325, Jan. 2003.
- [28] P. Mattavelli, G. Spiazzi, and P. Tenti, "Predictive digital control of power factor preregulators with input voltage estimation using disturbance observers," *IEEE Trans. Power Electron.*, vol. 20, pp. 140–147, Jan. 2005.
- [29] A. Nasiri, "Digital control of three-phase series-parallel uninterruptible power supply systems," *IEEE Trans. Power Electron.*, vol. 22, pp. 1116–1127, Jul. 2007.
- [30] S. Saggini, W. Stefanutti, E. Tedeschi, and P. Mattavelli, "Digital deadbeat control tuning for dc-dc converters using error correlation," *IEEE Trans. power. Electron.*, vol. 22, pp. 1566–1570, Jul. 2007.
- [31] A. Linder and R. Kennel, "Model predictive control for electrical drives," in *Proc. IEEE PESC*, (Recife, Brazil), pp. 1793–1799, 2005.
- [32] E. F. Camacho and C. Bordons, *Model Predictive Control*. New York: Springer-Verlag, 2007.
- [33] J. M. Maciejowski, *Predictive Control With Constraints*. Englewood Cliffs, NJ: Prentice-Hall, 2001.
- [34] J. Kleya, G. Papafotiou, K. Papadopoulos, P. Bohren, and M. Morari, "Performance evaluation of model predictive direct torque control," in *Proc. IEEE PESC*, (Recife, Brazil), pp. 4737–4744, Jun. 2008.
- [35] "Texas instruments." <http://www.ti.com>.
- [36] B. Paillard, "An Introduction to Digital Signal Processors," book, Genie electrique et informatique, Universite de Sherbrooke, Jan. 2002.
- [37] Zaks, Rodnay, and A. Wolfe, "From chips to systems: An introduction to microprocessors.," *Sybex, San Francisco, California, USA*, 1987.
- [38] C. Ilas, A. Sarca, R. Giuclea, and L. Kreindler, "Using TMS320 family DSPs in motion control systems," in *First European DSP Education and Research Conference*, (Paris), Sep. 1996.
- [39] "Berkeley design technology, inc.." <http://www.bdti.com>.
- [40] *Choosing a DSP Processor*. Berkeley Design Technology, Inc., 2000.
- [41] *DSP Selection Guide, TI DSP products: Making innovation possible*. Texas Instruments, 2007.
- [42] K. S. Lin, G. Frantz, and R. Simar, "TMS320 family of digital signal processors," in *Proceedings Of The IEEE*, vol. 2, pp. 1143–1159, 1987.
- [43] k. Astrom and B. Wittenmark, *Computer Controlled Systems*. Prentice-Hall, Englewood Cliffs, New Jersey, USA, 1984.

- [44] I. Ahmed, “Digital control applications with the TMS320 family - selected application notes,” in *Digital Signal Processing Products*, (Texas Instruments, Houston, Texas, USA), 1991.
- [45] S. Bierke, “Enhanced control of an AC motor using fuzzy logic and a TMS320 digital processor,” in *Application Note*, (Texas Instruments, Houston, Texas, USA), 1996.
- [46] F. Pourboghraat and I. Panahi, “Digital control of AC induction motors using TMS320 DSP family,” in *Application Note*, (Texas Instruments, Houston, Texas, USA), 1995.
- [47] B. K. Bose, “Microcomputer control of power electronics and drives,” in *IEEE Press*, (Piscataway, New Jersey, USA), 1987.
- [48] Kuo, S.M., and et al., “Design of active noise control systems with the TMS320 family,” in *Digital Signal Processing Solution*, (Texas Instruments, Houston, Texas, USA), 1996.
- [49] *TMS320F8335, TMS320F28334, TMS320F28332, TMS320F28235, TMS320F28234, TMS320F28232 Digital Signal Controllers (DSCs) data manual*. Texas Instruments, Tech. Rep., March 2010.
- [50] *TMS320F8335, TMS320F28334, TMS320F28332, TMS320F28235, TMS320F28234, TMS320F28232 Digital Signal Controllers (DSCs) data manual*. Texas Instruments, Tech. Rep., 2012.
- [51] J. Lettl, J. Bauer, and L. Linhart, “Comparison of different filter types for grid connected inverter,” in *Progress In Electromagnetics Research Symposium Proceedings PIERS*, (Marrakesh, MOROCCO), pp. 1426–1429, May 20–23, 2011.
- [52] I. S. Mohamed, S. A. Zaid, M. F. Abu-Elyazeed, and H. M. Elsayed, “Classical methods and model predictive control of three-phase inverter with output LC filter for UPS applications,” in *IEEE International Conference on Control, Decision and Information Technologies (CoDIT'13)*, (Hammamet, Tunisia), 6–8 May 2013.
- [53] S. V. Emeljanov, “*Automatische Regelsystem mit veränderlicher struktur* automatic control systems with variable structure,” *Munich, Vienna: R. Oldenbourg Verlag*, 2003.
- [54] M. Aaltonen, P. Tiitinen, J. Lalu, and S. Heikkila, “Direkte drehmomentregelung von drehstromantrieben (direct torque control of three-phase drives),” *ABB Technik*, vol. 3, pp. 19–24, 1995.
- [55] I. Takahashi and T. Noguchi, “A new quick response and high efficiency control strategy of an induction motor,” *IEEE IAS Annual Meeting*, pp. 496–507, 1985.
- [56] J. Holtz and S. Standtfeld, “A predictive controller for the stator current vector of AC machines fed from a switched voltage source,” in *International Power Electronics Conference IPEC*, vol. 2, (Tokio), pp. 1665–1675, 1983.

- [57] J. Holtz and U. schwellenberg, "A new fast response current control scheme for line controlled converters," in *International Semiconductor Power Converter Conference*, (Orlando), pp. 175–183, 1982.
- [58] A. Purcell and P. P. Acarnley, "Multilevel hysteresis comparator forms for direct torque control schemes," *Electronic Letters*, vol. 34, no. 6, pp. 601–603, 1998.
- [59] E. Flach, "Direkte Regelung des Drehmomentmittelwerts einer Induktions-Maschine direct control of the mean torque value of an induction motor," *Dissertation, Darmstadt: Technical University Darmstadt*, 1999.
- [60] O. Kukrer, "Discrete-time current control of voltage-fed three-phase PWM inverters," *IEEE Trans. Ind. Electron.*, vol. 11, pp. 260–269, Mar. 1996.
- [61] M. Depenbrock, "Direct self-control (DSC) of inverter-fed induction machine," *IEEE Trans. Power Electron.*, vol. 3, pp. 420–429, Oct. 1988.
- [62] E. Flach, R. Hoffmann, and P. Mutschler, "Direct mean torque control of an induction motor," in *Proc. Conf. Rec. EPE*, vol. 3, (Trondheim, Norway), pp. 672–677, 1997.
- [63] S. V. Emeljanov, "Automatic control systems with variable structure (automatische regelsystem mit veranderlicher struktur)," *Munich, Vienna: R. Oldenbourg Verlag*, 1969.
- [64] I. Takahashi and T. Noguchi, "A new quick response and high efficiency control strategy of an induction motor," in *Conf. Rec. IEEE IAS Annu. Meeting*, pp. 1665–1675, 1985.
- [65] P. Mutschler, "A new speed-control method for induction motors," in *Proc. Conf. Rec. PCIM*, pp. 131–136, May 1998.
- [66] G. Bode, P. C. Loh, M. J. Newman, and D. G. Holmes, "An improved robust predictive current regulation algorithm," *IEEE Trans. Ind. Appl.*, vol. 41, pp. 1720–1733, Nov. 2005.
- [67] Q. Zeng and L. Chang, "An advanced SVPWM-based predictive current controller for three-phase inverters in distributed generation systems," *IEEE Trans. Ind. Electron.*, vol. 55, pp. 1235–1246, Mar. 2008.
- [68] Y. Nishida, O. Miyashita, T. Haneyoshi, H. Tomita, and A. Maeda, "A predictive instantaneous-current PWM controlled rectifier with AC-side harmonic current reduction," *IEEE Trans. Ind. Electron.*, vol. 44, pp. 337–343, Jun. 1997.
- [69] S.-G. Jeong and M.-H. Woo, "DSP-based active power filter with predictive current control," *IEEE Trans. Ind. Electron.*, vol. 44, pp. 329–336, Jun. 1997.
- [70] W. Zhang, G. Feng, and Y.-F. Liu, "Analysis and implementation of a new PFC digital control method," in *Proc. Conf. Rec. PESC.*, pp. Acapulco, Mexico, 2003.
- [71] P. Mattavelli, G. Spiazzi, and P. Tenti, "Predictive digital control of power factor preregulators," in *Proc. Conf. Rec. PESC*, (Acapulco, Mexico), 2003.

- [72] P. Mattavelli, G. Spiazzi, and P. Tenti, "Predictive digital control of power factor preregulators with input voltage estimation using disturbance observers," *IEEE Trans. Power Electron.*, vol. 20, pp. 140–147, Jan. 2005.
- [73] S. Buso, S. Fasolo, and P. Mattavelli, "Uninterruptible power supply multiloop employing digital predictive voltage and current regulators," *IEEE Trans. Ind. Appl.*, vol. 37, pp. 1846–1854, Nov./Dec. 2001.
- [74] S. Saggini, W. Stefanutti, E. Tedeschi, and P. Mattavelli, "Digital deadbeat control tuning for dc-dc converters using error correlation," *IEEE Trans. Power Electron.*, vol. 22, pp. 1566–1570, Jul. 2007.
- [75] P. Correa, M. Pacas, and J. Rodriguez, "Predictive torque control for inverter-fed induction machines," *IEEE Trans. Ind. Electron.*, vol. 54, pp. 1073–1079, Apr. 2007.
- [76] S. J. Henriksen, R. E. Betz, and B. J. Cook, "Practical issues with predictive current controllers," in *Proc. Australasian Univ. Power Eng. Conf.*, (Perth WA, Australia), 2001.
- [77] H. Abu-Rub, J. Guzinski, Z. Krzeminski, and H. A. Toliyat, "Predictive current control of voltage source inverters," *IEEE Trans. Ind. Electron.*, vol. 51, pp. 585–593, Jun. 2004.
- [78] Y. A. R. I. Mohamed and E. F. El-Saadany, "An improved deadbeat current control scheme with a novel adaptive self-tuning load model for a three-phase PWM voltage-source inverter," *IEEE Trans. Ind. Electron.*, vol. 54, pp. 747–759, Apr. 2007.
- [79] Y. A. R. I. Mohamed and E. F. El-Saadany, "Robust high bandwidth discrete-time predictive current control with predictive internal model –a unified approach for voltage-source PWM converters," *IEEE Trans. Power Electron.*, vol. 23, pp. 126–136, Jan. 2008.
- [80] Y. A. R. I. Mohamed and E. F. El-Saadany, "Adaptive discrete-time gridvoltage sensorless interfacing scheme for grid-connected DG-inverters based on neural-network identification and deadbeat current regulation," *IEEE Trans. Power Electron.*, vol. 23, pp. 308–321, Jan. 2008.
- [81] P. Zanchetta, D. B. Gerry, V. G. Monopoli, J. C. Clare, and P. Wheeler, "Predictive current control for multilevel active rectifiers with reduced switching frequency," *IEEE Trans. Ind. Electron.*, vol. 55, pp. 163–172, Jan. 2008.
- [82] D. W. Clarke, "Adaptive predictive control," *Annual Review in Automatic Programming*, vol. 20, pp. 83–94, 1996.
- [83] D. W. Clarke, C. Mohtadi, and P. S. Tuffs, "Generalized predictive control. part I. the basic algorithm," *Automatica*, vol. 23, no. 2, pp. 137–148, 1987.
- [84] D. W. Clarke, C. Mohtadi, and P. S. Tuffs, "Generalized predictive control. part II. extensions and interpretations," *Automatica*, vol. 23, no. 2, pp. 149–160, 1987.

- [85] M. Tonnes and H. Rasmussen, "Robust self-tuning control of AC servo drive," in *Conf. Record EPE'91*, vol. 3, (Firenze), pp. 48–49, 1991.
- [86] H. R. Mayer and G. Pfaff, "Direct control of induction motor currents," in *European Conference on Power Electronics and Applications EPE 1985*, vol. 2, pp. 3.7–3.12, 1985.
- [87] G. M. Asher, M. Sumner, F. Cupertino, and A. Lattenzi, "Direct flux control of induction motor drives," in *European Conference on Power Electronics and Applications EPE 2001*, (Graz), 2001.
- [88] M. Depenbrock, "Direkte selbstregelung (DSR) für hochdynamische drehelantriebe mit stromrichterspeisung (direct self control for inverter supplied high dynamic AC drives)," *etzArchiv*, vol. 7, pp. 211–218, 1985.
- [89] P. Mutschler, "Verfahren zur direkten regelung der geschwindigkeit eines elektrischen antriebs (principle for direct control of the speed of an electric drive)," *German patent*, DE 196 35 981 C 2-1998.
- [90] R. Kennel, A. Linder, and M. Linke, "Generalized predictive control (GPC)– ready for use in drive applications," in *32nd IEEE Power Electronics Specialists Conference pres2001*, vol. 4, (Vancouver), pp. 1839–1844, 2001.
- [91] G. C. Goodwin, M. M. Seron, and J. D. Dona, *Constrained Control and Estimation—An Optimization Perspective*. London, U.K.: Springer-Verlag, 2005.
- [92] S. J. Qin and T. A. Badgwell, "A survey of industrial model predictive control technology," *Control Eng. Pract.*, vol. 11, pp. 733–764, Jul. 2003.
- [93] D. Q. Mayne, J. B. Rawlings, C. V. Rao, and P. O. M. Scokaert, "Constrained model predictive control: Optimality and stability," *Automatica*, vol. 36, pp. 789–814, Jun. 2000.
- [94] C. E. Garcia, D. M. Prett, and M. Morari, "Model predictive control: Theory and practice—a survey," *Automatica*, vol. 25, pp. 335–348, May 1989.
- [95] G. C. Goodwin, M. M. Seron, and J. D. Dona, *Constrained Control and Estimation*. New York: Springer-Verlag, 2004.
- [96] M. Veenstra and A. Rufer, "Control of a hybrid a symmetric multilevel inverter for competitive medium-voltage industrial drives," *IEEE Trans. Ind. Appl.*, vol. 41, pp. 655–664, Mar./Apr. 2005.
- [97] J. Rodriguez, J. Pontt, C. Silva, M. Salgado, S. Reesa, U. Ammann, P. Lezana, R. Huerta, and P. Cortes, "Predictive control of a three-phase inverter," *Electron. Lett.*, vol. 40, pp. 561–562, Apr. 2004.
- [98] P. Cortes, J. Rodriguez, P. Antoniewicz, and M. Kazmierkowski, "Direct power control of an AFE using predictive control," *IEEE Trans. Power Electron.*, vol. 23, pp. 2516–2523, Sep. 2008.

- [99] M. A. Perez, P. Cortes, and J. Rodriguez, “Predictive control algorithm technique for multilevel a symmetric cascaded h-bridge inverters,” *IEEE Trans. Ind. Electron.*, vol. 55, pp. 4354–4361, Dec. 2008.
- [100] P. Cortes, J. Rodriguez, S. Vazquez, and L. G. Franquelo, “Predictive control of a three-phase UPS inverter using two steps prediction horizon,” in *IEEE International Conference on Industrial Technology (ICIT)*, pp. 1283–1288, 2010.
- [101] B. C. Babu and B. V. Reddy, “An improved dynamic response of voltage source inverter using novel hysteresis dead band current controller,” in *18th Annual Symposium on Emerging Needs in Computing*, Aug. 2009.
- [102] ALTERA, “Hardware in the loop from the matlab/simulink environment,” white paper, Altera Corporation, Sep. 2013.
- [103] M. Bacic, “On hardware-in-the-loop simulation,” in *in 44th IEEE Conference on Decision and Control, 2005 and 2005 European Control Conference CDC-ECC05*, pp. 3194–3198, 2005.
- [104] B. Lu, X. Wu, H. Figueroa, and A. Monti, “A low-cost real-time hardware-in-the-loop testing approach of power electronics controls,” *IEEE Transactions on Industrial Electronics*, vol. 54, no. 2, pp. 919–931, 2007.
- [105] “ezdsp<sup>TM</sup> for the TMS320F28335DSP controller “Quick Start Installation Guide”.” <http://support.spectrumdigital.com>, 2014.